

**APPLICATION OF LOW SALINITY HOT WATER INJECTION IN  
CARBONATES**

by

**LEILA KARABAYANOVA**

**THESIS SUPERVISOR**

**PEYMAN POURAFSHARY**

**THESIS CO-SUPERVISOR**

**MUHAMMAD REHAN HASHMET**

Thesis submitted to the School of Mining and Geosciences of Nazarbayev  
University in Partial Fulfillment of the Requirements for the Degree of

**Master of Science in Petroleum Engineering**

**Nazarbayev University**

**April 2022**

## **Acknowledgements**

I would like to express my deepest appreciation and gratitude to my supervisors, Dr. Peyman Pourafshary and Dr. Muhammad Rehan Hashmet, for their continuous guidance and timely assistance throughout the laboratory experiments and thesis writing. Without their support, this thesis would not have been possible. I also wish to acknowledge the technical support and assistance provided by the staff and faculty of the Petroleum Engineering Department of the School of Mining and Geosciences.

I express my deep gratitude and love to my parents for their immense support during my study. I am forever grateful to my family for giving me the opportunities and experiences to make me who I am.

Finally, I would like to thank my colleague, Aizada Ganiyeva, with whom we learned to understand each other without words and became a real team.

## **Originality Statement**

I, Leila Karabayanova, hereby declare that this submission is my own work and to the best of my knowledge it contains no materials previously published or written by another person, or substantial proportions of material which have been accepted for the award of any other degree or diploma at Nazarbayev University or any other educational institution, except where due acknowledgement is made in the thesis.

Any contribution made to the research by others, with whom I have worked at NU or elsewhere is explicitly acknowledged in the thesis.

I also declare that the intellectual content of this thesis is the product of my own work, except to the extent that assistance from others in the project's design and conception or in style, presentation and linguistic expression is acknowledged.

Signed on 09.04.22



---

## ABSTRACT

The high efficiency of Low Salinity Water (LSW) injection in carbonates, leading to rock wettability alteration from oil-wet to water-wet and, hence, resulting in better oil displacement, has been confirmed by numerous studies. In recent years, the combination of LSW injection with other Enhanced Oil Recovery (EOR) techniques has been widely discussed to activate the synergistic effects of hybrid EOR methods leading to additional oil recovery. The idea of combining LSW injection with a thermal approach, known as Low Salinity Hot Water (LSHW) injection, is a highly promising hybrid EOR method for heavy oil carbonate formations. In this study, the performance of LSW and hybrid LSHW injection was experimentally evaluated for heavy oil carbonate cores by different measurements of rock-fluid interactions and core flooding experiments. Contact angle measurements were conducted to investigate the optimal dilution of seawater (SW) and evaluate the performance of different variations of Potential Determining Ions (PDIs) concentration on wettability change. Appropriate dilution and ion management were applied to design LSW and engineered water (EW) for oil displacement at different temperatures (from 20°C to 70°C) in order to evaluate the standalone LSW and hybrid LSHW injection performance. The injection of LSW and EW was estimated to be inefficient for heavy oil carbonates, while hybrid LSHW flooding showed a significant increase of oil recovery with the best performance of the brine spiked by PDIs, where 60% and 55% of the residual oil was displaced at 50°C and 70°C, respectively. Moreover, the injection of LSHW directly after SW was found to be more practical than following LSW flooding. The application of the hybrid EOR method activates different mechanisms, such as oil detachment from the rock surface, due to the wettability alteration by EW/LSW and viscosity reduction by the thermal methods. Combined active mechanisms result in better performance, compared to the standalone EOR methods. Rock dissolution and multi-ion exchange by PDIs were identified as the main mechanisms of wettability alteration by EW/LSW via the results of ion chromatography analyses. The synergy between EOR methods affects the active mechanisms of LSW/EW flooding. For example, an increase in temperature showed more active multi-ion exchange and rock dissolution, which resulted in higher oil release from the rock surface.

## TABLE OF CONTENTS

LIST OF FIGURES .....	6
LIST OF TABLES .....	8
1. INTRODUCTION .....	9
1.1. Oil Recovery Phases .....	9
1.2. Enhanced Oil Recovery Methods in Carbonates .....	10
1.3. Low Salinity Water Injection in Carbonates .....	12
1.3.1. Main Driving Mechanisms .....	16
1.4. Hot Water Injection .....	21
1.4.1. Main Driving Mechanisms .....	25
1.5. Hybrid EOR Methods .....	27
1.6. Low Salinity Hot Water Injection .....	30
1.7. Problem Statement .....	35
1.8. Research objectives .....	35
1.9. Thesis structure .....	36
2. METHODOLOGY .....	37
2.1. Materials .....	37
2.1.1. Crude oil .....	37
2.1.2. Rock samples .....	40
2.1.2. Low salinity and Engineered brines .....	43
2.2. Procedure of Experiments .....	44
2.2.1. Contact Angle Measurements .....	44
2.2.2. Core flooding experiments .....	46
2.2.3. Ion chromatography analyses .....	49
3. RESULTS AND DISCUSSION .....	50
3.1. Contact Angle Measurements .....	50
3.1.1. Effect of seawater dilution .....	50
3.1.2. Effect of PDIs .....	53
3.2. Core Flooding Experiments .....	56
3.2.1. Experiment 1: SW → Hot SW → Extra Hot SW .....	57
3.2.2. Experiment 2: SW → 5D SW → Hot 5D SW → Extra Hot 5D SW .....	59

3.2.3. Experiment 3: SW → 5D-2Mg*2SO <sub>4</sub> → Hot 5D-2Mg*2SO <sub>4</sub> → Extra Hot 5D-2Mg*2SO <sub>4</sub> ...	61
3.2.4. Experiment 4: SW → 5D-2Ca*2SO <sub>4</sub> → Hot 5D-2Ca*2SO <sub>4</sub> → Extra Hot 5D-2Ca*2SO <sub>4</sub> .....	63
3.2.5. Experiment 5: SW → 5D-2Ca*2Mg*2SO <sub>4</sub> → Hot 5D-2Ca*2Mg*2SO <sub>4</sub> → Extra Hot 5D-2Ca*2Mg*2SO <sub>4</sub> .....	65
3.2.6. Experiment 6: SW → Hot 5D-2Ca*2Mg*2SO <sub>4</sub> → Extra Hot 5D-2Ca*2Mg*2SO <sub>4</sub> .....	67
3.2.7. Comparison of core flooding experiments.....	69
3.3. Ion Chromatography Analysis .....	73
3.3.1. Analysis of Water Samples from Contact Angle Tests.....	73
3.3.2. Effluent Analysis.....	75
4. CONCLUSION AND RECOMMENDATIONS.....	79
5. REFERENCES .....	81

## LIST OF FIGURES

Figure 1. Main phases of a field production plan (Alvarado and Manrique, 2010).....	9
Figure 2. EOR methods by lithology (Manrique et al., 2010) .....	11
Figure 3. Waterflood with the formation brine, followed by 50-times diluted seawater brine in the tertiary mode (Chandrasekhar et al., 2013) .....	13
Figure 4. Results of coreflooding experiment: SW → 3.3D SW → 25D SW (Nasralla et al., 2018) .....	15
Figure 5. Diagram of oil recovery of OOIP during the injection of three different brines: 20dSW, 20dSW*3Mg, 20dSW*2Ca (Saw et al., 2020) .....	16
Figure 6. The schematic description of wettability alteration by multi-ion exchange at (a) low and (b) high temperatures (Zhang et al., 2007) .....	17
Figure 7. SEM images of the core before and after injection – pores enlargement and fines migration due to rock dissolution (Altahir& Hussain, 2017).....	18
Figure 8. Impact of salinity on electrical double layer (Knott, 2010).....	20
Figure 9. Comparison diagram of relative permeability curves under different temperatures (Yongmao et al., 2016) .....	23
Figure 10. Oil recovery factor (RF) vs. pore volume (PV) injected at 20°C, 40°C, 60°C, and 80°C (Masoomi and Torabi, 2022) .....	24
Figure 11. Contributions of different mechanisms in thermal EOR (Burger et. al., 1985).....	24
Figure 12. The predicted oil–water viscosity ratio ( $\mu_o/\mu_w$ ) as a function of temperature (T) by Masoomi and Torabi (2022) .....	26
Figure 13. Change of interfacial tension with temperature increase.....	26
Figure 14. Recovery factor of oil and cumulative water production at different salinity levels (0, 6, and 20%) during SWAG (Aleidan and Mamora, 2010) .....	28
Figure 15. The oil recovery curve of 2 core flooding experiment: hot water and LSHW flooding (Abass and Fahmi, 2013) .....	31
Figure 16. History of oil recovery for LSWF and hot LSWF in pilot-scaled reservoirs (Lee et al., 2016) 32	

Figure 17. Core flooding experiment in core La 1 at 100 °C (Strand et al., 2017).....	33
Figure 18. History of oil recovery (%) for SWI, LSWI, and hot LSWI (Lee and Lee, 2018). .....	34
Figure 19. Temperature dependency of crude oil dynamic viscosity and density .....	38
Figure 20. The schematic procedure of color-indicator titration method .....	39
Figure 21. Examples of core samples (left: core plug, right: core slice).....	40
Figure 22. Vinci HEP-P Helium Porosimeter .....	41
Figure 23. Vinci Vacuum desiccator.....	42
Figure 24. A schematic diagram of carbonate wettability conditions defined by the contact angle (Teklu et al., 2015) .....	44
Figure 25. OCA 15EC video-based optical contact angle measuring instrument.....	45
Figure 26. Core flooding system scheme.....	46
Figure 27. Dionex ICS-6000 high-level modular ion chromatography system .....	49
Figure 28. Prepared 5D, 10D, and 20D SW brines.....	51
Figure 29. Effect of temperature on the rock surface during aging in diluted brines .....	51
Figure 30. Change of CA in 5D SW after 168 hours SW at 20°C and 80°C .....	52
Figure 31. Effect of SW dilution on contact angle at 20°C and 80°C .....	53
Figure 32. Effect of temperature on the rock surface during aging in brines with PDI tuning.....	54
Figure 33. Change of CA in 5D 2Ca*2Mg*2SO <sub>4</sub> after 168 hours SW at 20°C and 80°C.....	55
Figure 34. Effect of PDIs on contact angle at 20°C and 80°C.....	56
Figure 35. Tubes with effluent from core flooding before separation .....	57
Figure 36. Oil recovery diagram of Experiment 1: SW (20°C) → Hot SW (50°C) → Extra Hot SW (70°C) .....	59
Figure 37. Oil recovery diagram of Experiment 2: SW → 5D SW → Hot 5D SW → Extra Hot 5D SW ...	61
Figure 38. Oil recovery diagram of Experiment 3: SW → 5D 2Mg*2SO <sub>4</sub> → Hot 5D 2Mg*2SO <sub>4</sub> → Extra Hot 5D 2Mg*2SO <sub>4</sub> .....	63
Figure 39. No oil production during the injection of 5D 2Ca*2SO <sub>4</sub> brine at 20°C .....	64
Figure 40. Oil recovery diagram of Experiment 4: SW → 5D 2Ca*2SO <sub>4</sub> → Hot 5D 2Ca*2SO <sub>4</sub> → Extra Hot 5D 2Ca*2SO <sub>4</sub> .....	65
Figure 41. Oil recovery diagram of Experiment 5: SW → 5D 2Ca*2Mg*2SO <sub>4</sub> → Hot 5D 2Ca*2Mg*2SO <sub>4</sub> → Extra Hot 5D 2Ca*2Mg*2SO <sub>4</sub> .....	67
Figure 42. Oil recovery diagram of Experiment 6: SW → Hot 5D 2Ca*2Mg*2SO <sub>4</sub> → Extra Hot 5D 2Ca*2Mg*2SO <sub>4</sub> .....	68
Figure 43. Oil recovery comparison for 3-stage core flooding experiments .....	70
Figure 44. Oil recovery comparison for 4-stage core flooding experiments .....	71
Figure 45. Incremental oil recovery (without SW injection) of 4-stage core flooding experiments .....	72
Figure 46. Incremental oil recovery (without SW injection) of 3-stage core flooding experiments .....	72
Figure 47. Comparison of displacement efficiency of 4-stage core flooding experiments.....	73
Figure 48. Comparison of displacement efficiency of 3-stage core flooding experiments.....	73
Figure 49. Change of PDIs concentration in 10-times diluted SW during aging of oil-wet cores (left: 20°C, right: 80°C) .....	74
Figure 50. Change of PDIs concentration in 10-times diluted SW during aging of clean cores (left: 20°C, right: 80°C) .....	75

Figure 51. Change of PDIs concentration during 5D SW brine injection.....	76
Figure 52. Change of PDIs concentration during 5D 2Ca*2SO4 brine injection.....	77
Figure 53. Change of PDIs concentration during 5D 2Mg*2SO4 brine injection.....	77
Figure 54. Change of PDIs concentration during 5D 2Mg*2Ca*2SO4 brine injection.....	78

## LIST OF TABLES

Table 1. Measured oil properties at different temperatures .....	37
Table 2. Core samples porosity values.....	41
Table 3. Core samples permeability values .....	43
Table 4. Ionic composition of formation, sea and low salinity water .....	44
Table 5. Design of core flooding experiments.....	47
Table 6. Results of contact angle measurements with diluted brines.....	53
Table 7. Results of contact angle measurements with different PDI concentration.....	55
Table 8. Characteristics of the core 1.....	58
Table 9. Oil recovery factors of Experiment 1: SW (20°C) → Hot SW (50°C) → Extra Hot SW (70°C).58	
Table 10. Characteristics of core 5.....	59
Table 11. Oil recovery factors of Experiment 2: SW → 5D SW → Hot 5D SW → Extra Hot 5D SW.....	60
Table 12. Characteristics of core 2.....	61
Table 13. Oil recovery factors of Experiment 3: SW → 5D 2Mg*2SO <sub>4</sub> → Hot 5D 2Mg*2SO <sub>4</sub> → Extra Hot 5D 2Mg*2SO <sub>4</sub> .....	62
Table 14. Characteristics of core 10.....	63
Table 15. Oil recovery factors of Experiment 4: SW → 5D 2Ca*2SO <sub>4</sub> → Hot 5D 2Ca*2SO <sub>4</sub> → Extra Hot 5D 2Ca*2SO <sub>4</sub> .....	64
Table 16. Characteristics of core 8.....	65
Table 17. Oil recovery factors of Experiment 5: SW → 5D 2Ca*2Mg*2SO <sub>4</sub> → Hot 5D 5D 2Ca*2Mg*2SO <sub>4</sub> → Extra Hot 5D 2Ca*2Mg*2SO <sub>4</sub> .....	66
Table 18. Characteristics of core 9.....	67
Table 19. Oil recovery factors of Experiment 5: SW → Hot 5D 2Ca*2Mg*2SO <sub>4</sub> → Extra Hot 5D 2Ca*2Mg*2SO <sub>4</sub> .....	69
Table 20. Summary of oil recovery factors of 3-stage core flooding experiments .....	70
Table 21. Summary of oil recovery factors of 4-stage core flooding experiments .....	71

# 1. INTRODUCTION

## 1.1. Oil Recovery Phases

Production of crude oil and gas can be classified into three oil recovery stages: primary, secondary, and tertiary. Primary recovery is the initial production step when oil can be displaced by reservoir natural energy, i.e., the differential pressure between the buried reservoir and the earth's surface (Alvarado and Manrique, 2010). When the reservoir energy decreases and is no longer sufficient to sustain oil production, secondary oil production can be implemented at the field. Despite the additional oil recovered from the reservoir by water or gas injection during secondary oil recovery, a considerable amount of oil remains in the pores of the rock (Vishnyakov et al., 2020). Tertiary oil recovery methods, also called Enhanced Oil Recovery (EOR), help produce crude oil from reservoirs that other methods cannot extract. EOR methods can displace from 30% to 60% of the original oil in place, compared to the other two recovery methods, which can extract only 20-40% of crude oil (ERPI, Palo Alto, CA, 1999). It is essential to mention that stages of oil recovery do not always follow the chronological sequence. For example, heavy and extra heavy oil reservoirs require thermal support to reduce the oil viscosity, because high viscous oil cannot be naturally displaced, as the economic cost will be higher than the minor oil inflows anyway. Figure 1 shows a schematic description of the main phases of a field production plan.

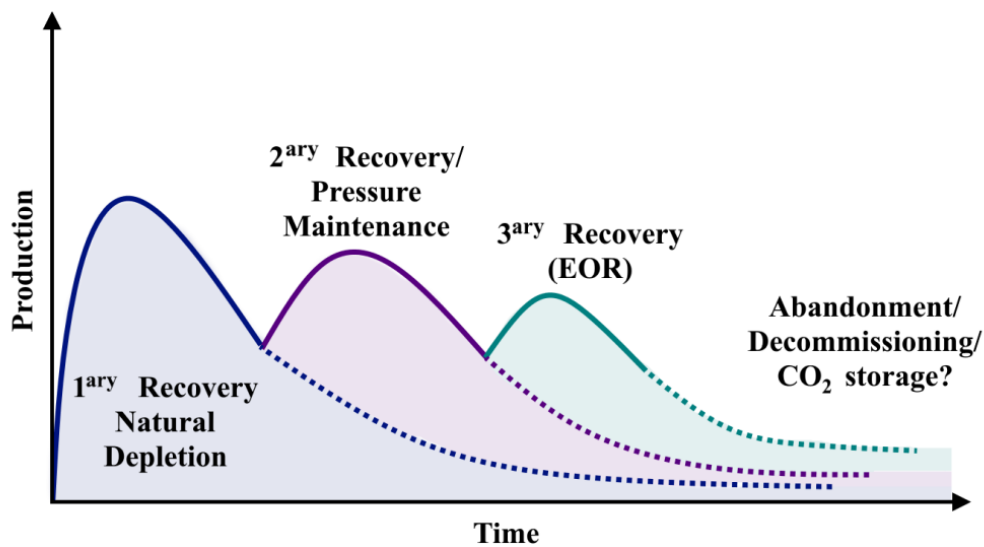


Figure 1. Main phases of a field production plan (Alvarado and Manrique, 2010)

The application of EOR methods is always associated with certain risks and requires considerable capital investments. Developing new EOR methods optimize many points: maximizing the oil recovery factor, reducing investment and environmental damage, etc., under certain conditions. These oil recovery methods must be technically and economically feasible; otherwise, their application in the fields will be impossible (Verma, 2015). EOR methods can be classified into three main types: thermal, chemical, and miscible (solvent) injections (Vishnyakov et al., 2020). Thermal EOR methods include steam, hot water flooding, stimulation, steam-assisted gravity drainage (SAGD). Chemical EOR methods are represented by injected interfacial-active components such as alkalis, surfactants, chemical mixtures, and polymers (Alvarado and E. Manrique, 2010). Miscible or solvent EOR methods can be described as gas injection, such as carbon dioxide (CO<sub>2</sub>), nitrogen (N<sub>2</sub>), and hydrocarbon gases (Verma, 2015).

### **1.2. Enhanced Oil Recovery Methods in Carbonates**

More than half of known oil and gas fields are represented in carbonate reservoirs. Since carbonates can form not only during the accumulation of sediments in the sea but also during chemical weathering, the physicochemical characteristics of carbonates vary greatly. However, in general, it can be noticed that carbonate rocks are often characterized by low porosity, high heterogeneity and may be fractured (Alvarado and E. Manrique, 2010; Myint and Firoozabadi, 2015). When pressure, temperature, or fluid composition in the pores of rocks change, chemical reactions may start in carbonates, resulting in dissolution, recrystallization, and other processes (Myint and Firoozabadi, 2015). Mixed and even oil-wet conditions, high heterogeneity of the mineral content, and the characteristics listed above lead to the lowered rates of oil recovery from carbonates to only 25-45% of OOIP (Alvarado and Manrique, 2010; Verma, 2015; Myint and Firoozabadi, 2015; Montaron et al., 2007; Burchette, 2012)

According to Alvarado and Manrique (2010), only 18% of EOR methods are applied worldwide in carbonate formations (Figure 2). Chemical EOR methods, especially polymer (Murayri et al., 2019; Lee et al., 2019; Diab and Al-Shalabi, 2019), surfactant (Standnes and T. Austad, 2000; Seethepalli et al., 2004; Ayirala et al. 2021), and surfactant-polymer (AlSofi et al., 2013; Ayirala et al. 2021) flooding have proven their high efficiency in carbonates in many studies and field applications. Up to now, surfactants are the only chemical method able to change the wettability of the rock from oil-wet to mixed or water-wet state to initiate the process

of water imbibition into the rock matrix (Alvarado and E. Manrique, 2010). On the other hand, thermal EOR is not as widely used in carbonate formations as chemical EOR (Alvarado and E. Manrique, 2010). Thermal EOR in heavy oil carbonates is mostly presented by steam (Penney et al., 2005), hot water injection (Askarova et al., 2020), and Steam-Assisted Gravity Drainage (SAGD) (Shafiei et al., 2007). Due to the high cost of application, low efficiency at great depths, and other characteristics, this type of EOR approach is highly limited (Alvarado and E. Manrique, 2010). Gas EOR methods are most commonly used for fractured and light oil carbonate formations compared to thermal and chemical recovery techniques. As of 2010, among the applications of gas EOR in carbonate reservoirs, CO<sub>2</sub> injection accounted for 61%, while 36% and 3% constituted hydrocarbon gas and N<sub>2</sub> injection, respectively (Koottungal, 2010).

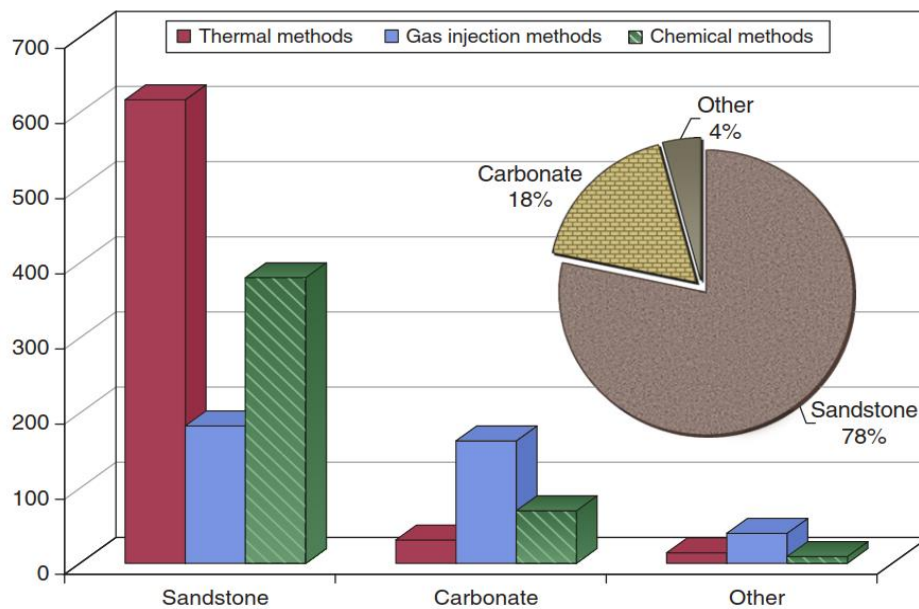


Figure 2. EOR methods by lithology (Manrique et al., 2010)

Conventional waterflooding can be considered one of the most cost-effective and applicable oil recovery methods compared to the techniques mentioned above (Yousef et al., 2011). Due to the strong bond between oil carboxylic groups and the rock surface leading to oil-wet conditions of carbonates, conventional water flooding is often inefficient for oil displacement from carbonate reservoirs. Thus, in recent studies, more attention has been paid to investigating the optimal injection method and changing the type of injected brine (Xu et al., 2020).

### 1.3. Low Salinity Water Injection in Carbonates

Low Salinity Water (LSW) injection is a relatively recent EOR method applied on sandstone and carbonate reservoirs. The approach of this technique is to inject several times diluted sea or formation water with possible alteration of ionic concentration into the reservoir. The oil recovery factor can be increased by adjusting the wettability from oil-wet to water-wet (Katende&Sagala, 2019). It should be pointed out that the mechanisms of LSW injection in sandstone reservoirs differ significantly from carbonate reservoirs due to internal structural and mineral differences in rocks. Despite the complex pore structure in carbonates, which complicates the displacement of oil and yields conflicting results in LSWI studies, the high efficiency of LSWI was proved by many laboratory studies with the help of rock-fluid interactions measurements and core flooding experiments (Alotaibi et al., 2011; Skrettingland et al., 2011; Yousef et al., 2012; Mahani et al., 2015; Ayirala et al., 2018). LSW can be designed in carbonate formations by diluting sea or formation water and/or altering the concentration of cations and anions, mostly  $\text{Ca}^{2+}$ ,  $\text{Mg}^{2+}$ , and  $\text{SO}_4^{2-}$ .

Interestingly, despite a significant number of active mechanisms, the dominant one has not yet been identified either in sandstones or in carbonate reservoirs due to contradictory results in many studies (Katende&Sagala, 2019). Literature about LSW injection is quite extensive for light oils and sandstone reservoirs. However, up to now, the number of studies and applications for heavy and extra heavy oils in carbonate reservoirs is limited.

In 1991, seawater injection in the Ekofisk chalk field showed unexpectedly high results compared to the pilot experiments, which began in 1986 (Hallenbeck et al., 1991). Austad et al. (2005) investigated the phenomenon of the Ekofisk field and concluded that the oil-wet wettability of carbonate surface could be affected by the composition, base number (BN)/acid number (AN) of crude oil, ionic concentration of injected fluid, and reservoir temperature. The authors found out that  $\text{SO}_4^{2-}$  ions act as a catalyst in the process of wettability alteration and, hence, a high concentration of  $\text{SO}_4^{2-}$  is crucial for the oil carboxylic groups released from the carbonate surface.

$\text{Ca}^{2+}$ ,  $\text{Mg}^{2+}$ , and  $\text{SO}_4^{2-}$  were firstly determined by Zhang et al. (2007) as Potential Determining Ions (PDI) that alter the wettability of rock surface and, hence, release more oil from the surface. It was concluded that  $\text{Ca}^{2+}$ ,  $\text{Mg}^{2+}$ , and  $\text{SO}_4^{2-}$  ions could adjust the wettability of

the carbonates due to absorption of the PDI on the surface, and  $Mg^{2+}$  ions potentially can affect the charge density on the rock surface. Injection of the brine with the excess of both  $Mg^{2+}$  and  $SO_4^{2-}$  ions showed a considerable increase of oil recovery, compared to initial seawater injection, due to the strong combined effect of  $Mg^{2+}$  and  $SO_4^{2-}$  ions on wettability alteration.

Chandrasekhar et al. (2013) studied the effect of ion tuning of injected brines on additional oil displacement from the carbonate surface with the help of contact angle measurements, spontaneous imbibition tests, and core flooding experiments. Proposed mechanisms were studied by geochemical modeling and zeta-potential measurements. The authors highlighted  $Ca^{2+}$ ,  $Mg^{2+}$ ,  $SO_4^{2-}Na^+$ , and  $Cl^-$  as the main active ions of LSW. Injection of seawater showed an additional oil recovery by 7% of OOIP compared to the formation brine injection with the recovery factor of 40%. Moreover, brines with diluted seawater and sulfate ions excess showed an increase of oil recovery to 65-80% of OOIP in secondary and tertiary oil recovery stages, respectively, which matches the results of Austad et al. (2005) about the positive effect of an excess of sulfate ions on the change in wettability (Figure 3). Release of naphthenic acids and, hence, the reduction of these acids in surface concentration was proposed as the main mechanism leading to the change of wettability from oil-wet to at least mix-wet state. Furthermore, minor calcite dissolution after 5 injected pore volumes of diluted seawater was noticed during the core flood experiments.

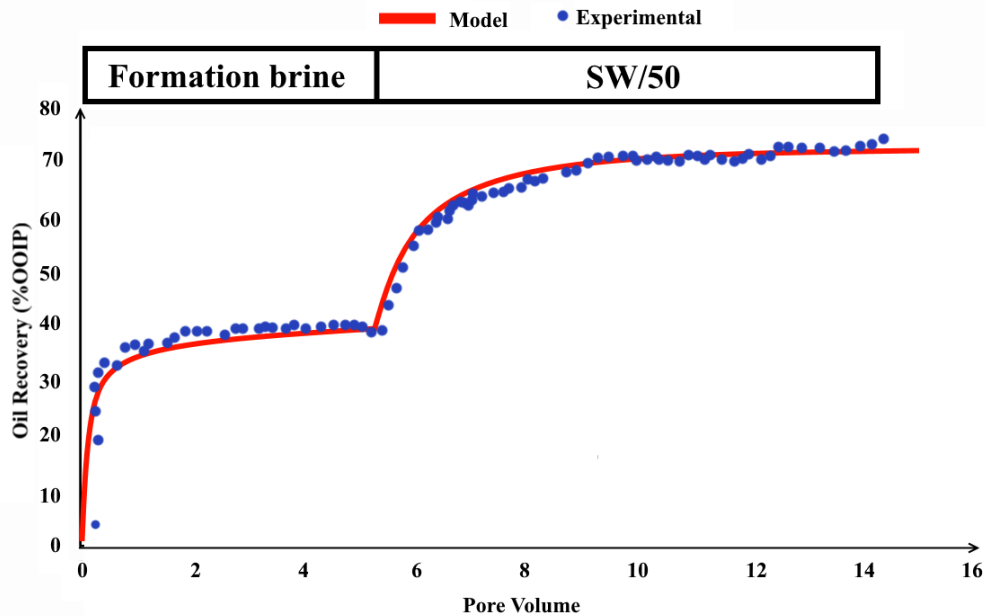


Figure 3. Waterflood with the formation brine, followed by 50-times diluted seawater brine in the tertiary mode (Chandrasekhar et al., 2013)

Mahani et al. (2015) explored the effect of water dilution, surface charge change, mineral dissolution, alteration of PDIs concentration, etc., on the wettability alteration of rock surface from oil-wet to water-wet condition. Wettability alteration was estimated by continuous contact angle measurements, while zeta-potential measurements investigated surface charge change. The effect of mineral dissolution was researched using the given solubility data and geochemical modeling. The authors concluded that surface change alteration was the leading mechanism of the salinity water flooding, while mineral dissolution could be identified as a secondary mechanism due to its significance only on a laboratory scale. Limestone mineral composition was more effective for low salinity water injection than dolomites, possibly due to fewer adhesion forces between oil and limestone.

The potential of low salinity water flooding in heavy oil carbonate reservoirs was firstly explored by José et al. (2015). Several core flooding experiments and numerical simulation techniques were carried out for secondary and tertiary oil recovery stages. The purpose of the experimental part was to collect data for relative permeability curves and further simulation. Several numerical simulations were carried out to explore the effect of reservoir parameters such as pressure, thickness, temperature, etc., well pattern, and injection time on the success of low salinity water injection under different conditions. The authors concluded that low salinity water injection leads to higher incremental oil recovery results during secondary oil recovery than tertiary stage but still promising for both stages. Ten times dilution of high salinity water was optimal for most simulations.

Nasrallaet al. (2018) conducted several laboratory experiments and numerical interpretations to study seawater dilution's effect and compare seawater's performance with LSW injection. It was found that additional oil recovery is possible when formation injection is switched to seawater and then several times diluted seawater. However, after a certain number of seawater dilutions, no more oil was produced, indicating an optimal dilution of seawater, beyond which the oil recovery factor will no longer increase. Estimated optimal salinity of seawater and effect of LSW injection differed in layers of the carbonate reservoir. Thus, it was concluded that depending on the conditions of the experiment (physical and chemical properties of the reservoir, oil, etc.), the optimal degree of dilution might vary, so for different conditions, it will always be different. LSW injection showed additional oil displacement by 7% compared to formation water injection (Figure 4).

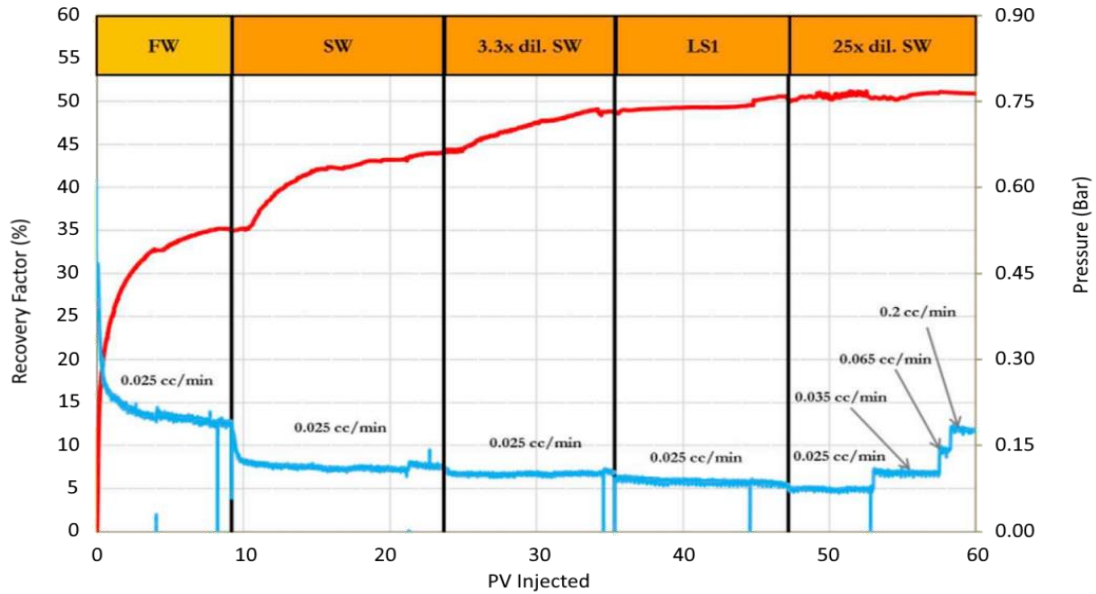


Figure 4. Results of coreflooding experiment: SW → 3.3D SW → 25D SW (Nasralla et al., 2018)

Zaeri et al. (2018) performed several spontaneous imbibitions and contact angle tests to investigate the effect of dilution and temperature on oil recovery factor during low salinity water injection and confirmed the statement of Nasralla et al. (2018) about the optimal dilution of the injected brine. Application of 20-times diluted seawater showed the tremendous contact angle change and oil recovery factor, while brines with lower and higher salinities were less potent. It was also found that temperature had a crucial effect on additional oil recovery increasing at optimal dilution. Multi-ion exchange and calcite dissolution were proposed as the main mechanisms of LSW.

Saw and Mandal (2020) studied the primary mechanisms of LSW flooding in carbonate core plugs by exploring the effect of optimal dilution and altering the concentration of PDI of the injected seawater. The effect of dilution was explored with the help of contact angle, zeta potential, and interfacial tension measurements. After finding the optimal seawater dilution, the most appropriate concentrations of PDI were tuned by contact angle and zeta potential tests. Several core flooding experiments with different low-salt water solutions were performed to find the highest rise of incremental oil recovery compared to seawater. The authors determined that 20-fold dilution was found to be optimal, showing an additional increase of 20% in oil recovery factor compared to seawater. The double concentration of  $\text{Ca}^{2+}$  and triple concentration of  $\text{Mg}^{2+}$  in 20-fold diluted seawater resulted in 17.51% and 20.58% of incremental oil recovery (Figure5).

Potential Determining Ions and calcite dissolution were identified as the primary mechanisms leading to change in wettability from oil-wet to water-wet conditions.

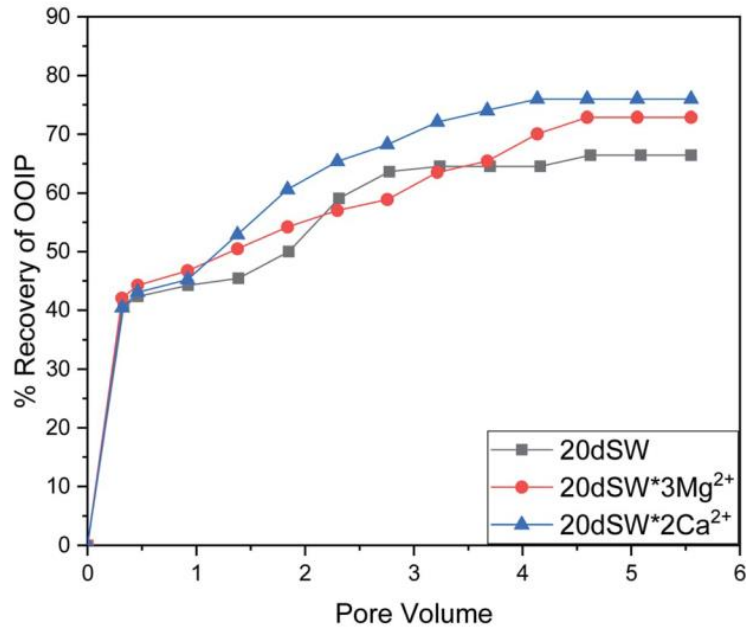


Figure 5. Diagram of oil recovery of OOIP during the injection of three different brines: 20dSW, 20dSW\*3Mg, 20dSW\*2Ca (Saw et al., 2020)

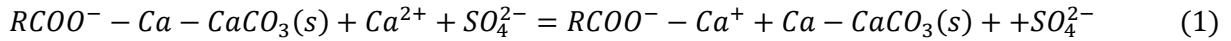
### 1.3.1. Main Driving Mechanisms

#### *Multi-ion Exchange by Potential Determining Ions*

The effect of PDIs on wettability alteration during LSW flooding was proposed by Zhang et al. (2007). The wettability of carbonate surface changes from an oil-wet to more water-wet due to the adsorption of PDIs onto the rock surface. A significant concentration of  $\text{SO}_4^{2-}$  ions presented in seawater adsorb on the rock surface, which leads to the reduction of surface charge density. After that,  $\text{Ca}^{2+}$  and  $\text{SO}_4^{2-}$  can also co-adsorb onto the surface and considerably reduce electrostatic repulsive force. Organic components of crude oil can be released from the surface after reacting with  $\text{Ca}^{2+}$  ions, which finally leads to wettability alteration (Lee & Lee, 2019). Furthermore, the effect of PDI on wettability change strongly depends on the types of carbonate rocks such as calcite, dolomite, or magnesite (Strand et al., 2006).

PDI exchange was proposed as one of the main LSW mechanisms in many studies (Tweheyo et al., 2006; Ding and Rahman, 2018; Saw et al., 2020; Kasha et al., 2021). The

reaction of co-adsorption of  $\text{Ca}^{2+}$  and  $\text{SO}_4^{2-}$  ions with the release of carboxylic groups was proposed by RezaeiDoust et al. (2009):



With the increase of temperature, especially in the range of 90-110°C,  $\text{Mg}^{2+}$  ions can replace  $\text{Ca}^{2+}$  ions, which are connected to carboxylic groups on the rock surface, resulting in the additional release of oil organic components and, therefore, higher wettability alteration (Figure 6). High concentration of  $\text{SO}_4^{2-}$  ions is crucial for more reactions of  $\text{Mg}^{2+}$  replacing  $\text{Ca}^{2+}$  (Austad et al., 2011). Strand et al. (2003) experimentally found that the process of multi-ion exchange becomes more active when sulfate ions have a concentration of more than 1g/L in the brine. An exchange of  $\text{Ca}^{2+}$  ions by  $\text{Mg}^{2+}$  at higher temperatures is shown by Equation (2):

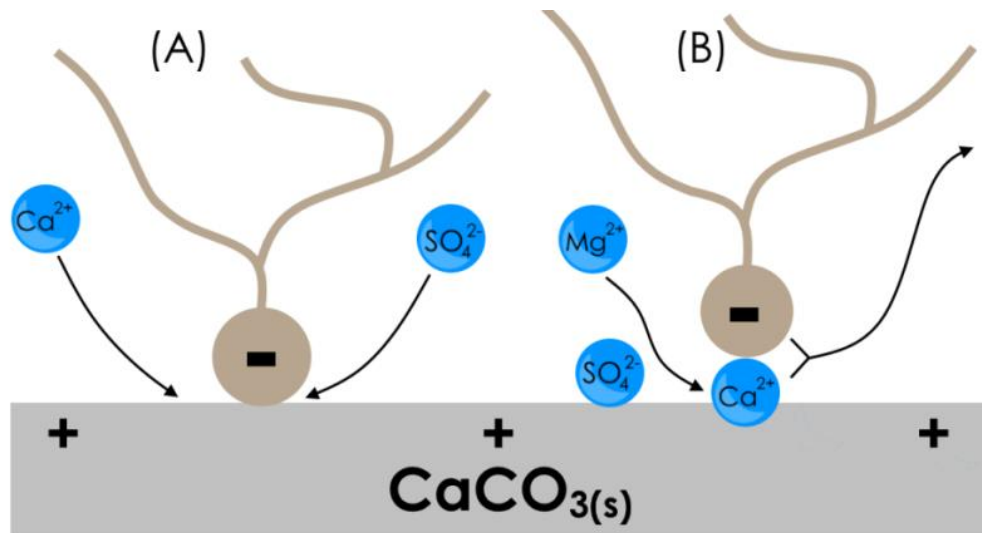
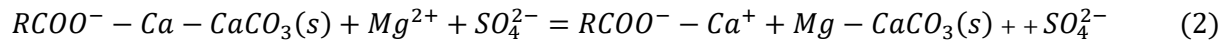
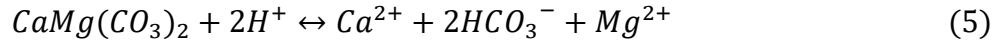
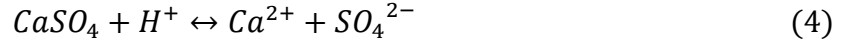
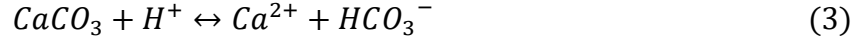


Figure 6. The schematic description of wettability alteration by multi-ion exchange at (a) low and (b) high temperatures (Zhang et al., 2007)

### ***Rock Dissolution***

Rock dissolution was firstly proposed as the active mechanism of LSW flooding leading to the wettability alteration by Hiorth et al. (2010). The degree of calcite dissolution strongly depends on the ionic concentration of water in pores, temperature, and pressure. It was confirmed in many studies [Hiorth et al., 2010, Zhang & Austad, 2006; Zhang et al., 2006, 2007] that rock dissolution is a temperature-sensitive mechanism. Organic components of crude oil are

released from the carbonate surface due to the calcite dissolution process, and it results in wettability alteration to water-wet conditions. Calcite and anhydrite dissolution/precipitation processes can be described by the following equations (Al-Shalabi, 2016):



Further reactions that take place in the aqueous phase:



Altahir and Hussain (2017) performed displacements with 3- and 6-times diluted seawater and deionized water in water-wet carbonate cores fully saturated with seawater to study the effect of calcite dissolution separately from other mechanisms. Results of ion chromatography analysis showed a considerable increase of  $Ca^{2+}$  ions, indicating an active calcite dissolution mechanism. SEM images of the carbonate rock surface showed pore enlargement resulting from calcite dissolution (Figure 7).

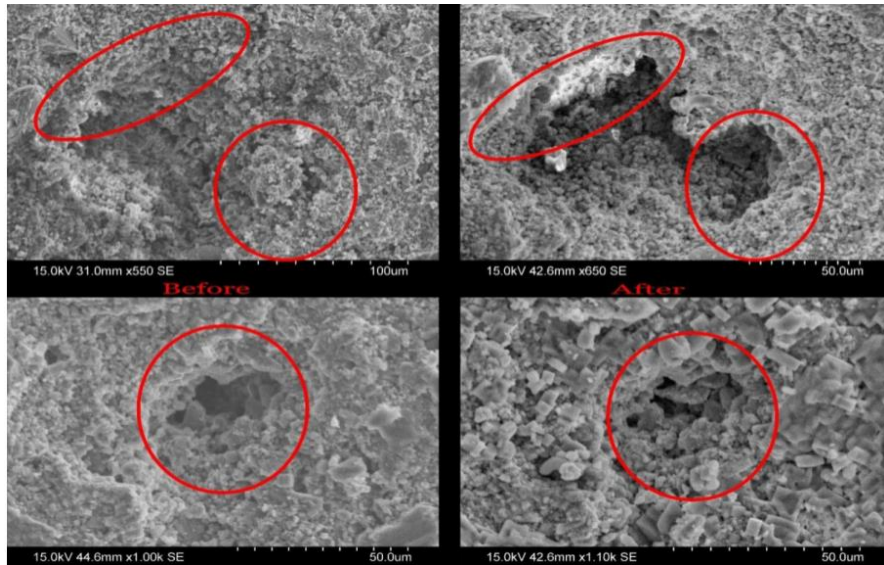


Figure 7. SEM images of the core before and after injection – pores enlargement and fines migration due to rock dissolution (Altahir& Hussain, 2017)

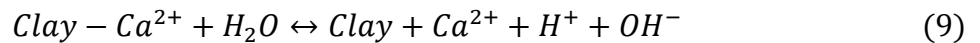
However, according to Mahani et al. (2017), enhanced oil recovery during LSW injection is still possible without the process of calcite dissolution, and other mechanisms such as PDI and surface charge behave as more active. Moreover, the effect of calcite dissolution becomes less significant as the study scale increases from core-scale to reservoir size. Thus, the effect of calcite dissolution on oil displacement during LSW injection requires more experimental and numerical studies, taking into account different scales of the carbonate rocks.

### ***Effect of pH***

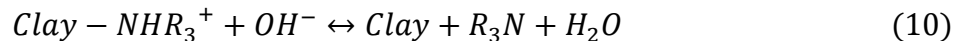
The effect of the increase in pH on the desorption of oil carboxylic groups from the carbonate surface was firstly proposed by Austad et al. (2010). The authors proposed three conditions under which the mechanism would work:

1. The presence of clay in the rock;
2. A high amount of acidic or base material in the crude oil;
3. PDI in connate water, especially  $Ca^{2+}$ .

Since the process is only possible with clay content in the rock, this effect is more noticeable in carbonate rocks. Before the injection of LSW, polar components of crude oil and potential determining cations of formation water adhere to the large rock surface. The crude oil-brine-rock (CBR) system is in chemical equilibrium at the constant reservoir pressure, temperature, pH (Austad et al., 2010). When LSW with a significantly lower amount of cations, especially  $Ca^{2+}$ , enters the porous media, the chemical balance is disturbed, which leads to desorption of  $Ca^{2+}$  and other cations from the rock surface.  $H^+$  ions substitute  $Ca^{2+}$  ions and adsorb on the clay surface to compensate for the cation loss (Vledder et al., 2010). This process results in pH increase close to the carbonate surface and can be described by the following equation (9):



According to Vledder et al. (2010), the local pH increasing near the chalk surface induces reactions between adsorbed basic and acidic components, as shown by Equations (10) and (11). After LSW injection, acidic and simple crude oil ions are partially desorbed from the chalk surface, changing the wettability to a more water-wet condition.





### ***Expansion of the Electrical Double Layer***

The concept of the electrical-double layer in reservoirs was firstly proposed by Winsauer and McCardell (1953). They concluded that PDI adsorption on the rock surface leads to the abnormal conductivity of the shales and limestones. The expansion of the double layer depends on the ionic concentration and presence of PDI in the electrolyte. Knott (2010) suggested the expansion of electrical double-layer as an active mechanism of LSW injection. According to his theory, an electrical double layer is formed around the negatively charged particles of clay on the carbonate surface. The ionic concentration of pore water strongly affects the thickness of the double-layer, consisting of the external diffusive layer with excess anions and the internal adsorbed layer with excess cations. Figure 8 shows the difference in the impact of ionic concentration on the double layer. When low-salinity water is injected into the reservoir, double-layers tend to expand compared to the compact thickness of EDL under high-salinity water.  $\text{Ca}^{2+}$  and  $\text{Mg}^{2+}$  ions strongly connect clay particles and oil components in the adsorbed layer. Injection of LSW helps to “destroy” the diffusive layer and allows  $\text{Na}^+$  and other monovalent ions to penetrate this layer and displace  $\text{Ca}^{2+}$  and  $\text{Mg}^{2+}$ . This displacement leads to the excess of the repulsive forces and, hence, oil desorption from the carbonate surface.

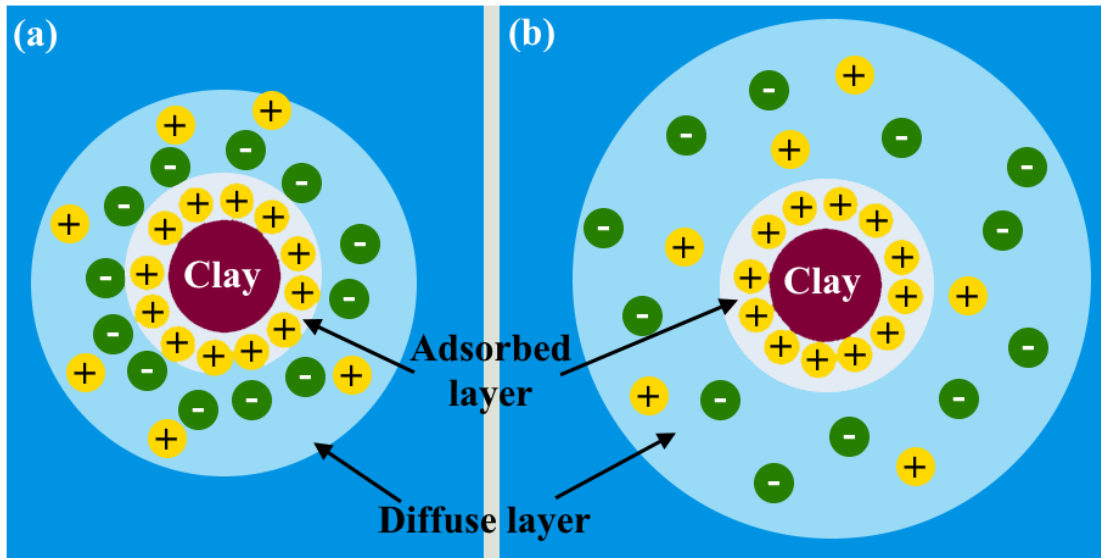


Figure 8. Impact of salinity on electrical double layer (Knott, 2010)

Alotaibi et al. (2011) investigated the electrokinetics of carbonate rocks suspensions at 25°C and 50°C with the help of zeta-potential measurements. It was found that chemical reactions between the rock surface and pore brine are controlled by electrical-double layer (EDL) forces. However, Mehana and Fahes (2018) observed EDL shrinkage during LSW injection, which completely contradicted the previous studies showing EDL expansion. Thus, they concluded that the efficiency of the double-layer expansion mechanism during LSW flooding is in doubt.

To summarize, LSW injection requires the presence of PDI with an excess of sulfates and at least mixed-wet conditions of the rock surface, i.e., the more oil-wetted wettability is, the better the oil displacement process will be. LSW injection can be successfully applied during secondary and tertiary oil recovery stages. The primary LSW mechanism is the wettability alteration from oil-wet to water-wet conditions, which can be reached by multi-ion exchange, pH increase, calcite dissolution, and other proposed mechanisms. Due to conflicting results, the main driving mechanisms are still not well defined. LSW injection of heavy oil carbonate reservoirs is a promising technique but accompanied by certain risks, such as unfavorable mobility ratio and poor sweep efficiency.

#### **1.4. Hot Water Injection**

Heavy oil and bitumen sandstone and carbonate reservoirs account for more than 65% of the world's oil reserves of approximately 5.6 trillion barrels (Frances, 2006; Meyer et al., 2007). In general, thermal EOR methods are widely used in heavy oil reservoirs to reduce the viscosity and increase the sweep efficiency of the crude oil, and, hence, increase the oil recovery (Al-Saedi et al., 2018). Hot water flooding is the process of injecting hot water under a specific temperature into a reservoir through special injection wells (Liu, 1998). When the hot water appears in porous media of the rock, the viscosity of the crude oil tends to reduce, and polar acidic components of crude oil, such as asphaltenes and resin substances release from the rock surface, making the wettability of the rock more water-wet (Yongmao et al., 2016).

Compared to steam EOR approaches, which require a tremendous amount of energy for steam production and lead to greenhouse gas emissions, hot water injection is the least expensive due to less heat loss during the flooding and the most environment-friendly technique for oil extraction (Yongmao et al., 2016). Furthermore, injection rates during hot water flooding are

considerably higher than during steam injection, which results in more effective reservoir pressure maintenance (Masoomi and Torabi, 2022). However, this EOR method has many limitations:

1. Lower sweep efficiency compared to steam injection;
2. An early water breakthrough in high-permeable reservoirs;
3. Considerable heat loss immediately after the contact with the rock;
4. Only a local increase in temperature near-horizontal injection wells.

Furthermore, according to Jamaloei and Singh (2016), hot water flooding is not practical for extra heavy oil with 10,000 – 100,000 cp viscosities. Thus, it can be concluded that hot water injection is a cost-effective thermal alternative for medium-heavy oil reservoirs when steam injection methods cannot be applied (Masoomi and Torabi, 2022).

Since hot water injection into high-permeable reservoirs may be accompanied by the risks of an early water breakthrough, the application of hot water in tight and medium-permeable heavy oil reservoirs is a high potential approach for effective oil displacement. Yongmao et al. (2016) experimentally investigated the role of hot water injection mechanisms and crude oil and reservoir petrophysical properties. Twenty-five tight heterogeneous core samples with the permeability of 0.38 mD were used for experimental hot water flooding at 20°C, 50°C, 90°C, 120°C, and 150°C to analyze the effect of oil viscosity, oil/water interfacial tension, relative permeability curves, and pores structure during the thermal approach. The authors concluded that the ratio of oil/water viscosity tends to decrease in heated reservoirs, which results in better sweep efficiency and waterflood performance. However, an increase of temperature to 150°C showed no effect on additional oil displacement due to a slight reduction of oil/water viscosity ratio with an increase in temperature in an already heated rock. Effect of temperature increase on oil/water interfacial tension is noticeable. Thermal expansion of oil crucially increased during the hot water flooding at higher temperatures, resulting in a formation pressure rise and better oil displacement. Residual oil saturation and irreducible water saturation started to decrease with the temperature rise, making the relative permeability curves shift right (Figure 9). It was found that hot water injection leads to the pore structure change, i.e., enlargement of pore radius, which also results in better oil displacement than cold water flooding.

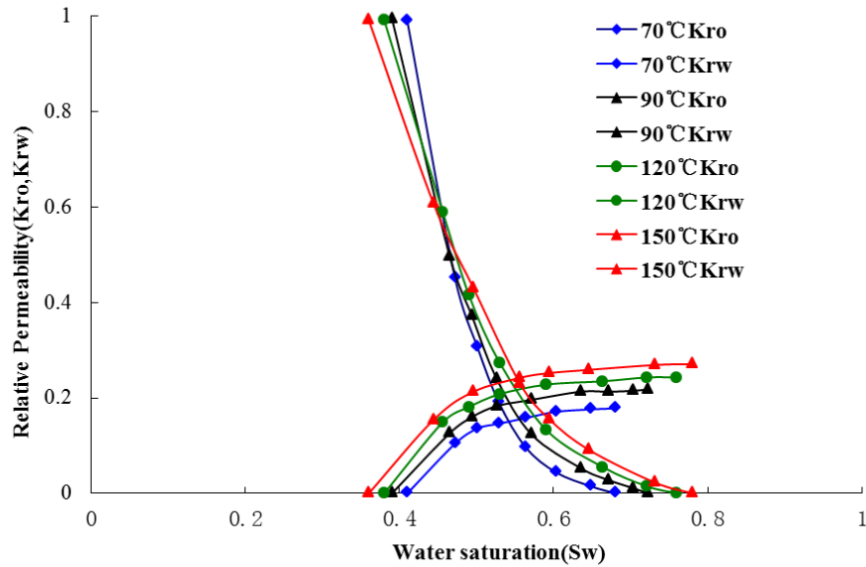


Figure 9. Comparison diagram of relative permeability curves under different temperatures (Yongmao et al., 2016)

Masoomi and Torabi (2022) conducted a novel numerical approach for unconsolidated heavy oil reservoirs to predict the distribution of temperature and oil-water viscosity ratio in the porous media and oil production and recovery factor. Data from 4 core flooding experiments at 20-80°C were used for further numerical simulation in CMG software. Conventional water injection at 20°C showed low oil displacement with a total oil recovery of 28.94% OOIP due to an unfavorable mobility ratio between oil and injected fluid (less than 1) and, hence, pure sweep efficiency. An increase in temperature showed better oil recovery due to a considerable reduction in the oil viscosity. Water flooding at 40°C, 60°C, and 80°C showed oil recoveries of 31.32%, 32.79%, and 38.55% OOIP (Figure 10). Moreover, an increase in temperature tended to prevent early breakthrough due to better control of mobility ratio. Relative permeability curves tended to shift right with the temperature increase, which indicated lower residual oil saturation and higher irreducible water saturation. Furthermore, temperature rise showed more effect on the oil relative permeability curve because oil viscosity decreases much more strongly than the viscosity of water. All results confirmed the study by Yongmao et al. (2016).

At the moment, all mechanisms of hot water injection have been studied quite well. Burger et al. (1985) proposed several active mechanisms, the effect of which changes with increasing crude oil density: vaporization, thermal expansion, wettability alteration, and viscosity reduction. In many studies, the viscosity reduction of crude oil is considered the leading mechanism. The

density of oil dramatically influences the activity of hot water mechanisms: viscosity reduction and wettability alteration have more impact on heavy oil displacement, while the effect of vaporization and thermal expansion are more noticeable with lighter oils (Figure 11).

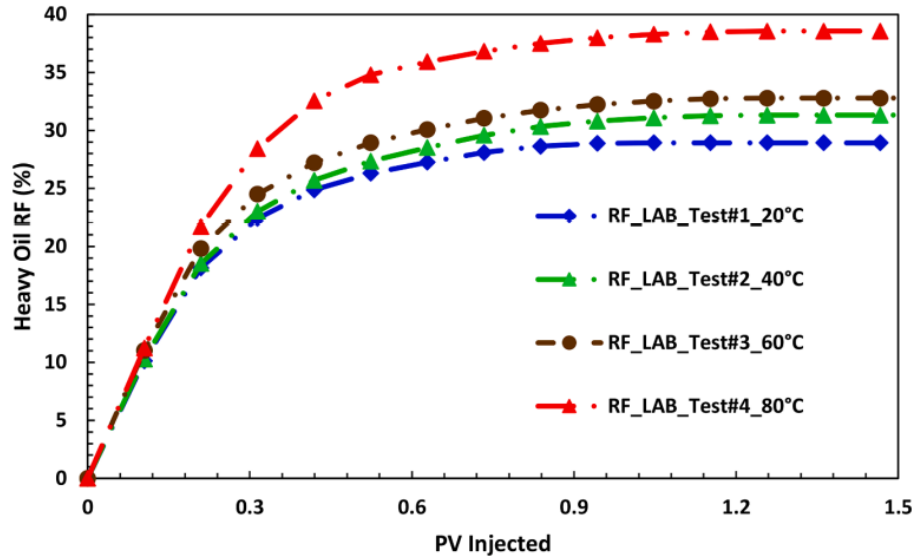


Figure 10. Oil recovery factor (RF) vs. pore volume (PV) injected at 20°C, 40°C, 60°C, and 80°C (Masoomi and Torabi, 2022)

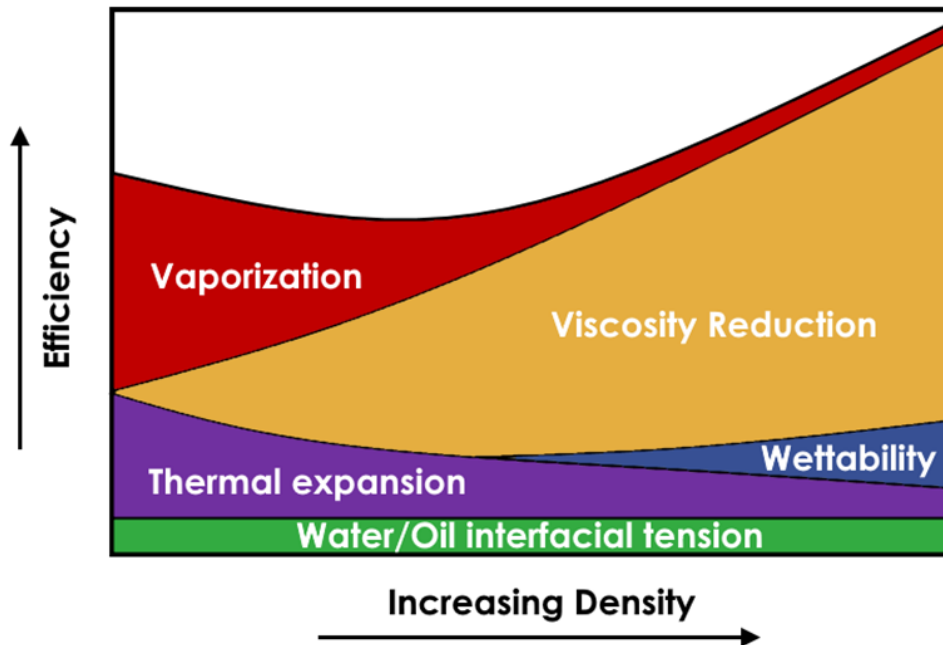


Figure 11. Contributions of different mechanisms in thermal EOR (Burger et. al., 1985)

### 1.4.1. Main Driving Mechanisms

#### *Viscosity reduction*

It is known that the more viscous the oil (and other liquids), the more sensitive it will be to temperature changes. Hot water injection affects the oil, making it less viscous and mobile. Viscosity change of the injected and formation water is negligible compared to the alteration of oil viscosity during the heating process, which is confirmed by a considerable right shifting of relative oil permeability curves and minor shifting of relative water permeability curves showing the higher sensitivity of oil to temperature change (Yongmao et al., 2016; Masoomi and Torabi, 2022).

There are many correlations between temperature and viscosity of different liquids in porous media, one of the most widely applicable equations was proposed by Kreith and Bohn (1977):

$$\mu_o = 0.6402 + 18.9612 * e^{(-0.074T)} \quad (12)$$

Where T is the temperature of the formation and  $\mu_o$  is the viscosity of crude oil. This correlation is applicable in the range of 0-100°C

Fournier (1965) estimated a correlation for oil-water viscosity ratio( $\mu_o/\mu_w$ )during hot water injection:

$$\frac{\mu_o}{\mu_w} = \beta_1 + \beta_2(1 - T_D)^{\beta_3} \quad (13)$$

$$T_D = \frac{T - T_R}{T_{inj} - T_R} \quad (14)$$

Where  $T_D$  is the dimensionless temperature,  $T_r$  is the initial reservoir temperature of the injected fluid, T is the current reservoir temperature,  $T_{inj}$  is the temperature of the injected fluid, and  $\beta_{1,2,3}$  are constants in the viscosity ratio curve fitting function.

Figure 12 shows the predicted oil-water viscosity ratio based on Equation (14) by Masoomi and Torabi (2022). As shown, with increasing temperature, oil viscosity initially decreases significantly, but after overcoming a certain point, viscosity reduction declines, indicating the hyperbolic correlation between the viscosity and temperature.

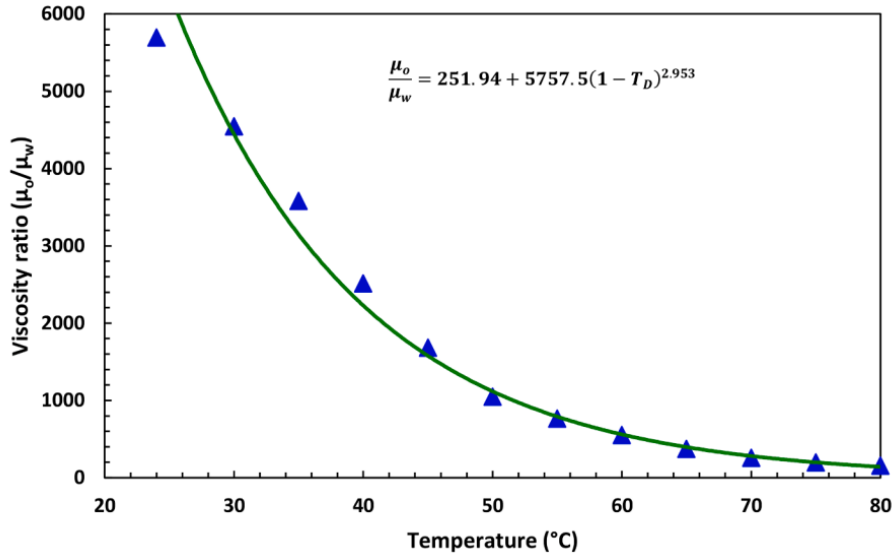


Figure 12. The predicted oil–water viscosity ratio ( $\mu_o/\mu_w$ ) as a function of temperature (T) by Masoomi and Torabi (2022)

***IFT reduction***

The interfacial tension between oil and water generally tends to decrease with the increase of temperature during hot water injection, which results in better sweep efficiency and, hence, an increase in the oil recovery (Lo and Mungan, 1973; Yongmao et al., 2016). Figure 13 shows a linear correlation between interfacial tension and temperature changes.

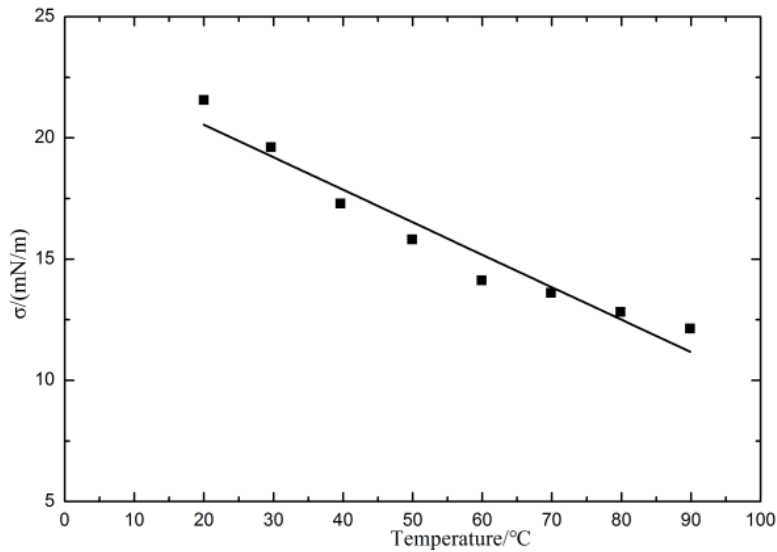


Figure 13. Change of interfacial tension with temperature increase

An increase in temperature leads to interfacial tension reduction due to more intense movement of molecules; hence, the molecular force field decreases. Furthermore, a decrease in interfacial tension affects the capillary forces, which is crucial for oil recovery. The correlation between interfacial tension and temperature was proposed by Yongmao et al. (2016):

$$\sigma = -0.13404(T - t_o) + \sigma_{t_o} \quad (15)$$

where  $\sigma$  is the interfacial tension between oil and water,  $\sigma_o$  is the initial interfacial tension,  $T$  is the temperature of the rock, and  $t_o$  is the initial temperature before the injection.

### 1.5. Hybrid EOR Methods

The idea of combining two or more different EOR techniques, known as hybrid EOR methods, was considered to enhance the driving oil recovery mechanisms for an increase in oil recovery. LSW injection has been already successfully applied in a hybrid scheme with surfactant (Alameri et al., 2015; Sekerbayeva et al., 2020; Shakeel et al., 2021), polymer (Torrijos et al., 2018; Shakeel et al., 2020; Karimov et al., 2020), nanofluid (Assef et al., 2014; Mahmoudpour&Pourafshary, 2021), hot water (Abbas and Fahmi, 2013; Strand et al., 2017; Lee and Lee, 2018), and gas (Aleidan and Mamora, 2010; Jiang et al., 2010; Moradpour et al., 2021). These hybrid EOR methods improve oil recovery due to the simultaneous effects of driving mechanisms such as wettability alteration, IFT reduction, and mobility control (Pourafshary and Moradpour, 2019).

The combination of LSW flooding and gas injection is a relatively new hybrid EOR technology. At the moment, the effectiveness of the hybrid method is questionable due to conflicting research results. There are many possible combinations of EOR methods, such as injection of LSW into simultaneous water alternating gas (SWAG) or water alternating gas (WAG) techniques and injection of gas following LSW flooding. Reducing water salinity improves gas solubility, increasing the stability of the injected fluid, mobility ratio, and waterfront (Pourafshary and Moradpour, 2019). However, several studies (Li and Nghiem, 1983; Enick and Klara, 1990; Duan and Sun, 2003) concluded that an increase in gas solubility reduces oil production due to higher oil mobility. Aleidan and Mamora (2010) performed several core flooding experiments in carbonate cores to evaluate the different schemes of hybrid gas-LSHW injection: (1) conventional water flooding, (2) SWAG injection, (3) WAG injection, (4) and continuous gas injection (CGI), where miscible CO<sub>2</sub> was used as a gas. It was concluded that the

process of CO<sub>2</sub> dissolution is a critical factor for better oil displacement and, hence, brines with lower salinity lead to higher oil recovery. However, standalone LSW was found to be ineffective, while the combination of miscible CO<sub>2</sub> and LSW showed better microscopic efficiency (Figure 14).

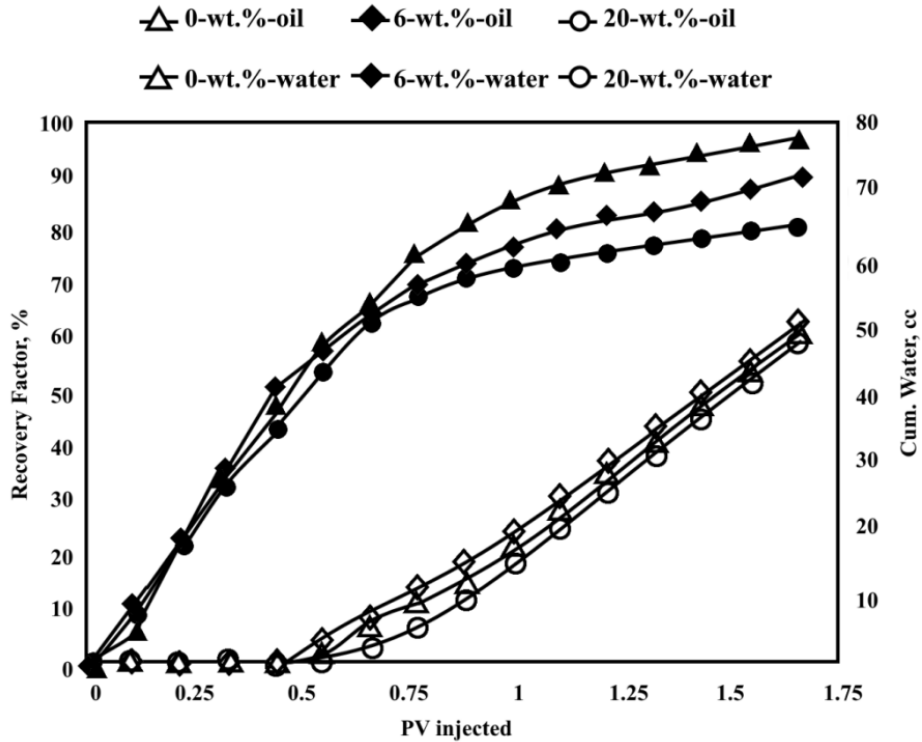


Figure 14. Recovery factor of oil and cumulative water production at different salinity levels (0, 6, and 20%) during SWAG (Aleidan and Mamora, 2010)

Polymer flooding can increase the mobility ratio of oil displacement and, hence, change the macroscopic sweep efficiency, while injection of LSW leads to chemical imbalance of CBR system and wettability alteration, resulting in a change of microscopic sweep efficiency (Pourafshary and Moradpour, 2019). Thus, a combination of LSW and polymers in the hybrid EOR approach is a potentially highly effective method. Alzayer and Sohrabi (2013) performed a simulation experiment for the heavy oil field case (20°API) by a hybrid method of LSW injection and polymer flooding. Numerical simulation led to a 5% oil recovery increase for LSW injection and 7.5% and 10% for the hybrid method of polymer flooding and LSW injection. Almansour et al. (2017) determined the increase of additional oil recovery from 12 to 29% in different cores by switching from LSW to polymer flooding. Tahir et al. (2018) concluded that polymer injection after LSW flooding shows better results than the case of injection LSW after polymer flooding.

Additional oil recovery (4%) in the primary polymer injection was assumed because of the viscoelastic response. Thus, it could be noted that in most cases, a combination of LSW flooding with other EOR methods gives additional percentages of ultimate oil recovery and other advantages.

Nanoparticles can be successfully combined with the LSW due to their free flow through porous media because of the small size and large surface area. Standalone nanoparticles can enhance the oil displacement by in situ emulsification, mobility ratio improvement, and IFT reduction (Moradi et al., 2017). As was mentioned before, fine migration is possible during LSW flooding due to the destruction of the equilibrium of the CBR system (Altahir& Hussain, 2017). Fine migrations disadvantages can be taken under control by combining LSW with nanoparticles by altering the zeta-potential of the rock surface (Assef et al., 2014; Assef et al., 2016). Sadatshojaei et al. (2016) investigated the synergistic effects of injection of LSW combined with silica nanoparticles to increase the oil recovery in carbonates with the help of zeta-potential, IFT, and contact angle measurements. It was concluded that the addition of silica nanoparticles helps increase wettability alteration from oil-wet to water-wet states; thus, leading to the additional oil recovery compared to standalone LSW injection. Ding et al. (2019) combined the LSW with  $\text{SiO}_2$  and  $\text{Al}_2\text{O}_3$  nanoparticles under high-temperature conditions. To investigate the synergistic effects of three EOR approaches in heavy oil silica sand reservoirs. Standalone LSW and hybrid low salinity water injection displacement experiments at different temperatures were carried out. Oil viscosity, interfacial tension reduction, and wettability alteration leading to better displacement efficiency were driving mechanisms of this hybrid EOR method. LSW injection with the addition of  $\text{Al}_2\text{O}_3$  showed the highest incremental oil recovery of 40.2% OOIP compared to conventional water flooding due to the more significant interfacial tension reduction.

Thus, it can be concluded that the application of the hybrid methods results in better sweep efficiency and other controlling mechanisms such as adsorption and lower residual oil. Hence, by this approach, the application of different EOR methods, such as LSWI, could be more effective in more complicated cases, such as heavy oil reservoirs.

## 1.6. Low Salinity Hot Water Injection

There are a few studies that show the application of LSW-based hybrid EOR approaches for heavy oil formations. To recover heavy oil, generally, thermal methods are used, and by application of a thermal method with LSW flooding, it is possible to develop a hybrid technique to enhance the recovery. Low Salinity Hot Water (LSHW) injection is a high-potential hybrid technique for sandstones and carbonates with heavy and extra heavy oil due to the simultaneous activation of mechanisms of different techniques in one hybrid approach. Heavy and extra heavy oil production in carbonate reservoirs is complicated not only due to the difficult recovery of high viscosity oil, which requires thermal approaches, but also because of the oil-wet condition of the porous media, which complicates the process of oil displacement. Even conventional water flooding is an economically unprofitable and inefficient method for oil recovery in such cases. However, the LSHW injection approach can be considered a promising EOR hybrid method that combines thermal and smart waterflooding techniques (Ismail et al., 2021). Increasing temperature leads to a significant acceleration of cation ion exchange and oil viscosity reduction (Lee and Lee, 2018). According to Zhang et al.(2007), at temperature conditions above 90°C, Mg<sup>2+</sup> ions displace Ca<sup>2+</sup> ions, which results in the additional release of the polar oil components and more water-wet conditions of the chalk surface. Hence, by the hybrid approach, different LSW mechanisms, such as multi-ion exchange, will also be involved besides thermal EOR mechanisms to increase the sweep efficiency in heavy oil formations.

The injection of LSHW was experimentally evaluated for the first time by Abass and Fahmi (2013). They compared the new hybrid method to the conventional water flooding, hot water injection, and steam injection in sandstone cores and unconsolidated sand packs. The hybrid method was operated at 95°C, and oil samples had different viscosity values from 700 to 1700 cp. The brine salinity was 24,000 ppm TDS for the high-salinity case and 200 ppm for the low-salinity case. During the first core flooding experiment, hot water and LSHW were injected in a sand pack system at 90°C. Conventional hot water injection was considered a secondary stage, and when water-cut reached 90%, the process of oil displacement was switched to the tertiary LSHW flooding. Resulted showed an additional increase of oil recovery by 20% OOIP during LSHW injection, indicating about active wettability modification mechanism of LSW (Figure 15). The second core flooding experiment had the same displacement design as the first, except that the temperature was lowered to 90°C and higher ionic concentration of connate water

and injected hot water. Results showed an increase of additional oil recovery by 29% OOIP compared to hot water injection. The third experiment consisted of an additional steam injection stage at 100°C after hot water and LSHW injection with a lower concentration than during the second experiment. Additional oil recovery by 52% and 8% OOIP was estimated during LSHW and steam injection, respectively, compared to the conventional hot water injection with the recovery factor of only 22% OOIP. Thus, the main driving mechanisms of oil viscosity reduction and thermal expansion were proposed, while LSW mechanisms were also active. Final results had shown that from 20% to 52% of incremental oil would be recovered by LSHW compared to the conventional hot water flooding, which proves the performance of the hybrid approach.

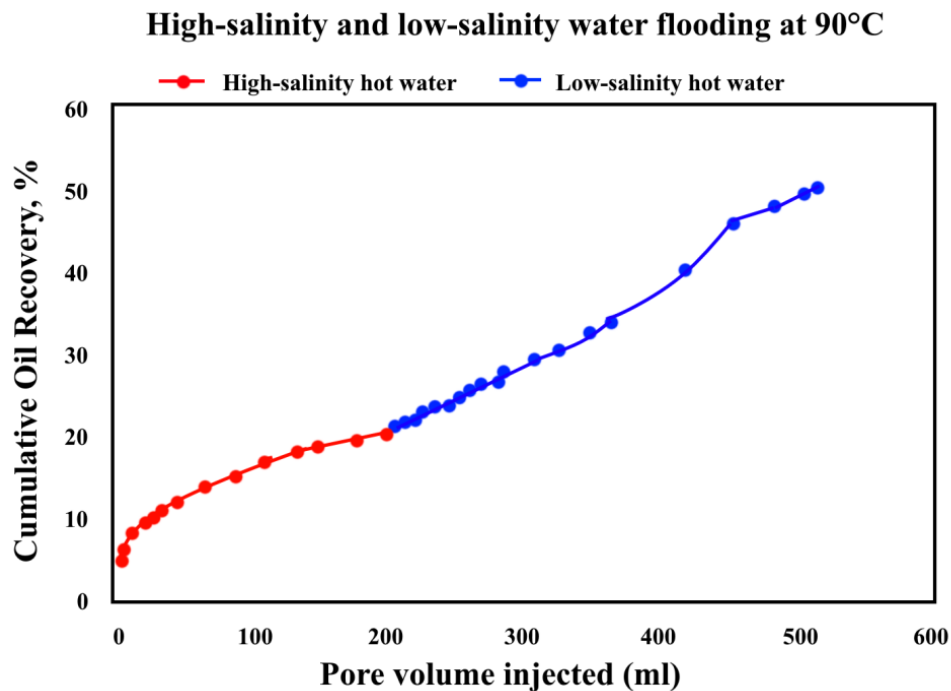


Figure 15. The oil recovery curve of 2 core flooding experiment: hot water and LSHW flooding (Abass and Fahmi, 2013)

Lee et al. (2017) performed several pilot-scaled numerical simulations in CMG software to compare the performances of LSW and LSHW injection in heavy oil carbonate reservoirs under different temperatures from 90 to 120°C. Ten times dilution of seawater was chosen as optimal case based on data from the study of Gachuz-Muro and Sohrabi (2014). The authors concluded that an increase in temperature leads to considerable oil reduction and wettability alteration, which results in better mobility control and, hence, additional oil displacement (Figure 16). The combination of LSW and thermal EOR approach accelerates the calcite dissolution and increases

pH near carbonate surface, i.e., increases the activity of LSW mechanisms. Furthermore, carbonates can control the loss of heat, which also helps to decrease oil viscosity.

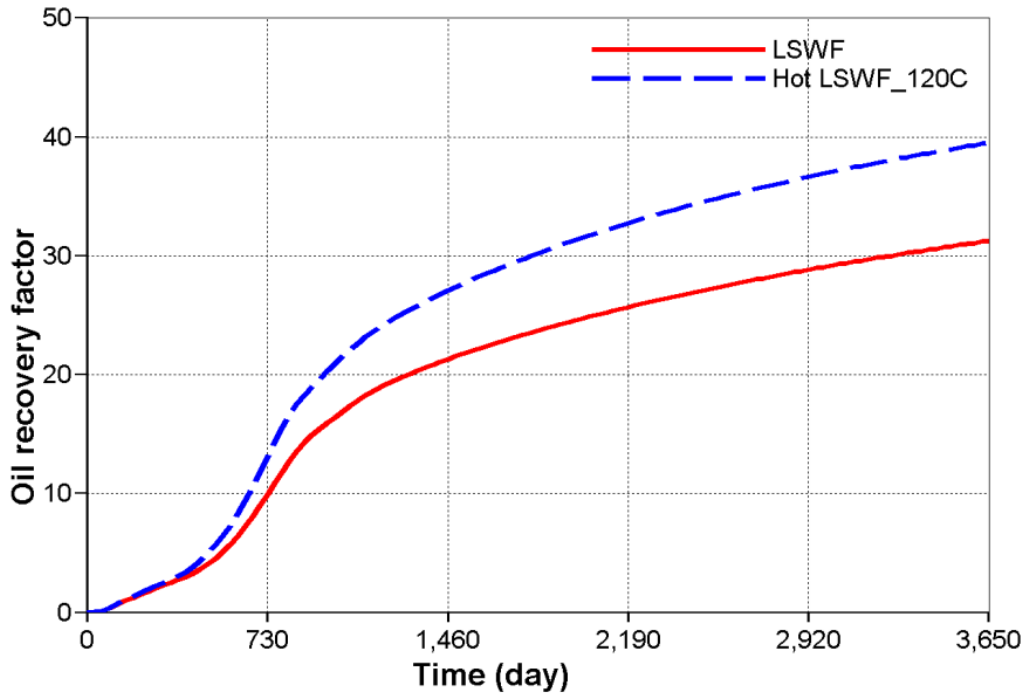


Figure 16. History of oil recovery for LSWF and hot LSWF in pilot-scaled reservoirs (Lee et al., 2016)

Strand et al. (2017) experimentally flooded two core plugs with 100 times diluted formation water, one at 20 °C and the other at different reservoir temperatures from 40 to 130 °C. Several effluent analyses were carried out to track the change of  $\text{Ca}^{2+}$ ,  $\text{Mg}^{2+}$ , and  $\text{SO}_4^{2-}$  ions concentration during the flooding process at a temperature from 20 °C to 130 °C. It was concluded that the highest incremental oil recovery was estimated during the 100 times diluted formation waterflooding at 100 °C (Figure 17). The injection rate during all experiments was constant at 1 pore volume per day. It was found that the high content of dissolvable anhydrite led to the generally positive impact on low salinity water flooding technique due to the maximum concentration of  $\text{Ca}^{2+}$  and  $\text{SO}_4^{2-}$  ions. The authors stated that temperature gradient increase led to the decrease of the anhydrite dissolution process. Mineral dissolution was proposed as the primary mechanism of low salinity water flooding in carbonates by changing the wettability of the rock surface.

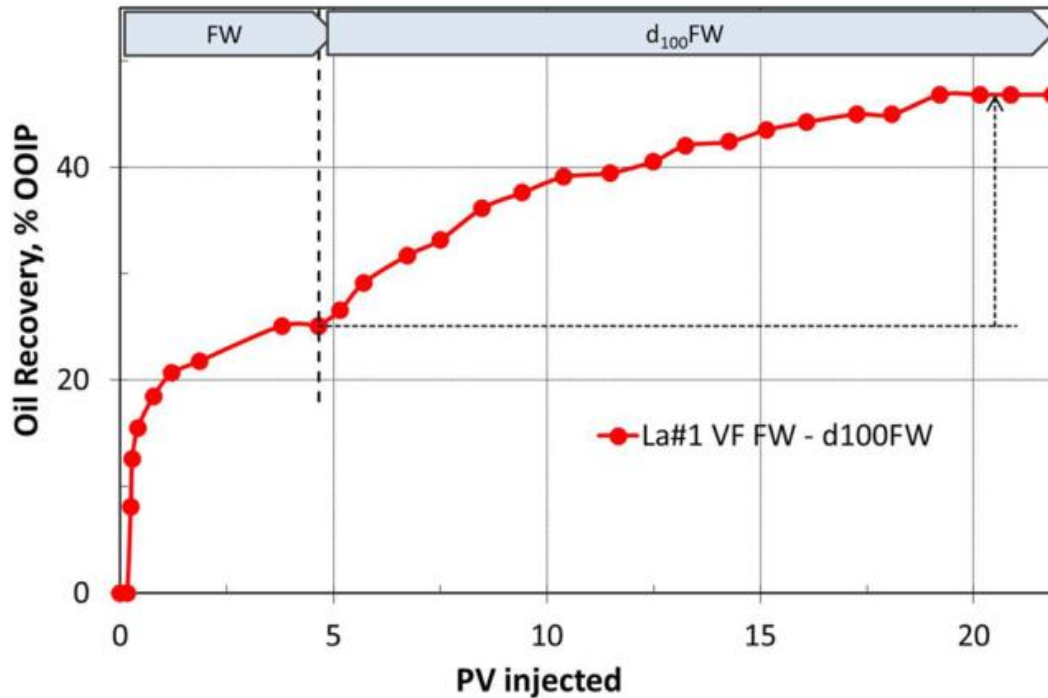


Figure 17. Core flooding experiment in core La 1 at 100 °C (Strand et al., 2017)

Al-Saedi et al. (2018) injected LSHW in four heavy oil sandstone cores under different temperature conditions (70 and 90°C). Two formation brines: the original one with the concentration of 97500 ppm and modified brine with the double concentration of  $\text{Ca}^{2+}$ , were used as connate water for cores saturation and second water flooding stage, while 100-times diluted formation water was prepared as low salinity brine for tertiary oil displacement. The first core flooding experiment was conducted at 70°C and showed an additional oil recovery of 8% OOIP compared to the conventional water flooding stage. The design of the second core flooding was similar to the first despite the temperature increase to 90°C. It showed 10% of additional oil recovery after formation water injection. The authors concluded that the application of hybrid LSHW leads to the viscosity reduction of heavy oil and thermal expansion mechanisms and wettability modification by the low salinity of injected brine. The remaining two experiments were performed with modified formation water to understand the role of  $\text{Ca}^{2+}$  ions during LSHW injection. Results showed a considerable increase of pH due to the double concentration of  $\text{Ca}^{2+}$  compared to the first and second experiments. However, temperature increase showed no effect on pH during all experiments. The third and fourth core flooding experiments showed lower amounts of displaced oil during the LSHW stage due to the excess of  $\text{Ca}^{2+}$  ions in formation

water. Furthermore, it was concluded that pH increase is not the main mechanism at different temperatures. It was concluded that ion tuning is crucial during LSHW injection, because it can improve or worsen the performance of flooding.

Lee and Lee (2018) observed and investigated the synergistic effects of the hybrid LSHW in heavy oil carbonate reservoirs by several numerical simulations of core-scale and pilot-scale models. Carbonate core-scale and pilot-scale models were used in several numerical simulations to quantify the effect of wettability alteration and viscosity reduction that were determined as the leading mechanisms of the hybrid method. Core-scaled system simulation of low salinity hot water injection showed higher multi-component ion exchange of  $\text{Ca}^{2+}$  and  $\text{Mg}^{2+}$  with an increase of  $\text{Ca}^{2+}$  fraction by 182% and  $\text{Mg}^{2+}$  fraction by 209% compared to conventional water flooding. Incremental oil recovery increased by 21% over seawater injection and 6% compared to low salinity water flooding (Figure 18). The pilot-scale system showed a rise of  $\text{Ca}^{2+}$  and  $\text{Mg}^{2+}$  fractions by 240% and 268% and oil recovery factor rise by 6% and 3% compared to seawater and low salinity water injections, respectively. For both systems, it was found that geochemical reactions led to additional wettability modification from a strong oil-wet to a water-wet state.

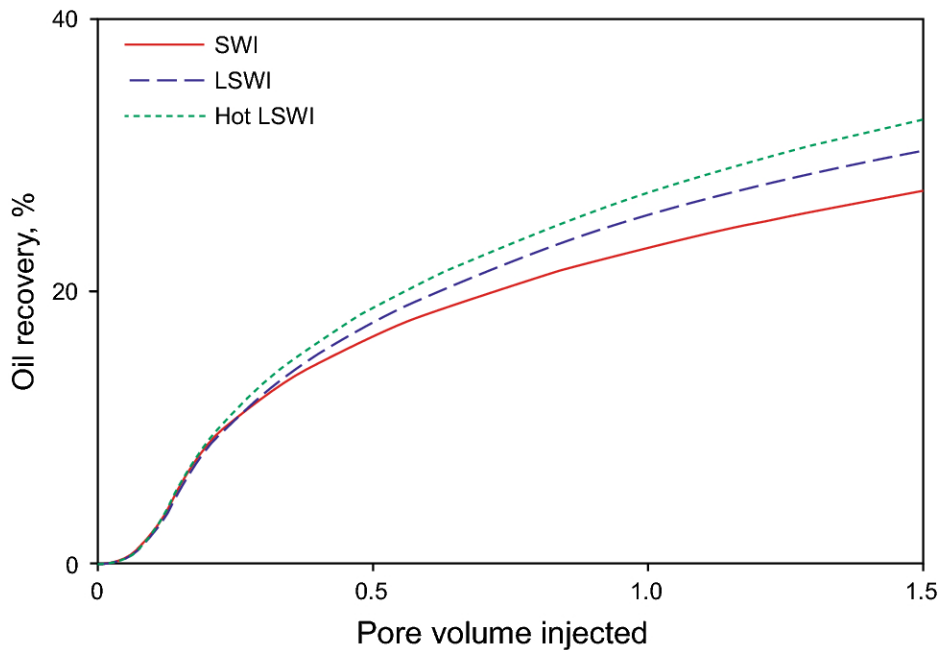


Figure 18. History of oil recovery (%) for SWI, LSWI, and hot LSWI (Lee and Lee, 2018).

## **1.7. Problem Statement**

LSW and hot water injection techniques are proven effective methods to displace oil from porous media. However, both methods have their limitations and potential risks. The combination of LSW and thermal approach in a hybrid LSHW injection can provide a considerable incremental oil recovery during secondary and tertiary oil recovery stages by the synergistic effects of the hybrid method. For example, the temperature increase of the injected problem solves the problem of unfavorable mobility ratio and poor volumetric sweep efficiency during LSW flooding, while PDI and optimal dilution of LSW help change wettability to a more water-wet state, which also leads to the additional oil displacement.

Due to contradictory results of laboratory and numerical studies, the main driving mechanisms of LSW for sandstone and carbonate reservoirs are still not well understood. Moreover, experimental studies on LSHW injection for carbonate reservoirs and heavy oil cases are limited. The performances of LSHW flooding were experimentally studied in light and heavy oil sandstone reservoirs and only in light oil carbonate reservoirs. There are also a few numerical simulation studies of LSHW injection in heavy oil carbonate reservoirs. However, mostly one-dimension homogeneous reservoirs were used for the flooding simulation, which can potentially show the performance of LSHW but not investigate the impact of driving mechanisms for different LSW brines at various temperature conditions. It is essential to mention that the performance of LSHW injection in heavy oil carbonates has not been experimentally investigated yet.

## **1.8. Research objectives**

This study aimed to show the performance of LSW injection in heavy oil carbonates and experimentally analyze the synergistic effects of thermal EOR and LSW flooding in a hybrid LSHW injection approach. The main objectives of the study are as follows:

1. To estimate the optimal dilution of LSW by contact angle measurements and compare the effect of dilution on the wettability alteration under different temperatures;
2. To investigate the effect of PDI and their various ionic combinations in different brines on the wettability alteration by contact angle measurements under different temperatures;

3. Design optimal injection scheme and core flooding stages for LSW and hybrid LSHW methods;
4. To carry out oil displacement experiments with different injected brines of LSHW following LSW flooding and direct injection of LSHW to compare the methods for higher incremental oil recovery and observe the effect of different PDI on oil displacement;
5. To perform ion chromatography analyses from contact angle measurements and core flooding experiments to track the change of PDI concentration and, hence, investigate the performance of main driving mechanisms of the LSHW method.

### **1.9. Thesis structure**

The thesis structure was designed to systematically cover all parts of the research and provide the work results. The chapters of the thesis are as follows:

#### 1. Introduction

This chapter provides a detailed literature review about EOR methods, namely LSW, hot water, and hybrid LSHW flooding methods, defines these methods' problems and limitations, and identifies the research objectives based on the problem statement.

#### 2. Methodology

Materials, equipment, and design of the contact angle measurements, core flooding experiments, and oil chromatography analyses were discussed in this chapter.

#### 3. Results and Discussion

This chapter describes the effect of dilution and PDI on wettability alteration by contact angle measurements, provides the evaluation of LSW and hybrid LSHW injection, compares incremental oil recovery of different injected brines at various temperatures, and evaluates the effect of LSHW driving mechanisms by ion-tracking by oil chromatography analysis.

#### 4. Conclusions and Recommendations

The chapter describes the main findings answering the research objectives and recommendations based on the obtained results.

#### 5. References

All sources used are listed at the end of the dissertation in alphabetical order.

## 2. METHODOLOGY

A consistent methodology was formulated to answer all research objectives, including preparation of materials, design of contact angle measurements, core flooding experiments, and ion chromatography analyses. Carbonate rocks with heavy oil of more than 900 cp and average permeability of 30 mD were used to compare the performance of standalone EOR methods and hybrid LSWI/thermal EOR. Different surface studies, such as contact angle measurements and ion chromatography analyses, were conducted at different temperatures (20 and 80°C) to study the effect of temperature on driving mechanisms. Several core flooding scenarios and effluent analyses were designed and conducted to propose leading mechanisms of LSHW injection and evaluate the efficiency of dilution and alteration of ion concentration at different temperatures.

### 2.1. Materials

#### 2.1.1. Crude oil

##### *Physical properties*

Highly viscous and resinous crude oil from a Western Kazakhstan field was used in the experiments. The average content of asphalt-resin substances in crude oil is 18.0 to 34.6%, and the sulfur content is 0.9 to 2.4% (Bealessio et al., 2020). Table 1 and Figure 19 show the physical properties of the oil measured by Anton Paar's viscometer SVM 3001 at different temperatures, from 20 to 70°C.

Table 1. Measured oil properties at different temperatures

Cell Temperature	Dynamic Viscosity	Kinematic Viscosity	Density
°C	cP	cP	g/cm <sup>3</sup>
20	967.36	1030.6	0.939
30	442.49	474.8	0.932
40	225.97	244.1	0.926
50	125.58	136.6	0.919
60	75.29	82.5	0.912
70	47.89	52.9	0.905

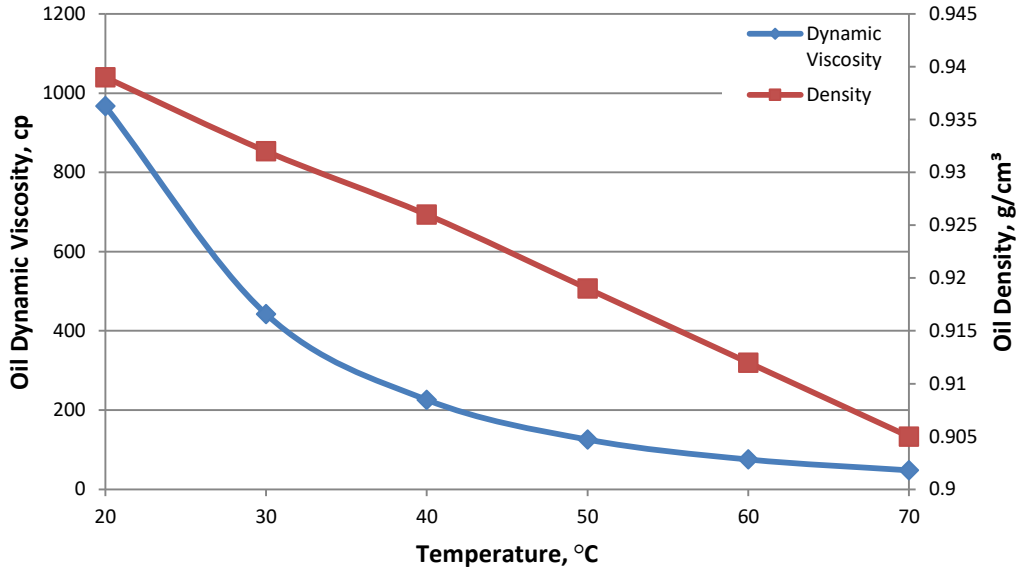


Figure 19. Temperature dependency of crude oil dynamic viscosity and density

### ***Determination of Acid Number***

Acid Number (AN) of crude oil is the crucial parameter for many EOR methods, especially LSW flooding, indicating the number of naphthenic acids (RCOOH) and bond between the oil's acidic components and the rock surface. The higher the AN, the more oil-wet surface will be. Thus, a high AN value is essential for LSW/LSHW flooding in carbonates because this EOR method does not affect oil displacement in water-wet carbonates. However, up to now, there is no exact value of AN for LSW screening. This parameter can be manually determined by the amount of potassium hydroxide (KOH) in milligrams required to neutralize the acids in one gram of oil (Sagbana et al., 2022).

AN of crude oil was manually estimated by the color-indicator titration method (ASTM D974-21). 0.1 mol of KOH diluted in isopropanol( $C_3H_8O$ ) was used as a titrant. 500 ml of toluene ( $C_7H_8$ ) was mixed with 5 ml of distilled water and 495 ml of isopropanol to prepare the solvent. Two color-indicator titrations were carried out. Firstly, 0.05 ml of phenolphthalein ( $C_{20}H_{14}O_4$ ) was added to 100 ml of solvent. After 30 seconds of stirring, the titrant was added drop by drop with a 1 ml syringe until the solution turned pink in color, and then the volume of titrant ( $V_{blank}$ ) used was noted. Secondly, the same procedure but with a crude sample was carried out by mixing 1g of the crude oil with 100 ml of solvent until complete dissolution. Again, 0.05 ml of phenolphthalein was added to the brown mixture of solvent with dissolved crude oil.

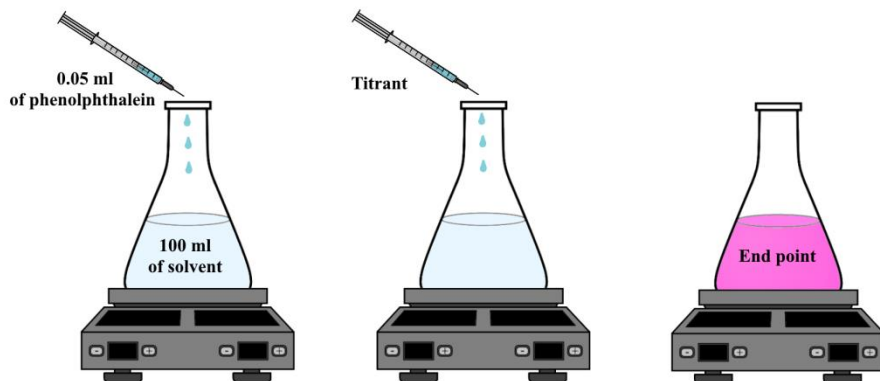
Titrant was used drop by drop after 30 seconds of stirring until the brown color became a noticeable pink tint. The new volume of titrant ( $V_{oil}$ ) used was noted again to calculate the AN value by Equation (16):

$$AN (mg KOH/g) = \frac{(V_{sample} - V_{blank}) \times C}{m_{sample}} \times 56.1 \quad (16)$$

Where  $C$  is the KOH concentration in titrant,  $V_{blank}$  is the volume of titrant for the first measurement without oil,  $V_{sample}$  is the volume of titrant for the second measurement without oil,  $m_{sample}$  is the weight of the sample (g).



### First color-indicator titration measurement



### Second color-indicator titration measurement

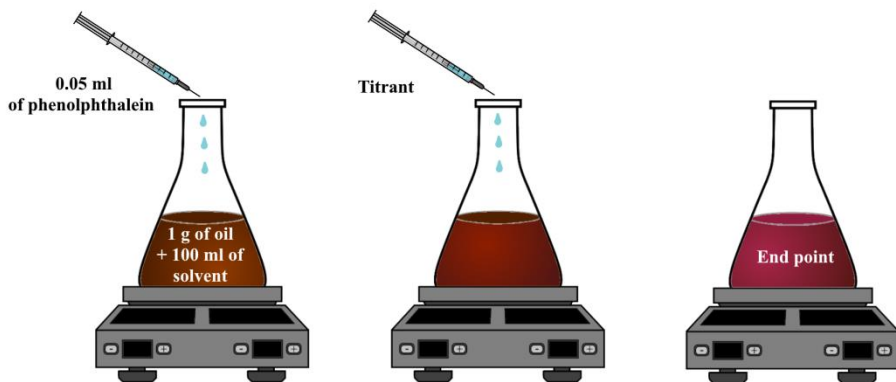


Figure 20. The schematic procedure of color-indicator titration method

The average AN was 4.72 mg KOH/g of oil by calculating an average value of 3 measurements. This value indicates a strong bond between the oil's acidic components and carbonate surface, which results in an oil-wet state of the rock surface. Thus, this crude oil is suitable for LSW/LSHW flooding experiments.

### 2.1.2. Rock samples

Carbonate outcrops were used for all measurements and experiments. X-ray diffraction (XRD) showed that the core samples mainly consisted of calcite (99.8%  $\text{CaCO}_3$ ). Six core plugs and 14 core slices were cut from these outcrops (Figure 21). The core plugs had a diameter of 3.7 cm and lengths ranging from 6.90 to 7.35 cm. Core slices were cut from two core plugs in the form of semicircles with a width of 0.5-1.5 cm. In appearance, the core samples were a solid gray rock with slight rare crystalline inclusions.



Figure 21. Examples of core samples (left: core plug, right: core slice)

#### *Core samples properties*

After cutting from the outcrop, all core plugs were dried in the oven at  $80^{\circ}\text{C}$  for three days to evaporate any remaining liquids. Vinci HEP-P Helium Porosimeter (Figure 22) was used to determine core samples' porosity and gas permeability. After that, core plugs were saturated with formation brine by Vinci Manual Saturator (AP-007-001-1) at least for one day at a constant pressure of 1400 psi. More accurate porosity and pore volume (PV) values were calculated by the weight method as shown in Equations (17) and (18), i.e., core samples were weighed before and after the saturation. Table 2 shows manual and equipment porosity measurements of core samples, which have a 6-8 % difference. Permeability measurements by Vinci HEP-P Helium Porosimeter are shown in Table 3 to compare with values obtained by Darcy Law.

$$V_p = \frac{w_{wet} - w_{dry}}{\rho_w} \quad (17)$$

$$\varphi = \frac{V_p}{V_{total}} = \frac{V_p}{\pi r^2 L} \quad (18)$$

Where  $V_p$  is the pore volume of the core sample,  $w_{dry}$  is the weight before saturation,  $w_{wet}$  is the weight after saturation,  $\rho_w$  is the formation water density at 20°C,  $\varphi$  is the porosity,  $V_{total}$  is the total volume of the rock including pores and bulk (cylinder volume in core cases),  $r$  is the radius,  $L$  is the length of the core.

Table 2. Core samples porosity values

Core Number	Diameter, mm	Length, mm	Dry weight, g	Wet weight, g	Pore Volume (PV)	Gas Porosity, %	Actual Porosity, %
Core 1	37.0	73.0	178.53	195.78	14.72	12.22	18.77
Core 2	37.0	69.0	175.33	190.57	13.00	12.95	17.54
Core 5	37.0	75.0	189.70	206.47	14.31	12.12	17.75
Core 8	37.0	73.5	188.99	205.55	14.13	11.50	17.88
Core 9	37.0	71.5	183.11	199.84	14.28	10.30	18.58
Core 10	37.0	69.0	175.77	191.20	13.16	9.03	17.76



Figure 22. Vinci HEP-P Helium Porosimeter

The core plugs were then flooded with the formation water, followed by the oil, to recreate initial reservoir conditions and measure absolute and effective permeability by Darcy Law (Equation 19) and initial water saturation (Equation 20). The backpressure was regulated at 600 psi, and the unit confining pressure was settled at 1100-1300 psi. The pressure drop was monitored for flow rates ranging from 1.0 to 10.0 cc/min. Core plugs were then placed in the aging cells saturated with the crude oil and left in the oven at 80°C for five weeks to change the wettability from water-wet to a strong oil-wet state. After aging, all core plugs were flooded again with crude oil to measure the new relative permeability of oil-wet cores. Core slices were also saturated with crude oil using a Vinci Vacuum desiccator (Figure 23) for 2 hours and aged to change the wettability. Contact angle measurements were taken before and after the aging process to confirm the wettability alteration of all core samples. Table 3 shows initial water saturation and permeability values before and after aging.

$$k = \frac{q\mu L}{A\Delta p} \quad (19)$$

Where  $q$  is the injected liquid flow rate,  $k$  is the permeability,  $\mu$  is the dynamic viscosity of the injected liquid,  $\Delta p$  is the pressure drop,  $L$  is the length of the core, and  $A$  is the circle area of the core.



Figure 23. Vinci Vacuum desiccator

$$S_{wi} = 1 - \frac{(V_{wd} - V_{dead})}{V_p} \quad (20)$$

Where  $S_{wi}$  is the initial water saturation of the core,  $V_{wd}$  is the volume of displaced water after the oil injection, and  $V_{dead}$  is the dead volume of the equipment.

Table 3. Core samples permeability values

Core Number	Gas Permeability, mD	Absolute permeability, mD	Effective permeability before aging, mD	Effective permeability after aging, mD	Initial water Saturation, %
Core 1	52.64	21.28	19.54	10.61	27.30
Core 2	36.37	35.67	18.59	8.49	18.33
Core 5	35.13	34.19	25.01	11.86	20.19
Core 8	35.28	31.24	17.31	9.5	24.13
Core 9	29.09	29.86	21.21	11.85	14.53
Core 10	32.31	23.56	15.58	9.17	22.37

### 2.1.2. Low salinity and Engineered brines

Three different types of brines (formation water (FW), seawater (SW), and engineered water (EW)) were used in the tests and prepared by mixing appropriate amounts of required salts in distilled water using a magnetic stirrer (IKA RH Digital). Formation water with a concentration of approximately 170,000 ppm was used for core sample saturation and prepared based on the formation water concentration in the field. Prepared seawater mimicked the Caspian Seawater's average ionic concentration and was considered the original brine, with a salinity of 13,000 ppm. Low salinity water was prepared by 5-, 10-, and 20-times dilution of seawater to find the optimal dilution, which provided the most effective wettability alteration. After determining the optimal dilution, the effect of PDIs on the enhancement of wettability alteration mechanisms was analyzed. Hence, three types of engineered water were prepared:

- $2Ca*2SO_4$  - double concentration of calcium and sulfate ions;
- $2Mg*2SO_4$  - double concentration of magnesium and sulfate ions;
- $2Ca*2Mg*2SO_4$  - double concentration of calcium, magnesium, and sulfate ions.

These formulas were selected to study the effect of combinations of PDIs on the wettability alteration. Table 4 shows the ion concentration of all presented brines.

Table 4. Ionic composition of formation, sea and low salinity water

	Cations concentration, ppm				Anions concentration, ppm		Total concentration, ppm
	Na <sup>+</sup> ,	K <sup>+</sup> ,	Ca <sup>2+</sup>	Mg <sup>2+</sup>	Cl <sup>-</sup>	SO <sub>4</sub> <sup>2-</sup>	
FW	54500	0	9450	1450	105000	0	170400.00
SW	3300	155.00	360	740	5400	3050.00	13005.00
5X Dilution	660	31.00	72	148	1080	610.00	2601.00
10X Dilution	330	15.50	36	74	540	305.00	1300.00
20X Dilution	165	7.75	18	37	270	152.00	650.25
5X 2Ca*2SO <sub>4</sub>	660	31.00	144	148	1080	1220.00	3283.00
5X 2Mg*2SO <sub>4</sub>	660	31.00	72	296	1080	1220.00	3359.00
5X 2Ca*2Mg*2SO <sub>4</sub>	660	31.00	144	296	1080	1220.00	3431.00

## 2.2. Procedure of Experiments

### 2.2.1. Contact Angle Measurements

Contact angle measurements were performed to estimate the wettability of the core slices by measuring the angle formed by an oil drop at the carbonate surface. Twelve core slices were used for contact angle measurements after a four-week aging process. Figure 24 shows how the wettability condition of the rock surface can be estimated by contact angle measurements. Two other slices were put in the 10-times diluted seawater to observe the LSW active mechanisms, such as the rock dissolution at different temperatures.

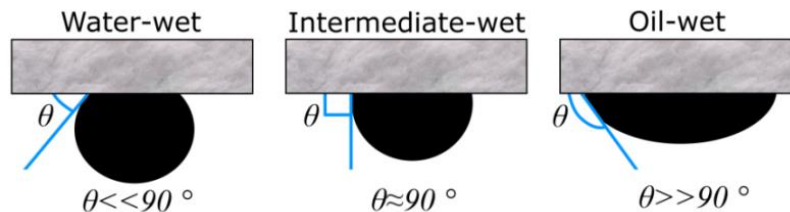


Figure 24. A schematic diagram of carbonate wettability conditions defined by the contact angle (Teklu et al., 2015)

Before aging the core slices by different engineered brines, the contact angles of the core slices were measured to check the oil-wet condition of the chalk surfaces. All contact angle measurements were performed using an OCA 15EC video-based optical contact angle measuring instrument (Figure 25). The procedure was the same for all measurements. The core slice was placed in the brine, and then one drop of oil dripped onto the surface using a special syringe. A special high-resolution camera recorded the attachment of a drop of oil, while a computer program automatically calculated the contact angle. For all core slices, measurements were repeated three times to neglect the effect of heterogeneous rock mineralogy or uneven rock surface.

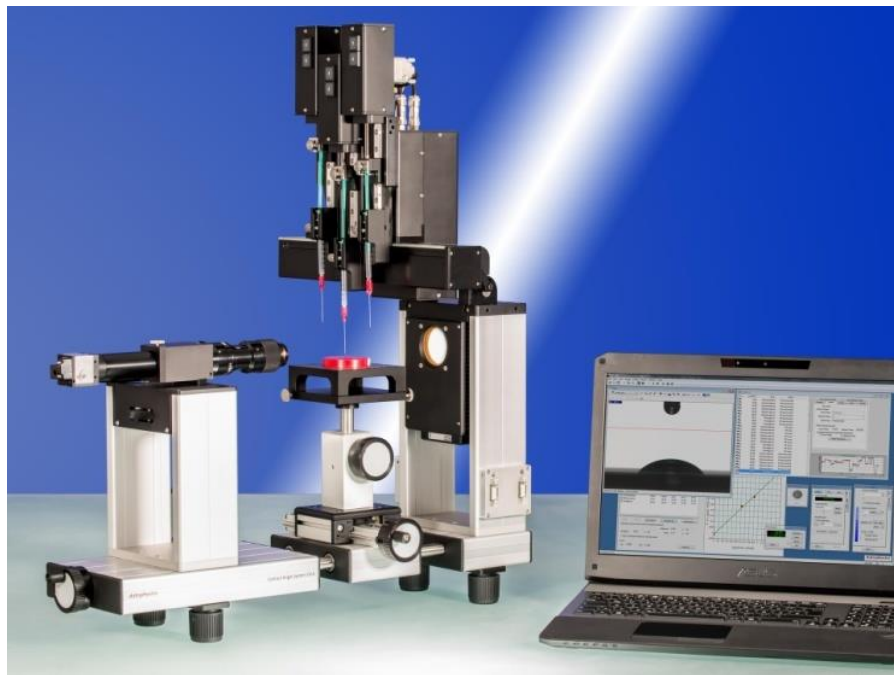


Figure 25. OCA 15EC video-based optical contact angle measuring instrument

Core slices were then aged by 5-, 10-, and 20-times diluted seawater at room temperature and in an oven at 80°C, to investigate the effect of temperature on wettability alteration. After 168 hours, the contact angle was measured to select the optimal dilution of seawater. After identifying the optimal dilution, the effect of PDIs on wettability alteration at 20°C and 80°C was also investigated by the contact angle measurement after 168 hours of aging in different designed engineered brines:  $2Ca \cdot 2SO_4$ ,  $2Mg \cdot 2SO_4$ , and  $2Ca \cdot 2Mg \cdot 2SO_4$ .

### 2.2.2. Core flooding experiments

Before the start of core flooding experiments, all core plugs were cleaned, saturated with the formation brine, then flooded again with the formation brine and oil to measure core physical properties, aged for 5 weeks at 80°C, and then flooded again with crude oil to make sure that no additional formation water is produced and core samples are ready for experiments.

The core flooding system is schematically shown in Figure 26. The system consists of two-piston accumulators (one was always filled with crude oil, and another with injected brine), pump regulating the flow rates, a core holder, a Hydraulic Hand Pump injecting the confining oil into the core holder, a back pressure regulator (BPR). Pressure changes of the system were noted manually.

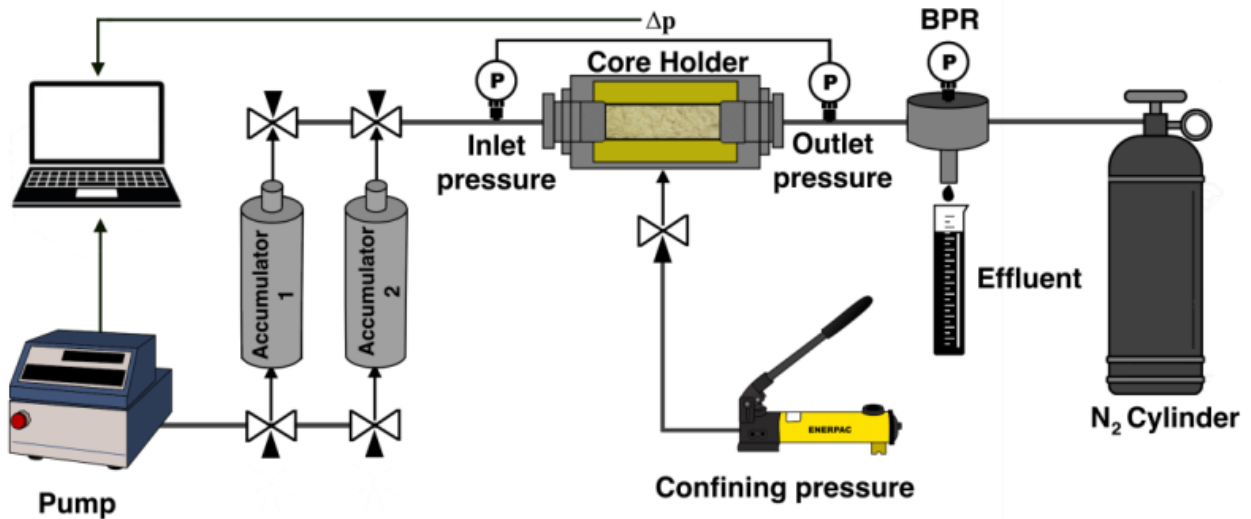


Figure 26. Core flooding system scheme

Six core flooding experiments were performed with LSW and three types of EW on heavy oil carbonate cores at different temperatures (20, 50, and 70°C) to investigate the effect of temperature on LSW and EW and the performance of LSHW flooding. Four core flooding experiments consisted of four stages: (1) SW injection, (2) LSW/EW injection, (3) hot LSW/EW injection at 50°C, and (4) extra hot LSW/EW injection at 70°C. The remaining two core floods included three stages: (1) SW injection, (2) hot SW/EW injection at 50°C, and (3) extra hot SW/EW injection at 70°C. These experiments were designed to answer the following questions:

- a) How effective is LSW injection in recovery of incremental heavy oil in tight carbonates?
- b) Is there synergy between thermal and LSW EOR methods for heavy oil in carbonates?
- c) Which mechanisms are dominant during oil recovery by the hybrid LSHW EOR?

Table 5 shows the whole design of all core flooding experiments. The first stage of the SW injection was performed with various injection rates (0.1, 0.3, 0.6, 0.9, 1.5, 2.0, and 5.0 cc/min) and a total of 19 pore volumes (PV). After SW injection, four experiments proceeded with LSW/EW injection, with injection rates of 0.1, 0.5, 1.0, 1.5, 2.0, and 5.0 cc/min and a total injection amount of 8 PV. After that, a core holder and accumulator with LSW/EW were heated for 2 hours to 50°C, and oil displacement continued at injection rates of 1, 2, and 5cc/min and a total of 10 PV injected. When no more oil was produced, the temperature in the water accumulator was increased to 70°C, and LSW/EW injection started again with the same injection rates as at 50°C, ending when another 11 PV were injected. Another two core flooding experiments were undertaken, using the same procedure with the same injection rates, even though there was no LSW/EW injection at room temperature. The injection rate was only changed when no more oil was produced, and the pressure gradient was stable for at least 2 PV. The backpressure was regulated at 550-650 psi, and the unit confining pressure was settled at 1100-1300 psi. When the accumulator and core holder were heated, the unit confining pressure dropped to 500-600 and needed additional lift to 1100-1300 psi. The recovery factor and residual oil saturation of core flooding were manually calculated by noting the oil produced in every 10 ml graduated tube after oil and water separation.

Table 5. Design of core flooding experiments

Core Number	Number of Stages	Subsequence of Injected Brines	Temperature of Injected Brine	Injection Rates	Number of PV injected	
Core 1	3	1	SW	20°C	0.1, 0.3, 0.6, 0.9, 1.5, 2.0, and 5.0 cc/min	19
		2	Hot 5D SW	50°C	1.0, 2.0, and 5.0 cc/min	10.5
		3	Extra Hot 5D SW	70°C	1.0, 2.0, and 5.0 cc/min	6.5
Core 5	4	1	SW	20°C	0.1, 0.3, 0.6, 0.9, 1.5, 2.0, and 5.0 cc/min	19

		2	5D SW	20°C	0.1, 0.5, 1.0, 1.5, 2.0, and 5.0 cc/min	8
		3	Hot 5D SW	50°C	1.0, 2.0, and 5.0 cc/min	10
		4	Extra Hot 5D SW	70°C	1.0, 2.0, and 5.0 cc/min	11
Core 10	4	1	SW	20°C	0.1, 0.3, 0.6, 0.9, 1.5, 2.0, and 5.0 cc/min	19
		2	5D 2Ca*2SO <sub>4</sub>	20°C	0.1, 0.5, 1.0, 1.5, 2.0, and 5.0 cc/min	8
		3	Hot 5D 2Ca*2SO <sub>4</sub>	50°C	1.0, 2.0, and 5.0 cc/min	10
		4	Extra Hot 5D 2Ca*2SO <sub>4</sub>	70°C	1.0, 2.0, and 5.0 cc/min	11
Core 2	4	1	SW	20°C	0.1, 0.3, 0.6, 0.9, 1.5, 2.0, and 5.0 cc/min	19
		2	5D 2Mg*2SO <sub>4</sub>	20°C	0.1, 0.5, 1.0, 1.5, 2.0, and 5.0 cc/min	8
		3	Hot 5D 2Mg*2SO <sub>4</sub>	50°C	1.0, 2.0, and 5.0 cc/min	10
		4	Extra Hot 5D 2Mg*2SO <sub>4</sub>	70°C	1.0, 2.0, and 5.0 cc/min	11
Core 8	4	1	SW	20°C	0.1, 0.3, 0.6, 0.9, 1.5, 2.0, and 5.0 cc/min	19
		2	5D 2Ca*2Mg*2SO <sub>4</sub>	20°C	0.1, 0.5, 1.0, 1.5, 2.0, and 5.0 cc/min	8
		3	Hot 5D 2Ca*2Mg*2SO <sub>4</sub>	50°C	1.0, 2.0, and 5.0 cc/min	10
		4	Extra Hot 5D 2Ca*2Mg*2SO <sub>4</sub>	70°C	1.0, 2.0, and 5.0 cc/min	11
Core 9	3	1	SW	20°C	0.1, 0.3, 0.6, 0.9, 1.5, 2.0, and 5.0 cc/min	19
		2	Hot 5D 2Ca*2Mg*2SO <sub>4</sub>	50°C	1.0, 2.0, and 5.0 cc/min	10.5
		3	Extra Hot 5D 2Ca*2Mg*2SO <sub>4</sub>	70°C	1.0, 2.0, and 5.0 cc/min	6.5

### 2.2.3. Ion chromatography analyses

Water samples were collected during contact angle and core flooding experiments. All ion chromatography analyses were carried out using a Dionex ICS-6000 high-level modular ion chromatography system (Figure 27). Only  $\text{Ca}^{2+}$ ,  $\text{Mg}^{2+}$ , and  $\text{SO}_4^{2-}$  ions were traced by Dionex ICS-6000. Water samples were multiply diluted in distilled water until all ions of one sample were not supposedly in the range of 0-100 ppm.

To observe the effect of LSW/oil/rock interactions on the rock dissolution, multi-ion exchange, and detachment of oil from the rock surface, clean and oil-coated core slices were aged in 10-times diluted SW samples at high and low temperatures in beakers. Water samples were collected from the beakers at the start of the experiments, and then 24, 72, 120, and 168 hours thereafter, to track the change of PDI concentration by an ion chromatography approach. By this analysis, the main mechanisms of rock wettability alteration were observed and studied.

During core flooding, effluent samples were collected and analyzed. Water samples were taken at the start, at the middle, and at the end of each injection stage to monitor PDI alteration in the injected LSW/EW solutions at different temperatures and propose the primary mechanism of LSW injection and synergistic effects of the LSHW hybrid EOR approach.



Figure 27. Dionex ICS-6000 high-level modular ion chromatography system

### **3. RESULTS AND DISCUSSION**

This chapter presents the results that were designed in the methodology part. The results obtained can be divided into three parts:

1. The effect of SW dilution and PDI tuning on wettability alteration at different temperatures;
2. Oil displacement analysis by standalone EOR methods (LSW and hot water flooding) and by hybrid LSHW flooding;
3. Tracking of multi-ion exchange during contact angle tests and core flooding experiments.

The main objective of the first part was to identify the optimal dilution of seawater, i.e., LSW, and investigate the effect of PDI tuning on wettability alteration by contact angle measurements over 168 hours at 20°C and 80°C. Optimal dilution of SW and brines with various PDI concentrations, which showed the best result of wettability alteration, were selected as injected fluids for core flood experiments. Heavy oil displacement experiments were conducted with various injected fluids to evaluate the performance of LSW and hybrid LSHW at different temperatures and, hence, investigate the synergistic effects of the hybrid approach and estimate the influence of various PDI on incremental oil recovery. Ion chromatography analyses were conducted to track the change of PDI concentration during core flooding experiments and the aging of core slices for contact angle tests. Obtained ion tracking results were used to determine the main driving mechanisms of LSW injection and the change of their influence at different temperatures.

#### **3.1. Contact Angle Measurements**

##### **3.1.1. Effect of seawater dilution**

The main objective of this part was to determine the most significant wettability alteration of the carbonate rock surface in different diluted SW brines and observe the effect of temperature on wettability alteration in diluted SW. According to Nasralla et al. (2018), there is an optimal SW dilution level, beyond which the oil recovery factor no longer increases and starts to decrease. An optimal degree of dilution will also vary depending on the conditions of the experiment (physical and chemical properties of the rock and oil). 5, 10, and 20-times diluted

(5D, 10D, and 20D) SW were prepared to measure the highest wettability alteration level in our study (Figure 28). Aging was conducted for 168 hours (8 days) at 20°C and 80°C to investigate the effect of temperature and dilution on the wettability alteration.



Figure 28. Prepared 5D, 10D, and 20D SW brines.

Contact angles measurements were performed before aging and after 168 hours. Initial contact angles showed that the wettability of all core slices had a strong oil-wet state from 145° to 160°, which is essential for experiments because the performance of LSW/LSHW is not effective in water-wet carbonate rocks. Core slices had a different external change of the rock surface at 20°C and 80°C over time. In all brines, core slices had tiny liquid drops and "spots" on their surface only at the higher temperature, which indicates the higher release of oil carboxylic groups from the carbonate surface. Figure 29 shows the effect of temperature on the rock surface change on different brines; photos were taken 120 hours after the start of aging. It can be noticed that the higher the dilution, the fewer bubbles and "spots" were observed.

	20 C	80 C
5D		
10D		
20D		

Figure 29. Effect of temperature on the rock surface during aging in diluted brines

20D SW showed the lowest contact angle difference after 168 hours, even at the higher temperature, due to lack of PDI concentration. Wettability alteration was still observed, but a change of contact angle was only  $9.82^\circ$  and  $10.63^\circ$  for  $20^\circ\text{C}$  and  $80^\circ\text{C}$ , respectively. Thus, it can be concluded that a brine concentration of 650 ppm was not enough for the considerable wettability alteration. Furthermore, according to the results, the effect of temperature is negligible when the concentration of the diluted SW is too low. 10D SW showed better contact angle difference results than the previous case. Contact angle changed by  $7.70^\circ$  at  $20^\circ\text{C}$  and  $15.37^\circ$  at  $80^\circ\text{C}$ . The effect of temperature was more significant in 10D SW because the contact angle changed twice as much at the higher temperature.

5D SW was determined as the optimal dilution with the highest wettability alteration by  $13.77^\circ$  and  $17.43^\circ$  at  $20^\circ\text{C}$  and  $80^\circ\text{C}$ , respectively (Figure 30). In all cases, wettability altered from a strong oil-wet state ( $145\text{-}160^\circ$ ) to a moderate oil-wet ( $135\text{-}140^\circ$ ) condition in 168 hours, proving the effect of LSW on wettability alteration. The wettability alteration was higher at  $80^\circ\text{C}$  than at room temperature in all diluted brines, proving that LSW mechanisms are more active at higher temperatures. Figure 31 shows the results of contact angle change by aging with different diluted SW.

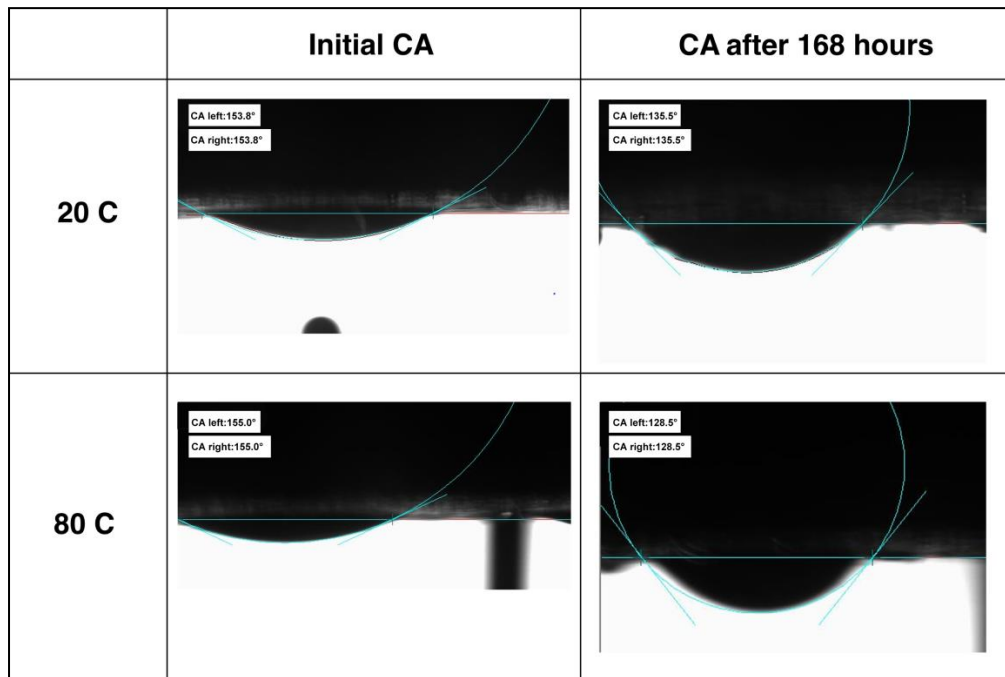


Figure 30. Change of CA in 5D SW after 168 hours SW at  $20^\circ\text{C}$  and  $80^\circ\text{C}$

Table 6. Results of contact angle measurements with diluted brines

	Initial contact angle				Contact angle after 168 hours				Difference
	# 1	#2	#3	Final	#1	#2	#3	Final	
<b>5D at 20°C</b>	153.8	150.8	155.0	153.20	142.7	140.1	135.5	139.43	13.77
<b>5D at 80°C</b>	160.2	155.0	150.6	155.27	140.4	128.5	144.6	137.83	17.43
<b>10D at 20°C</b>	145.3	150.1	143.6	146.33	137.2	137.9	140.8	138.63	7.70
<b>10D at 80°C</b>	154.7	153.3	152.4	153.47	139.0	142.0	133.3	138.10	15.37
<b>20D at 20°C</b>	155.0	152.7	152.7	153.47	142.4	147.5	141.1	143.65	9.82
<b>20D at 80°C</b>	151.1	146.0	152.6	149.9	137	140.4	140.4	139.27	10.63

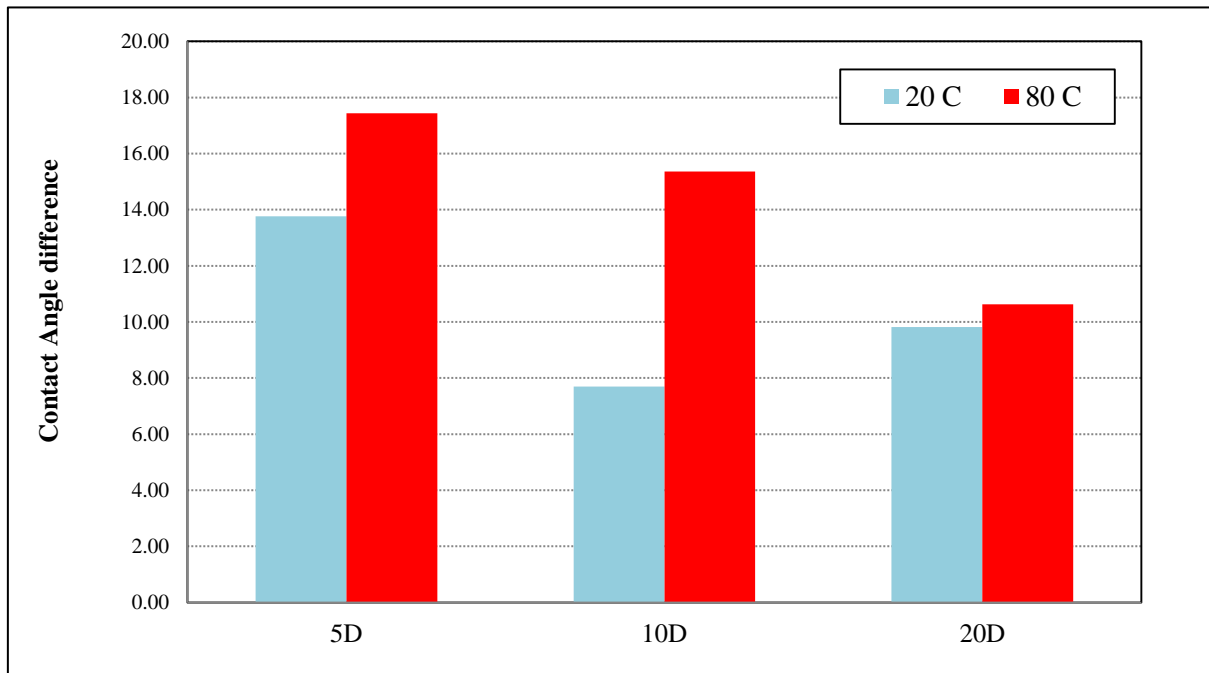


Figure 31. Effect of SW dilution on contact angle at 20°C and 80°C

### 3.1.2. Effect of PDIs

One of proposed mechanisms of wettability alteration of carbonate surfaces from oil-wet to more water-wet is the multi-ion exchange, i.e. an adsorption of PDIs onto the rock surface. A significant concentration of  $\text{SO}_4^{2-}$  ions, presented in SW, adsorb on the rock surface, which leads to the reduction of surface charge density. After that,  $\text{Ca}^{2+}$  and  $\text{SO}_4^{2-}$  can also co-adsorb onto the surface and considerably reduce electrostatic repulsive force. Organic components of crude oil

can be released from the surface after its reaction with  $\text{Ca}^{2+}$  ions, which finally leads to wettability alteration (Lee & Lee, 2019).

After determining that 5-times dilution of SW is the optimal dilution state, three different combinations of PDIs are spiked in the EW solutions: 5D  $2\text{Ca} \cdot 2\text{SO}_4$ , 5D  $2\text{Mg} \cdot 2\text{SO}_4$ , and 5D  $2\text{Ca} \cdot 2\text{Mg} \cdot 2\text{SO}_4$ . 2Ca, 2Mg, and 2Ca\*2Mg combinations were prepared to determine the effect of  $\text{Mg}^{2+}$  and  $\text{Ca}^{2+}$  ions and combinations of them. The double concentration of  $\text{SO}_4^{2-}$  was performed to create the excess sulfate concentration, which leads to the acceleration of adsorption of cations on the rock surface. Similar to diluted brines, aging in 5D  $2\text{Ca} \cdot 2\text{SO}_4$ , 5D  $2\text{Mg} \cdot 2\text{SO}_4$ , and 5D  $2\text{Ca} \cdot 2\text{Mg} \cdot 2\text{SO}_4$  at higher temperatures resulted in the appearance of many bubbles and spots on the rock surface (Figure 32). However, different PDI concentrations showed a similar external change of the rock surface at  $20^\circ\text{C}$  and  $80^\circ\text{C}$ .

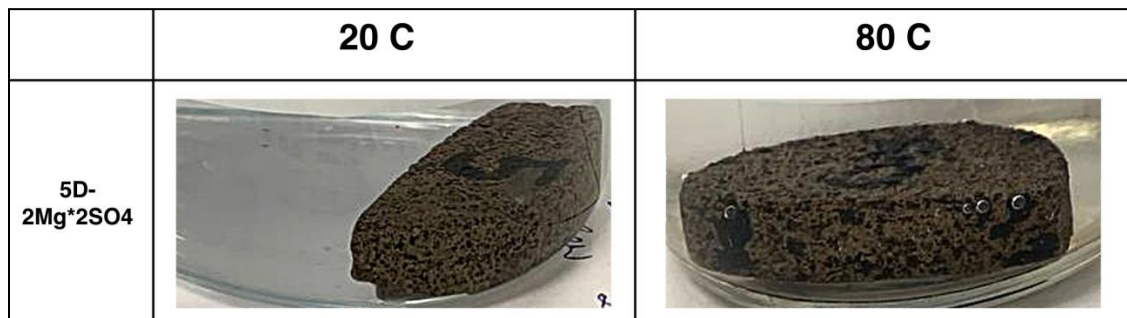


Figure 32. Effect of temperature on the rock surface during aging in brines with PDI tuning

Figure 34 shows the contact angle difference for various PDI solutions at  $20^\circ\text{C}$  and  $80^\circ\text{C}$ . The contact angle changed by  $5\text{-}15^\circ$  from a strong oil-wet state ( $145\text{-}150^\circ$ ) to a moderate oil-wet condition ( $135\text{-}140^\circ$ ) in 168 hours.  $\text{Ca}^{2+}$  ions were the most active beyond all combinations at room temperature and the least effective at  $80^\circ\text{C}$ . It could be explained by the fact that  $\text{Mg}^{2+}$  ions behave more actively at higher temperatures and can replace  $\text{Ca}^{2+}$  ions. However,  $\text{Mg}^{2+}$  ions showed average results of contact angle difference for both temperatures. The difference between the results for  $\text{Mg}^{2+}$  at  $20^\circ\text{C}$  and  $80^\circ\text{C}$  was only 2.5 degrees, and so, at this stage, it was impossible to prove that  $\text{Mg}^{2+}$  ions are more active at higher temperatures (Zhang and Austad, 2006). However, the combination of double concentration of all three PDIs showed interesting results with the lowest contact angle change at  $20^\circ\text{C}$  and the highest values at  $80^\circ\text{C}$  (Figure 33). Thus, it was proposed that  $\text{Mg}^{2+}$  ions become more active, especially at higher temperatures, with the excess of  $\text{Ca}^{2+}$  and  $\text{SO}_4^{2-}$  ions. Our results are similar to other findings in the literature

(Austad et al., 2005; Zhang et al., 2007; Chandrasekhar and Mohanty, 2013). All brines with PDI tuning showed slightly inconsistent results, thus, it was decided to keep all these solutions for core flooding experiments.

Table 7. Results of contact angle measurements with different PDI concentration

	Initial CA				8 days after				Difference
	# 1	#2	#3	Final	#1	#2	#3	Final	
<b>2Ca at 20°C</b>	153.9	155.3	149.1	152.77	143.9	135.4	133.3	137.53	15.23
<b>2Ca at 80°C</b>	151.2	151.1	147.1	149.8	141.9	147.6	143.4	144.30	5.50
<b>2Mg at 20°C</b>	151.6	147.5	148.3	149.13	136.1	141.4	135.2	137.57	11.57
<b>2Mg at 80°C</b>	149.2	149.0	147.4	148.53	137.1	140.1	141.6	139.60	8.93
<b>2Ca*2Mg at 20°C</b>	150.4	150.3	151.1	150.60	141.4	141.9	138.8	140.70	9.90
<b>2Ca*2Mg at 80°C</b>	148.6	150.9	151.9	150.47	135.2	136.55	135.2	135.65	14.82

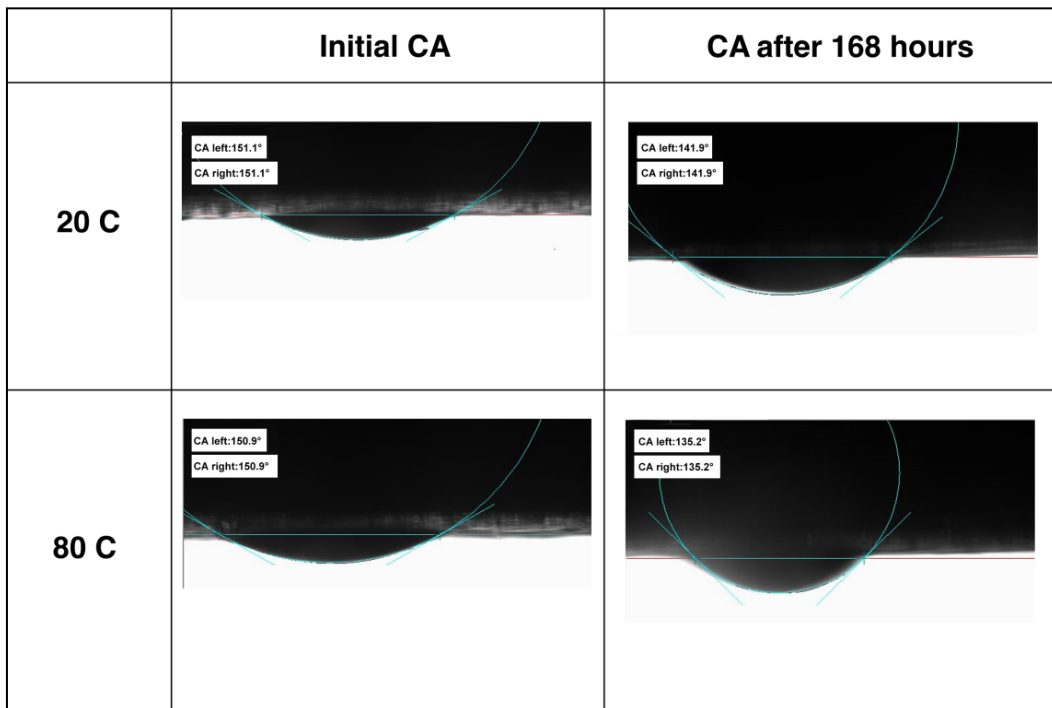


Figure 33. Change of CA in 5D 2Ca\*2Mg\*2SO<sub>4</sub> after 168 hours SW at 20°C and 80°C

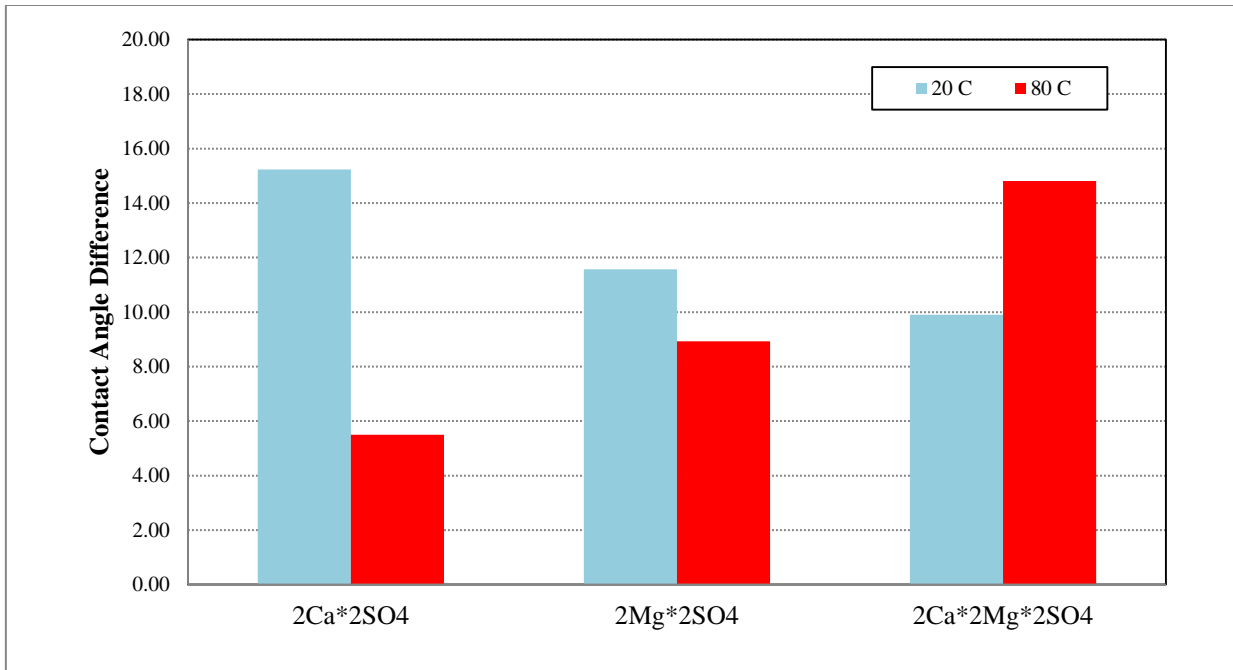


Figure 34. Effect of PDIs on contact angle at 20°C and 80°C

### 3.2. Core Flooding Experiments

Six coreflooding experiments were carried out to study the standalone LSW/hot water flooding and synergistic effects of hybrid LSHW injection at 20°C, 50°C, and 70°C, under normal, hot, and extra hot LSW flooding conditions:

- Experiment 1: SW → Hot SW → Extra Hot SW;
- Experiment 2: SW → 5D SW → Hot 5D SW → Extra Hot 5D SW;
- Experiment 3: SW → 5D 2Mg\*2SO<sub>4</sub> → Hot 5D 2Mg\*2SO<sub>4</sub> → Extra Hot 5D 2Mg\*2SO<sub>4</sub>;
- Experiment 4: SW → 5D 2Ca\*2SO<sub>4</sub> → Hot 5D 2Ca\*2SO<sub>4</sub> → Extra Hot 5D 2Ca\*2SO<sub>4</sub>;
- Experiment 5: SW → 5D 2Ca\*2Mg\*2SO<sub>4</sub> → Hot 5D 2Ca\*2Mg\*2SO<sub>4</sub> → Extra Hot 5D 2Ca\*2Mg\*2SO<sub>4</sub>;
- Experiment 6: SW → Hot 5D 2Ca\*2Mg\*2SO<sub>4</sub> → Extra Hot 5D 2Ca\*2Mg\*2SO<sub>4</sub>.

Since brines were injected at various flow rates from 0.1 to 5 cc/min, displaced oil and water needed at least 1 day for full separation. The recovery factor was calculated for every stage of all experiments by the amount of displaced oil in every tube (Figure 35) by the following formula:

$$RF = \frac{\text{Volume of displaced oil}}{\text{Total PV of oil in the core}} * 100\% \quad (21)$$

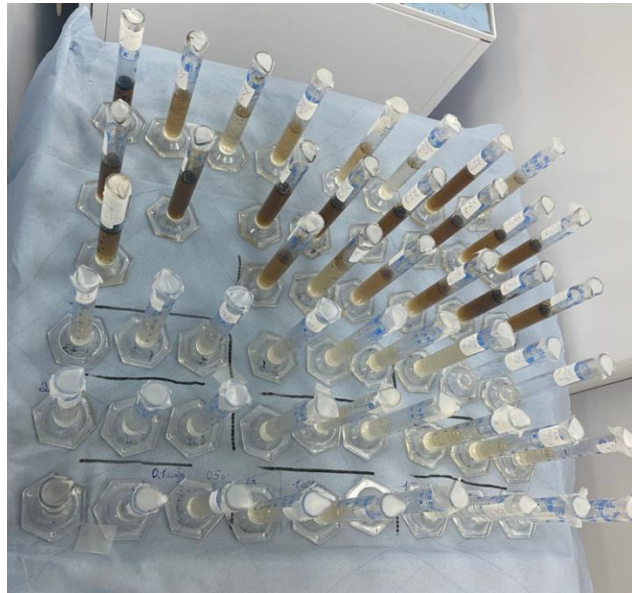


Figure 35. Tubes with effluent from core flooding before separation

Since the amount of displaced oil in tubes was recorded visually, there was a possibility of 2-4% error of the recovery factor. Every tube contained 4 to 7 ml of effluent, which was further used for ion chromatography analysis.

### 3.2.1. Experiment 1: SW → Hot SW → Extra Hot SW

As the base case, conventional hot water flooding was conducted to measure the oil recovery by a thermal EOR approach. The main objective of this core flooding was to evaluate the effect of the temperature increase on heavy oil displacement. Table 8 shows the characteristics of Core 1, which was used for the first experiment. Core flooding started with the injection of Caspian seawater at 0.1 cc/min. This low initial flow rate was chosen due to the high viscosity of the crude oil. Every time pressure drop stabilized and production of oil had decreased significantly, the flow rate was increased from 0.1 to 0.3 cc/min, then from 0.3 to 0.6 cc/min, and so on, until the flow rate reached 1.5 cc/min. After that, the flow rate was increased only after no oil was produced and pressure drop was stable for a significant period, at least 30 min of injection. The core flooding was also performed at 2.0 and 5.0 cc/min to minimize the possible capillary end effect. This procedure was the same for all further experiments. Injection of 19 PV of SW at 20°C resulted in the oil recovery of 46.78 OOIP.

Table 8. Characteristics of the core 1

	Diameter, mm	Length, mm	Pore Volume	Porosity, %	Absolute permeability, mD	Effective permeability after aging, mD	Initial water saturation, %	Residual oil saturation, %
<b>Core 1</b>	37.0	73.0	14.72	18.76	21.28	10.61	27.30	22.22

At the second stage of the first experiment, the core holder and accumulator with seawater were heated to 50°C for 2 hours. Since almost half of the oil was displaced from the core in the previous stage at 20°C and heating caused a considerable pressure decrease in the confining pressure, the injection of hot water started at 1.0 cc/min and continued at 2.0 and 5.0 cc/min. Thus, injected 10.5 PV of hot seawater resulted in additional oil recovery of 18.74% OOIP (or 35.21% of the remaining oil in the core).

Finally, the accumulator with seawater was heated to 70°C to perform the extra hot water injection, while the core holder was still maintained at 50°C to save the reservoir conditions. The design of injection was completely similar to the previous hot case, apart from the fact that a total of 6.5 PV were injected. Injection of hot seawater at 70°C resulted in incremental oil recovery of 3.91% OOIP compared to injection at 50°C or 11.36% of the remaining oil in the core.

Figure36 and Table 9 show the observed results. The application of thermal EOR showed a total incremental oil recovery of 22.65% OOIP, which can be considered as a good result for a core-scale experiment. An increase in temperature led to the considerable viscosity reduction from 967.36 cp to 125.58cp at 50°C and to 47.89 cp at 70°C. Since seawater has a concentration of 13.000 ppm, the main mechanism of this water flooding was the reduction in viscosity due to the higher temperature.

Table 9. Oil recovery factors of Experiment 1: SW (20°C) → Hot SW (50°C) → Extra Hot SW (70°C)

Test	Recovery Factor (RF)	Seawater 20°C	Hot SW 50°C	Extra Hot SW 70°C
<b>Experiment 1</b>	RF (% OOIP)	46.78	65.52	69.43
	Additional RF	-	<b>18.74</b>	<b>3.91</b>
	RF of the remaining oil (%)	46.78	35.21	11.36
	Total RF by EOR			<b>22.65</b>

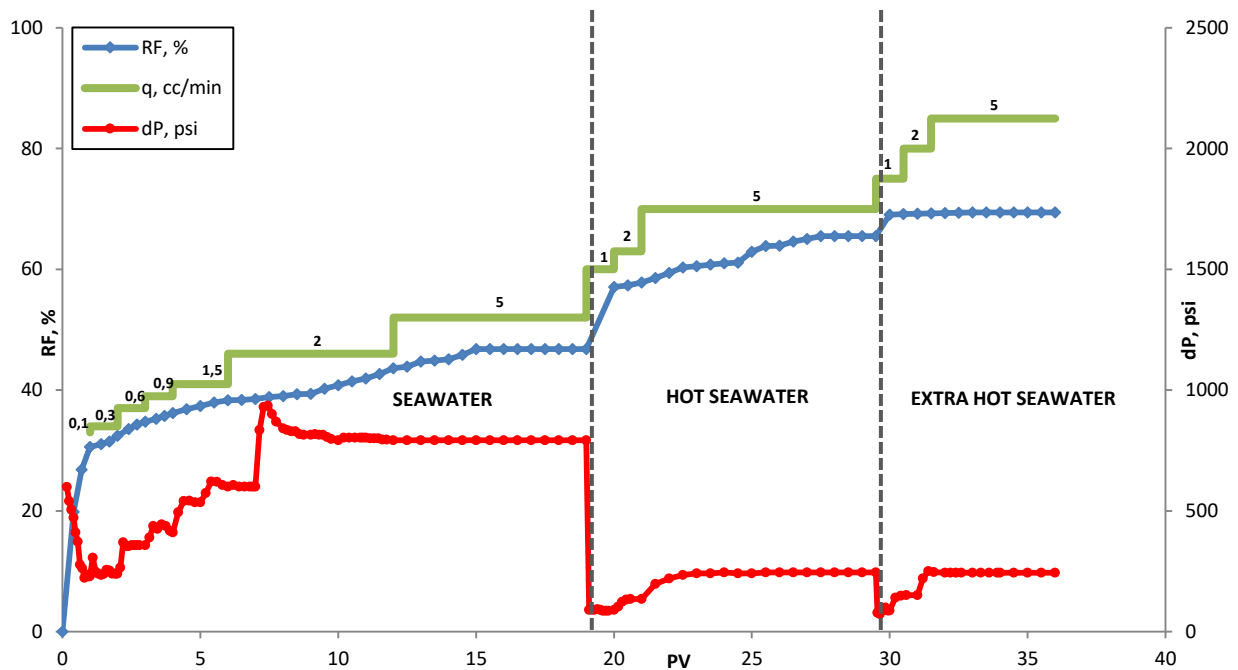


Figure 36. Oil recovery diagram of Experiment 1: SW (20°C) → Hot SW (50°C) → Extra Hot SW (70°C)

### 3.2.2. Experiment 2: SW → 5D SW → Hot 5D SW → Extra Hot 5D SW

The second experiment consisted of four stages, i.e., with the additional step of LSW injection at room temperature. The main objective of this core flooding was to evaluate the performance of standalone LSW and following hybrid LSHW without PDI tuning in heavy oil carbonate core. Table 10 shows the characteristics of Core 5, which was used for the second experiment.

Table 10. Characteristics of core 5

	Diameter, mm	Length, mm	Pore Volume	Porosity, %	Absolute permeability, mD	Effective permeability after aging, mD	Initial water saturation, %	Residual oil saturation, %
<b>Core 5</b>	37.0	75.0	14.31	17.75	34.19	11.86	20.19	14.35

Similar to the previous experiment, the injection of seawater started at 0.1 cc/min and proceeded with the rates of 0.3, 0.6, 0.9, 1.5, 2.0, and 5.0 cc/min. A total of 19 PV of seawater, imitating primary recovery, was injected into the carbonate core and resulted in oil recovery of 67.51% OOIP. A considerable difference in recovery factors of conventional seawater injection

between the first and second experiments can be explained by different characteristics of the cores, i.e., pore structure, porosity, and permeability values.

LSW flooding started at 0.1 cc/min and continued at 0.5, 1.0, 1.5, 2.0 and 5.0 cc/min, 8 PV were injected. The amount of flow rate steps for the second stage was reduced because of the lower amount of remaining oil after SW injection. Unfortunately, results showed only 0.41% OOIP (or 1.24% of the remaining oil) of additional oil recovery, i.e., almost no oil was recovered. It can be explained by too high viscous oil, which cannot be displaced by diluted seawater.

At the third stage, the core holder and accumulator with diluted seawater were heated to 50°C, and 10 PV of LSHW were injected at 1.0, 2.0, and 5.0 cc/min. Results showed that the increase of temperature favorably affected additional oil recovery by 9.55% of OOIP (or 29.75% of the remaining oil) compared to LSW at 20°C. Finally, the temperature of brine was increased to 70°C to perform the extra hot LSW injection with the similar design of injection rates to the previous stage. 11 PV of LSHW were injected. Additional oil recovery of 4.55% OOIP (or 20.20% of the remaining oil) was observed during the flooding at 70°C.

Figure 33 and Table 11 show the results of the second experiment. It can be concluded that injection of LSW without thermal support showed no effect on incremental oil recovery since almost no oil was displaced. However, an increase in temperature and, hence, viscosity reduction from 967.36 cp to 125.58 cp showed considerable additional oil recovery, indicating about successful LSHW approach.

Table 11. Oil recovery factors of Experiment 2: SW → 5D SW → Hot 5D SW → Extra Hot 5D SW

Test	RF	Seawater	5D SW	Hot 5D SW	Extra Hot 5D SW
		20°C	20°C	50°C	70°C
<b>Experiment 2</b>	RF (% OOIP)	67.51	67.92	77.47	82.02
	Additional RF	-	<b>0.41</b>	<b>9.55</b>	<b>4.55</b>
	RF of the remaining oil (%)	67.51	1.24	29.75	20.20
	Total RF by EOR				<b>14.51</b>

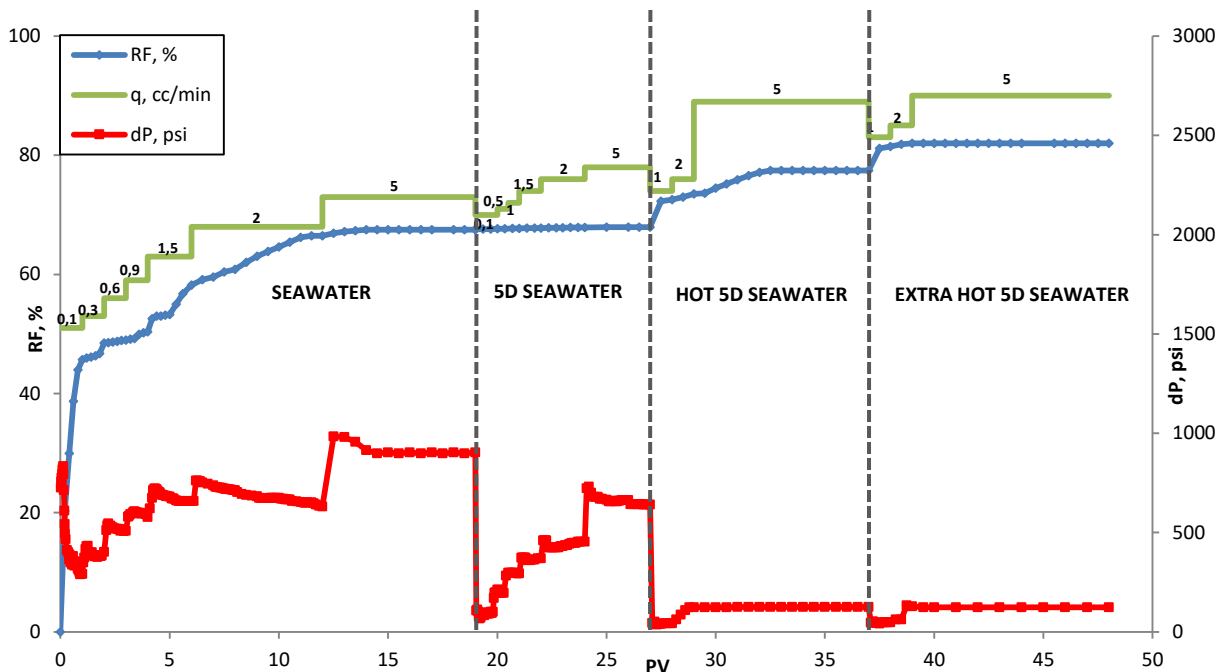


Figure 37. Oil recovery diagram of Experiment 2: SW → 5D SW → Hot 5D SW → Extra Hot 5D SW

### 3.2.3. Experiment 3: SW → 5D-2Mg\*2SO<sub>4</sub> → Hot 5D-2Mg\*2SO<sub>4</sub> → Extra Hot 5D-2Mg\*2SO<sub>4</sub>

The third experiment was performed to study the effect of PDI tuning in LSW brine, namely double concentration of Mg<sup>2+</sup> and SO<sub>4</sub><sup>2-</sup> ions, on the incremental oil recovery at 20, 50, and 70°C. Design of the third experiment was completely similar to the second, except for the ionic concentration of the injected brine. Table 12 shows the characteristics of Core 2, which was used for the third experiment.

Table 12. Characteristics of core 2

	Diameter, mm	Length, mm	Pore Volume	Porosity, %	Absolute permeability, mD	Effective permeability after aging, mD	Initial water saturation, %	Residual oil saturation, %
<b>Core 2</b>	37.0	69.0	13.0	17,54	35.67	8.49	18.33	6.56

Coreflooding of Caspian seawater started at 0.1 cc/min and continued at 0.3, 0.6, 0.9, 1.5, 2.0, and 5.0 cc/min with a total amount of 19 injected PV. Conventional SW flooding at 20°C resulted in the oil recovery of 74.95% OOIP. Injection of 5D 2Mg\*2SO<sub>4</sub> brine at the same temperature was performed at 0.1, 0.5, 1.0, 1.5, 2.0, and 5.0 cc/min until a total of 8 PV was

injected. Results showed an increase of oil recovery by 1.98% OOIP (or 7.89% of the remaining oil). Excess of magnesium and sulfate in the brine showed the higher incremental oil recovery compared to LSW injection (7.89% compared to 1.24% of the remaining oil), which could possibly indicate the positive effect of Mg<sup>2+</sup> and SO<sub>4</sub><sup>2-</sup> combination on the wettability alteration of the rock surface.

At the third stage, the core holder and accumulator with engineered seawater were heated to 50°C, and 10 PV of 5D 2Mg\*2SO<sub>4</sub> brine was injected at 1.0, 2.0, and 5.0 cc/min. Results showed an additional oil recovery of 7.68% of OOIP (or 33.31% of the remaining oil). Finally, the brine was heated to 70°C, and the core flooding was performed at the same injection rates as in the previous stage (at 50°C). Incremental oil recovery by 7.36% OOIP (or 47.79% of the remaining oil) was observed at the last stage of the experiment.

Table 13 and Figure 38 provide the results of oil recovery factors and pressure drop during the different stages of the experiment. It can be concluded that the increase of Mg<sup>2+</sup> and SO<sub>4</sub><sup>2-</sup> concentration led to the higher incremental oil recovery compared to diluted seawater without PDI tuning. This finding corresponds to the results of Chandrasekhar and Mohanty (2013), who observed that Mg<sup>2+</sup> and SO<sub>4</sub><sup>2-</sup> were the leading PDIs changing chalk surface wettability, as well as an excess of SO<sub>4</sub><sup>2-</sup> in the injected brine led to the increase of OOIP from 40 to 80% in both secondary and tertiary recovery stages for carbonate cores. A greater influence of the excess of magnesium and sulfate in the brine was observed at higher temperatures, indicating successful hybrid LSHW performance. A total of 17.02% OOIP of additional oil recovery injection was estimated during the standalone LSW and hybrid LSHW injection.

Table 13. Oil recovery factors of Experiment 3: SW → 5D 2Mg\*2SO<sub>4</sub> → Hot 5D 2Mg\*2SO<sub>4</sub> → Extra Hot 5D 2Mg\*2SO<sub>4</sub>

Test	RF	Seawater 20°C	5D 2Mg*2SO <sub>4</sub> 20°C	Hot 5D 2Mg*2SO <sub>4</sub> 50°C	Extra Hot 5D 2Mg*2SO <sub>4</sub> 70°C
<b>Experiment 3</b>	RF (% OOIP)	74.95	76.93	84.61	91.97
	Additional RF	-	<b>1.98</b>	<b>7.68</b>	<b>7.36</b>
	RF of the remaining oil (%)	74.95	7.89	33.31	47.79
	Total RF by EOR				<b>17.02</b>

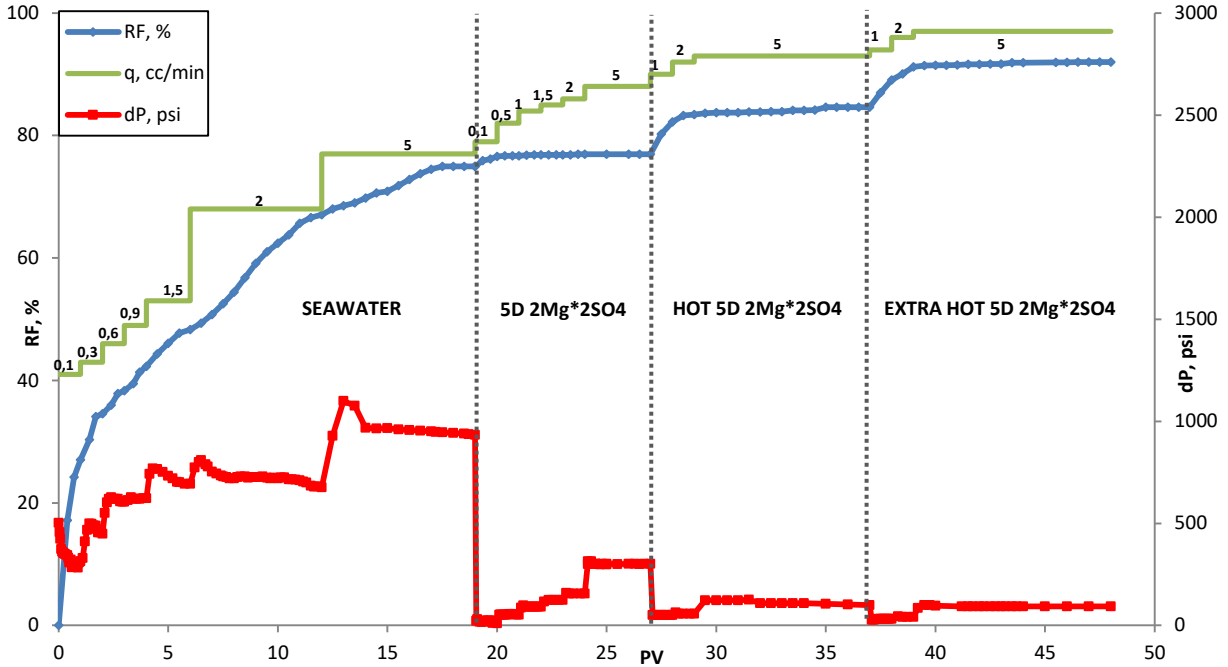


Figure 38. Oil recovery diagram of Experiment 3: SW → 5D 2Mg\*2SO<sub>4</sub> → Hot 5D 2Mg\*2SO<sub>4</sub> → Extra Hot 5D 2Mg\*2SO<sub>4</sub>

### 3.2.4. Experiment 4: SW → 5D-2Ca\*2SO<sub>4</sub> → Hot 5D-2Ca\*2SO<sub>4</sub> → Extra Hot 5D-2Ca\*2SO<sub>4</sub>

The main objective of this experiment was to evaluate the performance of standalone LSW and hybrid LSHW with the double concentration of Ca<sup>2+</sup> and SO<sub>4</sub><sup>2-</sup> ions at 20, 50, and 70°C. Table 14 shows the characteristics of Core 5, which was used for the fourth experiment.

Table 14. Characteristics of core 10

	Diameter, mm	Length, mm	Pore Volume	Porosity, %	Absolute permeability, mD	Effective permeability after aging, mD	Initial water saturation, %	Residual oil saturation, %
<b>Core 10</b>	37.0	69.0	13.16	17.755	32.31	9.17	22.37	9.31

As in previous experiments, the injection of Caspian seawater started at 0.1 cc/min. The experiment proceeded at higher flow rates of 0.3, 0.6, 0.9, 1.5 cc/min. The injection rate was increased to 2.0 and 5.0 cc/min to minimize the capillary end effect. 19 PV of 2Ca\*2SO<sub>4</sub> was injected to imitate the primary oil recovery. Results of conventional seawater injection showed an oil recovery of 72.7% OOIP.

At the next stage, 5D 2Ca\*2SO<sub>4</sub> brine flooding was performed at 0.1, 0.5, 1.0, 1.5, 2.0, and 5.0 cc/min at 20°C. A total of 19 PV was injected. Unfortunately, no oil was produced during the 5D 2Ca\*2SO<sub>4</sub> injection, even at high injection rates (Figure 39). Thus, the application of standalone LSW with the double concentration of Ca<sup>2+</sup> and SO<sub>4</sub><sup>2-</sup> was ineffective for the heavy oil displacement at 20°C, in total, as in previous experiments.

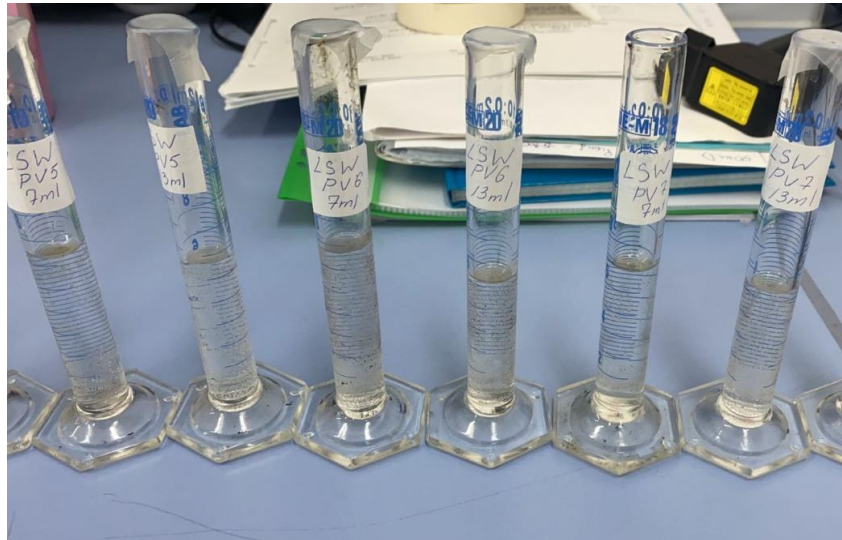


Figure 39. No oil production during the injection of 5D 2Ca\*2SO<sub>4</sub> brine at 20°C

An increase of temperature to 50°C and then to 70°C favorably affected the incremental oil recovery by 7.75% OOIP (or 28.39% of the remaining oil) and 7.55% OOIP (or 38.64 of the remaining oil), respectively (Table 15 and Figure 40). The procedure of the third and fourth stages of experiment #4 was completely the same as in previous experiments. Compared to the injection of 5D 2Mg\*2SO<sub>4</sub> brine, the performance of 5D 2Ca\*2SO<sub>4</sub> showed less incremental oil recovery at 50°C and 70°C. In total, 15.3% OOIP of incremental oil recovery was displaced during the hot and extra hot LSW injection.

Table 15. Oil recovery factors of Experiment 4: SW → 5D 2Ca\*2SO<sub>4</sub> → Hot 5D 2Ca\*2SO<sub>4</sub> → Extra Hot 5D 2Ca\*2SO<sub>4</sub>

Test	RF	Seawater	5D 2Ca*2SO <sub>4</sub>	Hot 5D 2Ca*2SO <sub>4</sub>	Extra Hot 5D 2Ca*2SO <sub>4</sub>
		20°C	20°C	50°C	70°C
<b>Experiment 4</b>	RF (% OOIP)	72.70	72.70	80.45	88.00
	Additional RF	-	<b>0</b>	<b>7.75</b>	<b>7.55</b>
	RF of the remaining oil (%)	72.70	0.00	28.39	38.64
	Total RF by EOR				<b>15.30</b>

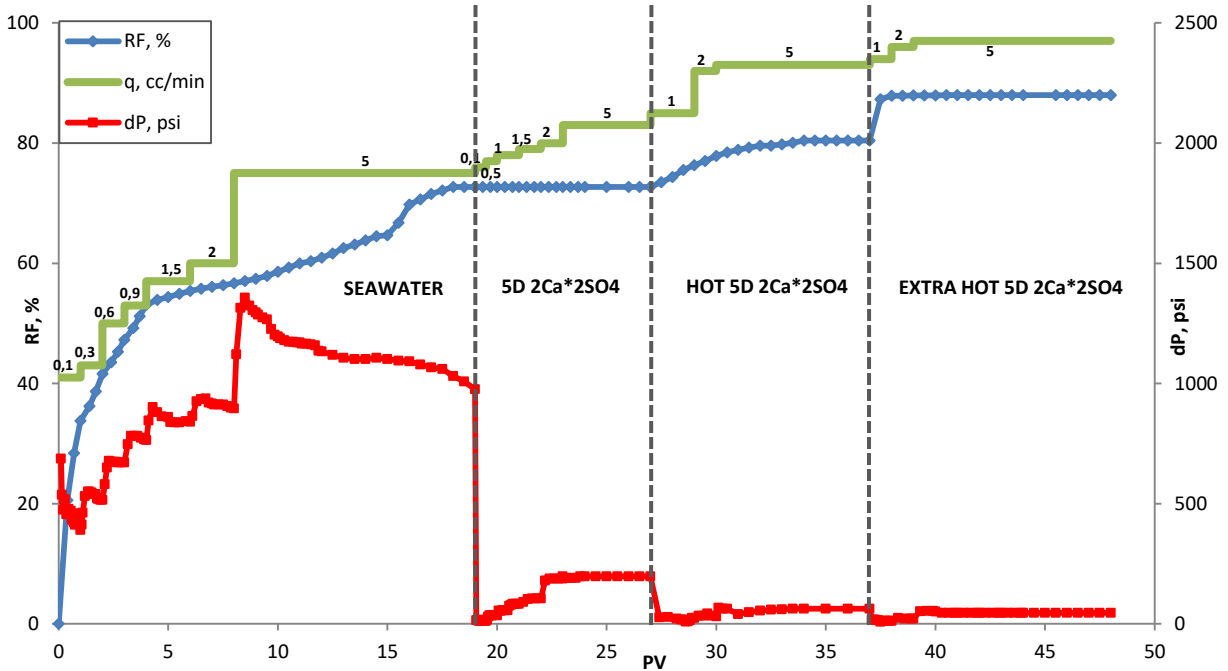


Figure 40. Oil recovery diagram of Experiment 4: SW → 5D 2Ca\*2SO<sub>4</sub> → Hot 5D 2Ca\*2SO<sub>4</sub> → Extra Hot 5D 2Ca\*2SO<sub>4</sub>

### 3.2.5. Experiment 5: SW → 5D-2Ca\*2Mg\*2SO<sub>4</sub> → Hot 5D-2Ca\*2Mg\*2SO<sub>4</sub> → Extra Hot 5D-2Ca\*2Mg\*2SO<sub>4</sub>

The main objective of the fifth experiment was to investigate the effect of the combination of all PDI, i.e., the double concentration of Ca<sup>2+</sup>, Mg<sup>2+</sup>, and SO<sub>4</sub><sup>2-</sup>, during the LSW at 20°C and hybrid LSHW at 50°C and 70°C. Table 16 shows the characteristics of Core 8, which was used for the fifth experiment.

Table 16. Characteristics of core 8

	Diameter, mm	Length, mm	Pore Volume	Porosity, %	Absolute permeability, mD	Effective permeability after aging, mD	Initial water saturation, %	Residual oil saturation, %
<b>Core 8</b>	37.0	73.5	14.13	17.88	31.24	9.50	24.13	4.08

Injection of conventional Caspian seawater, imitating the primary oil recovery, was performed at 0.1, 0.3, 0.6, 0.9, 1.0, 1.5, 2.0, and 5.0 cc/min at 20°C. Injection of 19 PV of seawater resulted in oil recovery of 66.79% OOIP. Injection of 5D-2Ca\*2Mg\*2SO<sub>4</sub> was performed at 0.1, 0.5, 1.0, 1.5, 2.0, and 5.0 cc/min. The number of low injection rates, which are

reasonable when the pressure difference is too high, was reduced because more than 2/3 of oil was displaced during the SW injection. 8 PV of the injected 5D-2Ca\*2Mg\*2SO<sub>4</sub> resulted in additional oil recovery of 3.37% OOIP (or 10.14% of the remaining oil), which was the best result beyond all LSW brines at 20°C but still not significant enough to evaluate the performance of this brine as the effective for heavy oil displacement without thermal support.

At the third stage of the experiment, the temperature was increased to 50°C, and core flooding was carried out at 1.0, 2.0, and 5.0 cc/min. The number of low injection rates, which are reasonable when the pressure difference is too high, was reduced because more than 2/3 of oil was displaced during the SW injection. Injection of 10 PV of 5D-2Ca\*2Mg\*2SO<sub>4</sub> resulted in considerable incremental oil recovery by 17.91% OOIP (or 60.02% of the remaining oil). When 11 PV of 5D-2Ca\*2Mg\*2SO<sub>4</sub> was injected at 70°C with the same injection rates, it resulted in the additional oil recovery by 6.55 % of OOIP (or 54.89% of the remaining oil, i.e., recovery factors of the remaining oil at 50°C and 70°C were almost similar).

Table 17 and Figure 41 show the obtained results of the fifth experiment. According to the obtained results of all 4-stage core flooding experiments, it can be noticed that the combination of double calcium, magnesium, and sulfate in 5-times diluted seawater showed the highest oil recovery factors at all temperatures.

Table 17. Oil recovery factors of Experiment 5: SW → 5D 2Ca\*2Mg\*2SO<sub>4</sub> → Hot 5D 5D 2Ca\*2Mg\*2SO<sub>4</sub> → Extra Hot 5D 2Ca\*2Mg\*2SO<sub>4</sub>

Test	RF	Seawater 20°C	5D 2Ca*2Mg*2S O <sub>4</sub> 20°C	Hot 5D 2Ca*2Mg*2S O <sub>4</sub> 50°C	Extra Hot 5D 2Ca*2Mg*2S O <sub>4</sub> 70°C
<b>Experiment 5</b>	RF (% OOIP)	66.79	70.16	88.07	94.62
	Additional RF	-	<b>3.37</b>	<b>17.91</b>	<b>6.55</b>
	RF of the remaining oil (%)	66.79	10.14	60.02	54.89
	Total RF by EOR				<b>27.83</b>

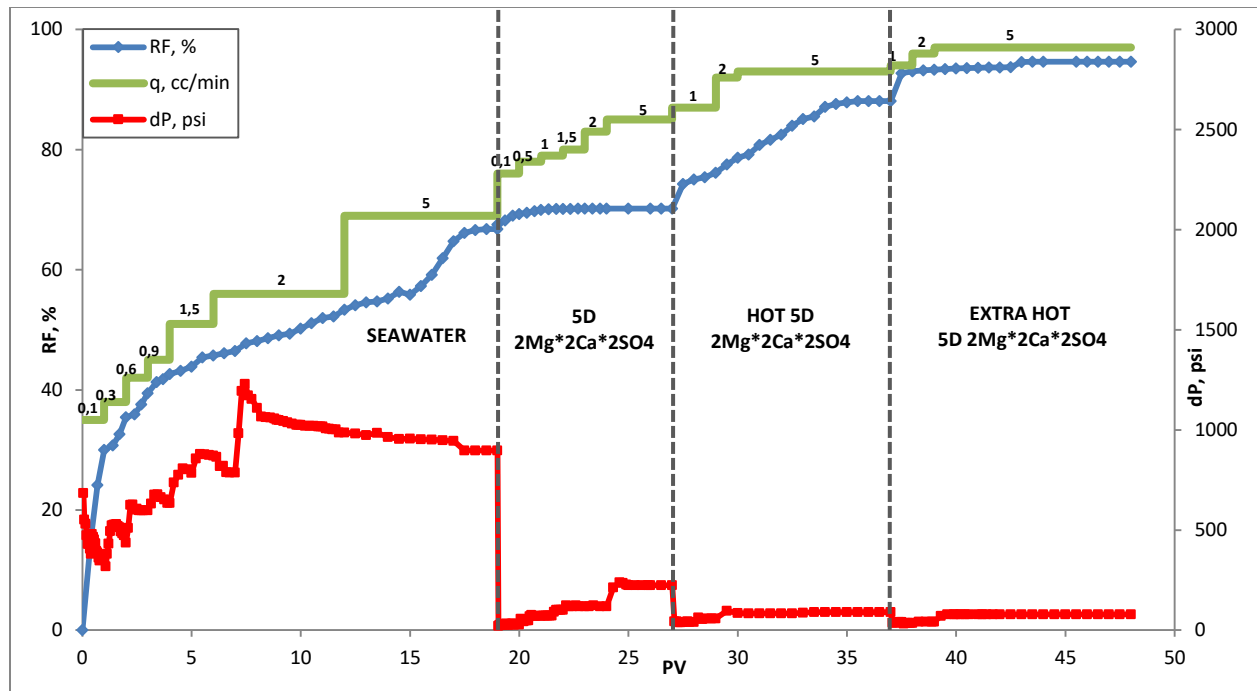


Figure 41. Oil recovery diagram of Experiment 5: SW → 5D 2Ca\*2Mg\*2SO<sub>4</sub> → Hot 5D 2Ca\*2Mg\*2SO<sub>4</sub> → Extra Hot 5D 2Ca\*2Mg\*2SO<sub>4</sub>

### 3.2.6. Experiment 6: SW → Hot 5D-2Ca\*2Mg\*2SO<sub>4</sub> → Extra Hot 5D-2Ca\*2Mg\*2SO<sub>4</sub>

The procedure of the last experiment was similar to the first and fifth core flooding. The sixth core flooding consisted of three stages: seawater injection at 20°C → injection of the diluted brine with PDI tuning at 20°C → injection of the diluted brine with PDI tuning at 50°C → injection of the diluted brine with PDI tuning at 70°C. 2Ca\*2Mg\*2SO<sub>4</sub> was selected as the injected brine, because it showed the highest recovery factors between all 4-stage core flooding experiments. The main purpose of this core flooding was the evaluation of hybrid LSHW injection directly after SW injection at 50°C and 70°C, since LSW flooding at 20°C showed no considerable effect on incremental oil recovery. Table 18 provides the characteristics of the core 9, which was used for the sixth experiment.

Table 18. Characteristics of core 9

	Diameter, mm	Length, mm	Pore Volume	Porosity, %	Absolute permeability, mD	Effective permeability after aging, mD	Initial water saturation, %	Residual oil saturation, %
Core 9	37.0	71.5	14.28	18.58	29.86	11.85	14.53	10.51

Injection of seawater was performed at 0.1, 0.3, 0.6, 0.9, 1.5, 2.0, 5.0 cc/min with a total of 19 injected PV. Results showed an oil recovery of 60.33% during the first stage, imitating primary oil recovery. After that, brine was changed to  $2Ca*2Mg*2SO_4$  solution, and the accumulator with core holder were heated to  $50^{\circ}C$  for 2 hours. Injection of  $2Ca*2Mg*2SO_4$  brine started at 1 cc/min and proceeded with 2 and 5 cc/min. Injected 10.5 PV showed an incremental oil recovery of 22.79% OOIP (or 57.44% of the remaining oil). At the last stage of the experiment, the accumulator was heated to  $70^{\circ}C$ , and the flooding was performed with the same injection rates as in the previous stage. A total of 6.5 PV was injected. Results showed an additional oil recovery by 4.59% OOIP (or 27.18% of the remaining oil). Table 19 and Figure 42 show the obtained oil recovery factors during the three stages of the experiment. Compared to the results of the first experiment, oil recovery factors were higher by 4.05% OOIP (or 22.23% of the remaining oil) at  $50^{\circ}C$  and by 0.68% OOIP (or 15.82% of the remaining oil), which proves the effectiveness of direct hybrid LSHW injection and positive effect of PDI tuning on additional oil release from the rock surface.

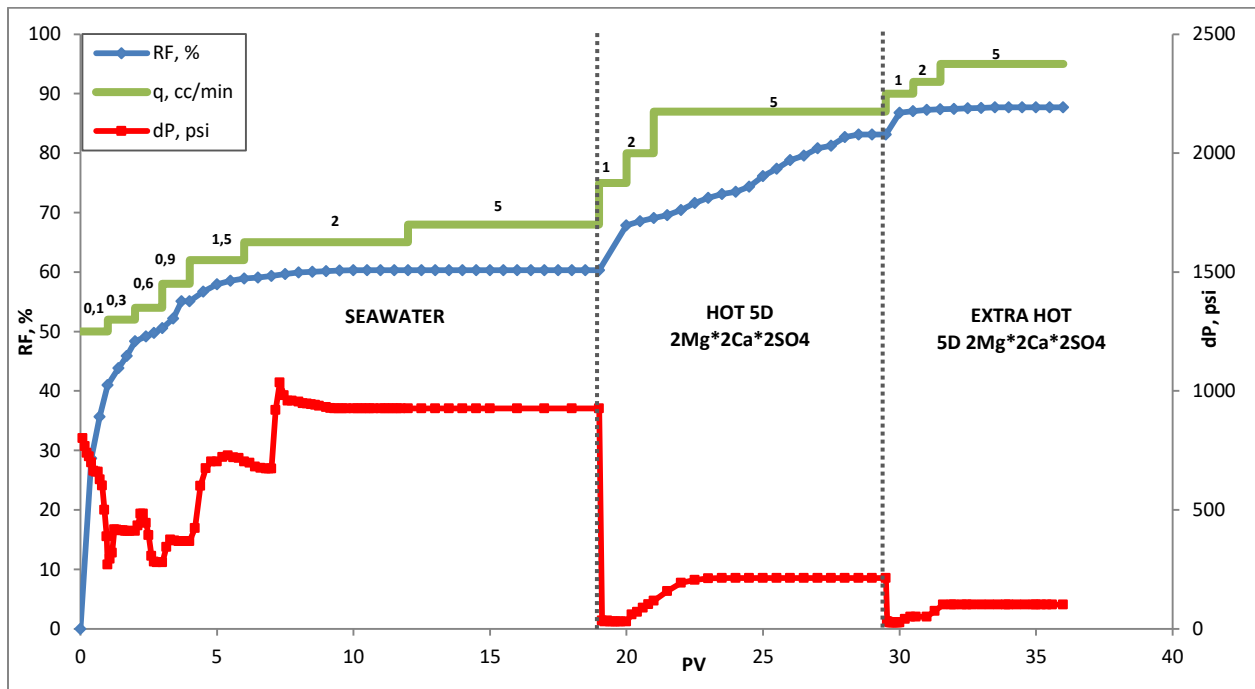


Figure 42. Oil recovery diagram of Experiment 6: SW → Hot 5D  $2Ca*2Mg*2SO_4$  → Extra Hot 5D  $2Ca*2Mg*2SO_4$

Table 19. Oil recovery factors of Experiment 5: SW → Hot 5D 2Ca\*2Mg\*2SO<sub>4</sub> → Extra Hot 5D 2Ca\*2Mg\*2SO<sub>4</sub>

Test	Recovery Factor (RF)	Seawater	Hot SW	Extra Hot SW
		20°C	50°C	70°C
<b>Experiment 6</b>	RF (% OOIP)	60.33	83.12	87.71
	Additional RF	-	<b>22.79</b>	<b>4.59</b>
	RF of the remaining oil (%)	60.33	57.44	27.18
	Total RF by EOR			<b>27.38</b>

### 3.2.7. Comparison of core flooding experiments

Figures 43-46 and Tables 20-21 show the results of these core flooding experiments. As the first stage of the EOR approach, standalone LSW/EW was injected, and, as observed, the recovery factor was very low (almost zero in some cases). Only 5D 2Mg\*2SO<sub>4</sub> and 5D 2Ca\*2Mg\*2SO<sub>4</sub> solutions showed an increase in oil recovery factor by 1.98 and 3.37% of OOIP compared to SW, while 5D SW and 5D 2Ca\*2SO<sub>4</sub> injection displaced no oil. It was concluded that the application of LSW/EW is not effective as an EOR method for highly viscous oil. Our experiments showed that the hybrid combination of the thermal method with an effective EW injection could enhance this recovery. For example, if adequate PDIs are considered in the injected hot water, more than 60% of the residual oil can be recovered, which shows the strong synergy between the two approaches. Wettability alteration by the interactions between rock, oil, and PDIs detach the oil from the surface, and higher temperatures reduce the viscosity. The two mechanisms together enhance microscopic and macroscopic sweep efficiencies, as observed during the injection to core 8. Other EW designs (5D SW, 5D 2Mg\*2SO<sub>4</sub>, and 5D 2Ca\*2SO<sub>4</sub>) recovered almost a similar amount of the residual oil in the range of 30-35%. This effect is more noticeable at a higher temperature (70°C). In this case, conventional hot water flooding recovered about 27% of the available residual oil, but it was observed that, by changing the composition of the brine and increasing PDIs, this recovery could be significantly increased. By spiking Mg<sup>2+</sup> cations, about 48% of the residual oil can be recovered. This number can even reach 55% by adjusting both Mg<sup>2+</sup> and Ca<sup>2+</sup> cation concentrations. All of these observations prove the performance of the hybrid EW/thermal method is better than the standalone approach, and it is recommended that the ions composition is tuned to the heavy oil carbonates during hot water flooding.

Table 20. Summary of oil recovery factors of 3-stage core flooding experiments

Test	Core#	RF	Seawater	Hot SW/5D EW	Extra Hot SW/5D EW
			20°C	50°C	70°C
<b>5D Seawater</b>	1	RF (% OOIP)	46.78	65.52	69.43
		Additional RF	-	<b>18.74</b>	<b>3.91</b>
		RF of the remaining oil (%)	46.78	35.21	11.36
		Total RF by EOR			<b>22.65</b>
<b>5D 2Ca*2Mg*2SO<sub>4</sub></b>	9	RF (% OOIP)	60.33	83.12	87.71
		Additional RF	-	<b>22.79</b>	<b>4.59</b>
		RF of the remaining oil (%)	60.33	57.44	27.18
		Total RF by EOR			<b>27.38</b>

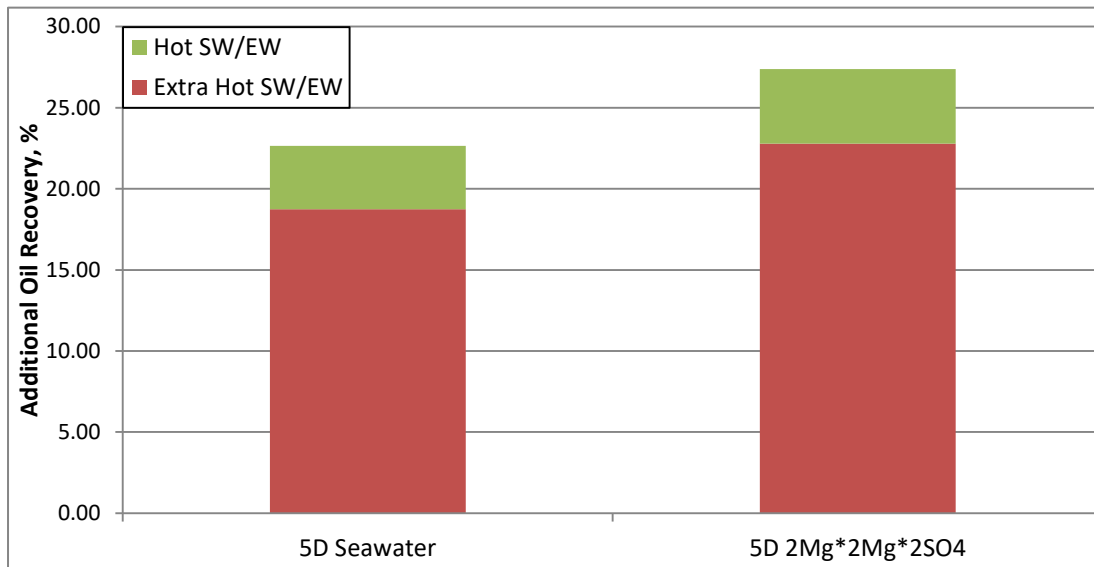


Figure 43. Oil recovery comparison for 3-stage core flooding experiments

Our observations showed that a more effective and practical design is the injection of the hybrid method directly after the seawater flooding. Our tests showed that the EOR by conventional LSW/EW is not productive, and it is better to avoid it. Hence, as the last coreflooding, hot 5D 2Ca\*2Mg\*2SO<sub>4</sub> brine was flooded at 50°C and 70°C to represent the best hybrid design. As can be seen in Figure 42, the final recovery factor reached almost 90%, and the highest oil production was observed, which proved our successful design. Figures 47 and 48 show the displacement efficiency values ( $E_D$ ) for 3- and 4-stage core flooding experiments, which were calculated using Equation (21). As expected, standalone LSW and hybrid LSHWinjection techniques provided better displacement efficiency compared to seawater injection.

$$E_D = \frac{S_{oi} - S_{or}}{S_{oi}} \times 100 \quad (22)$$

Table 21. Summary of oil recovery factors of 4-stage core flooding experiments

Test	Core #	RF	Seawater	5D LSW/EW	Hot 5D LSW/EW	Extra Hot 5D LSW/EW
			20°C	20°C	50°C	70°C
<b>5D Seawater</b>	5	RF (% OOIP)	67.51	67.92	77.47	82.02
		Additional RF	-	<b>0.41</b>	<b>9.55</b>	<b>4.55</b>
		RF of the remaining oil (%)	67.51	1.24	29.75	20.20
		Total RF by EOR				<b>14.51</b>
<b>5D 2Mg*2SO<sub>4</sub></b>	2	RF (% OOIP)	74.95	76.93	84.61	91.97
		Additional RF	-	<b>1.98</b>	<b>7.68</b>	<b>7.36</b>
		RF of the remaining oil (%)	74.95	7.89	33.31	47.79
		Total RF by EOR				<b>17.02</b>
<b>5D 2Ca*2SO<sub>4</sub></b>	10	RF (% OOIP)	72.70	72.70	80.45	88.00
		Additional RF	-	<b>0</b>	<b>7.75</b>	<b>7.55</b>
		RF of the remaining oil (%)	72.70	0.00	28.39	38.64
		Total RF by EOR				<b>15.30</b>
<b>5D 2Ca*2Mg*2SO<sub>4</sub></b>	8	RF (% OOIP)	66.79	70.16	88.07	94.62
		Additional RF	-	<b>3.37</b>	<b>17.91</b>	<b>6.55</b>
		RF of the remaining oil (%)	66.79	10.14	60.02	54.89
		Total RF by EOR				<b>27.83</b>

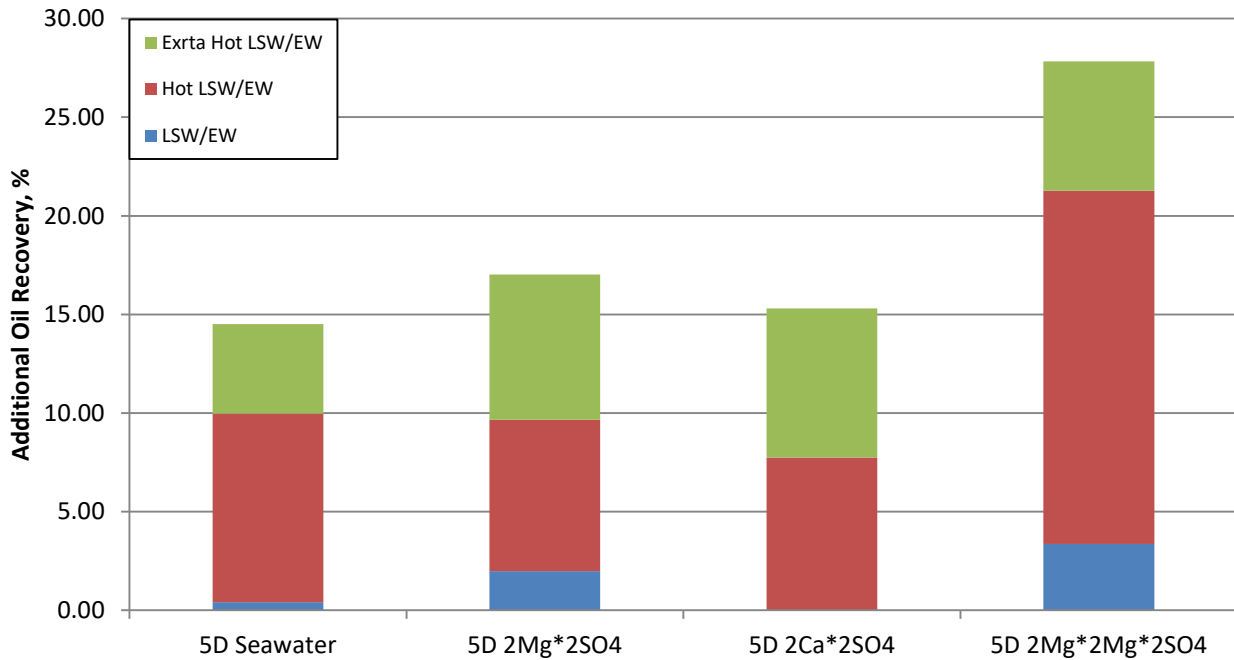


Figure 44. Oil recovery comparison for 4-stage core flooding experiments

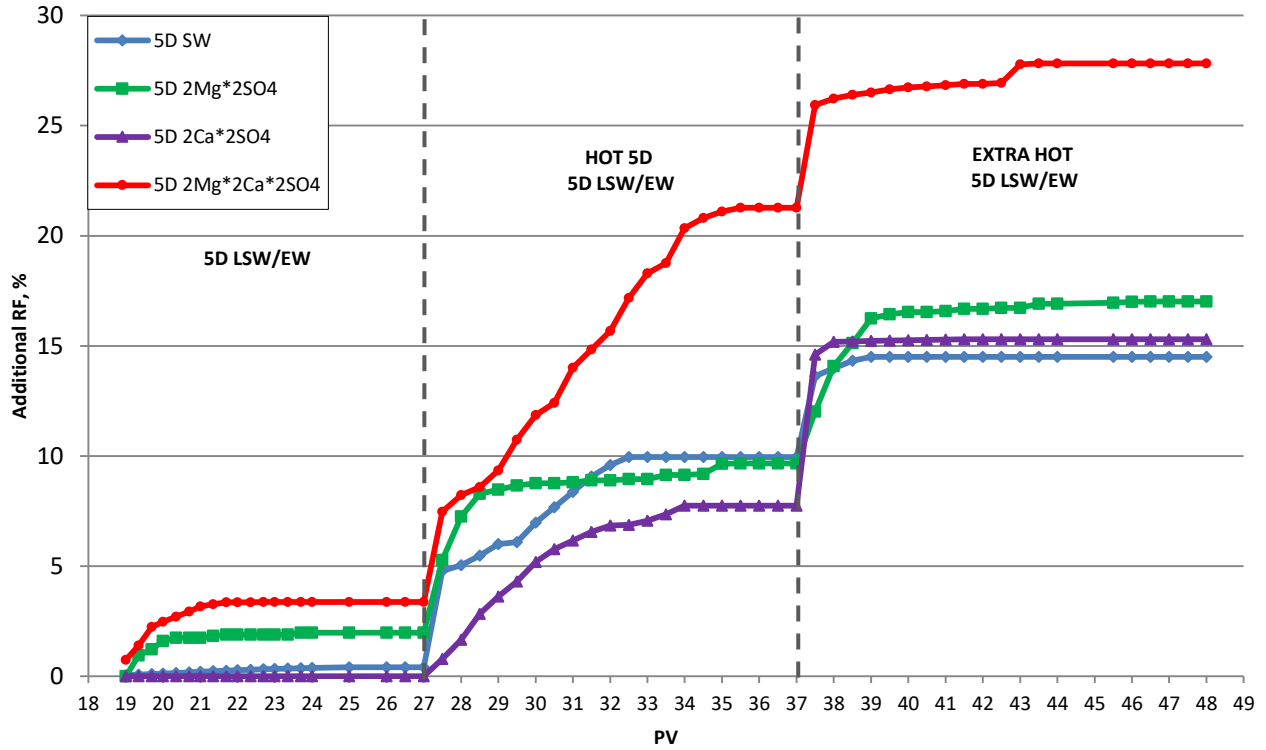


Figure 45. Incremental oil recovery (without SW injection) of 4-stage core flooding experiments

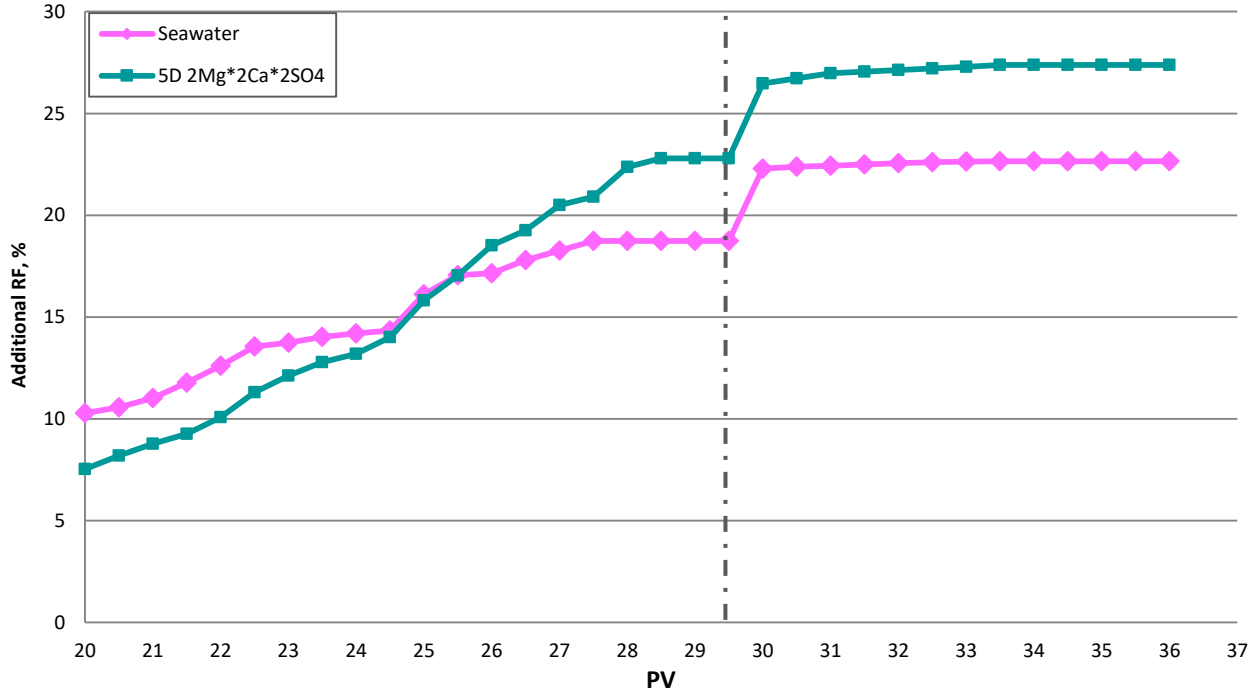


Figure 46. Incremental oil recovery (without SW injection) of 3-stage core flooding experiments

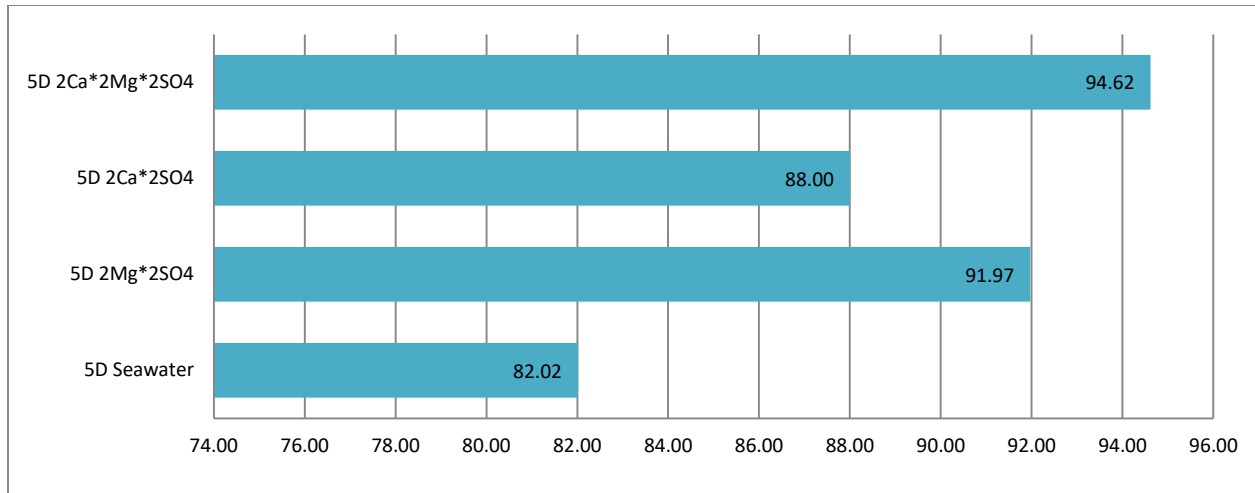


Figure 47. Comparison of displacement efficiency of 4-stage core flooding experiments

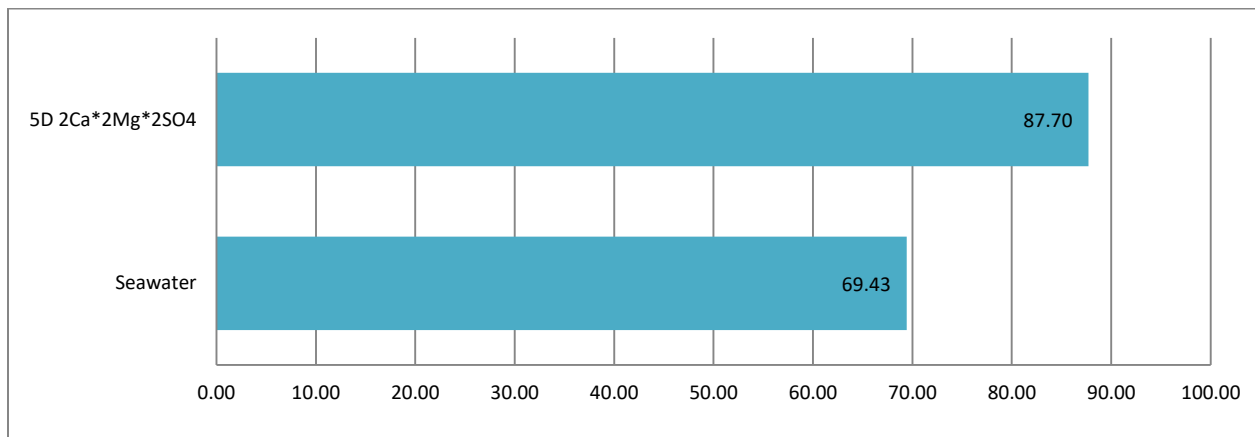


Figure 48. Comparison of displacement efficiency of 3-stage core flooding experiments

### 3.3. Ion Chromatography Analysis

#### 3.3.1. Analysis of Water Samples from Contact Angle Tests

To analyze the ion exchange on the rock surface during the LSW contact with core samples, two oil-saturated and two clean core slices were aged in 10-times diluted SW at 20°C and 80°C. By investigating the dynamic change of ion composition in the water and on the rock surface, it is possible to better clarify the active mechanisms.

The aging of the oil-saturated cores in 10-times diluted SW at 20°C and 80°C resulted in ion exchange and the release of the oil from the surface. Figures 12 and 13 show the results of ion chromatography analyses, where  $C/C_0$  is defined as the change in ion concentration,  $C_0$  is the

initial ion concentration of the brine, and  $C$  is a concentration at a given time  $t$ . Figure 50 shows the concentration of active ions in the solution during the aging process of cores already saturated by oil. Both rock dissolution and multi-ion exchange mechanisms can be observed during the aging process.  $CaCO_3$  is dissolved in the brine via rock dissolution, which results in an increase in the concentration of  $SO_4^{2-}$  and, as observed, the concentration of  $Mg^{2+}$  ions only slightly fluctuated, while the concentration of  $SO_4^{2-}$  and  $Ca^{2+}$  ions increased significantly, as can be seen during the first 120 hours of the measurements. It should be noted that the mechanism is a bit stronger at higher temperatures, and the rate of the dissolution is faster, which proves our core flooding results, i.e., higher oil recovery at higher temperatures. Multi-ion exchange occurs at a later time which results in the decrease of the cation concentration in the brine. Both ion exchange and calcite dissolution mechanisms affect the rock surface leading to a change in wettability to a more water-wet state.

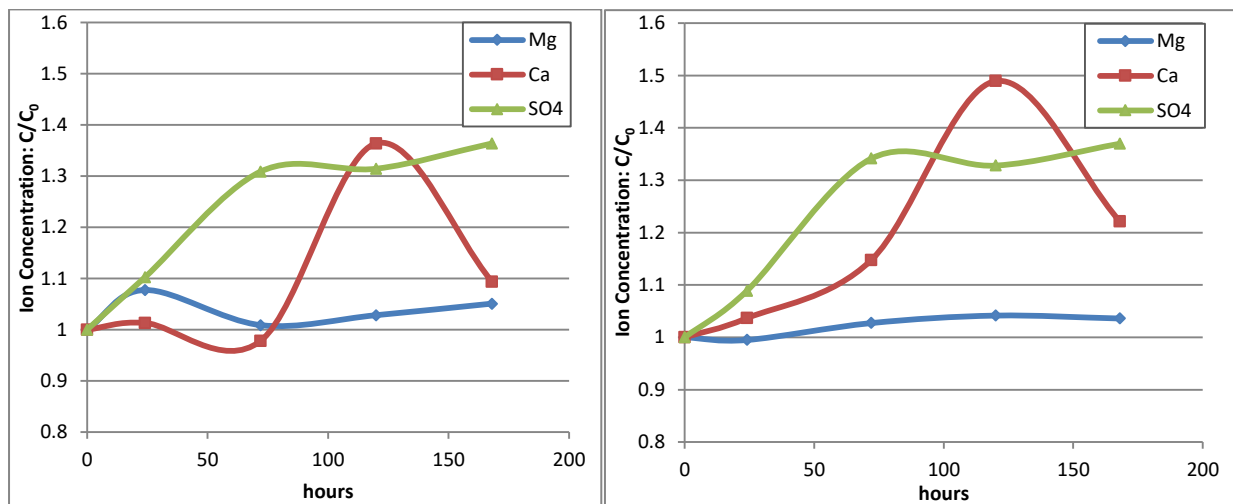


Figure 49. Change of PDI's concentration in 10-times diluted SW during aging of oil-wet cores (left: 20°C, right: 80°C)

Two clean core slices with no oil were used to investigate the effect of temperature on the rock dissolution mechanism. Figure 51 shows the results for 168 hours. It can be seen that the concentration of  $SO_4^{2-}$  increased significantly at both temperatures, but sulfate ions were released faster at 20°C, which does not contradict the study of Yousef et al. (2011), who observed that sulfate concentration increases faster in low-temperature conditions. The  $Ca^{2+}$  ions concentration increased at the same time as  $SO_4^{2-}$ , indicating the dissolution process at both temperatures.  $Mg^{2+}$  ion concentrations did not change within seven days, indicating that dolomite dissolution is

very weak at both temperatures. The calcite dissolution rate is faster at the higher temperature, which confirms the findings shown in Figure 12.

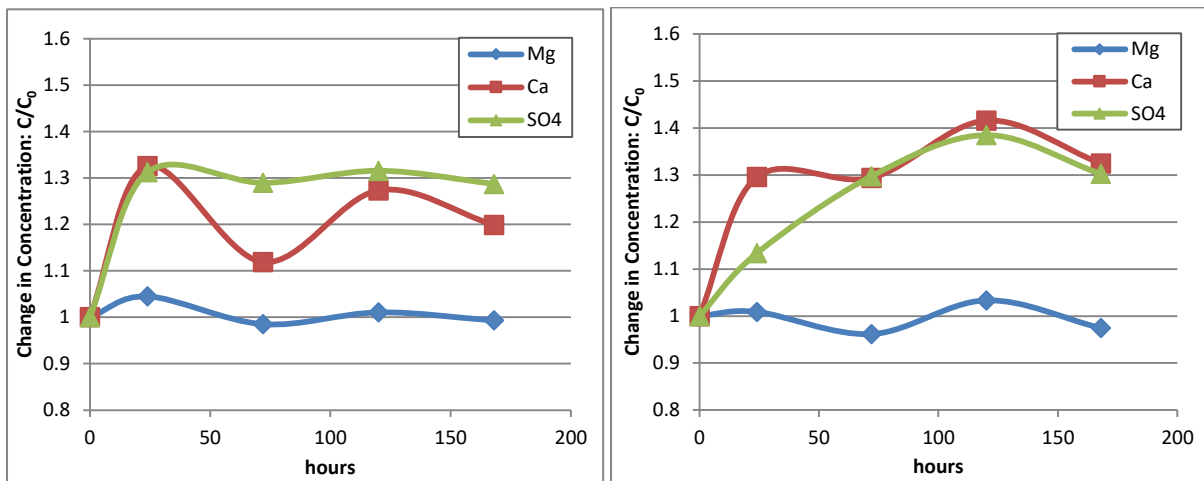


Figure 50. Change of PDIs concentration in 10-times diluted SW during aging of clean cores (left: 20°C, right: 80°C)

### 3.3.2. Effluent Analysis

Water samples were taken three times from each step of the 4-stage core flooding experiments to observe the multi-ion exchange and calcite dissolution mechanisms at different temperature conditions, from 20°C to 70°C. Figure 51-54 shows the effluent analysis results, where  $C/C_0$  is defined as the change in ion concentration,  $C_0$  is an initial concentration of a specific ion at the start of LSW injection (22<sup>nd</sup> PV), and  $C$  is an ion concentration at the current injected PV. It was decided to take 22<sup>nd</sup> PV as the  $C_0$  instead of 19-21<sup>th</sup> PVs because injection of LSW/EW started after SW injection with 5-times higher ionic concentration and, hence first pore volumes of effluent during LSW/EW injection contained SW.

Results of ion chromatography analysis show the rapid fluctuation of  $Ca^{2+}$ ,  $Mg^{2+}$ , and  $SO_4^{2-}$  during the core flooding process, indicating active chemical processes in the CBR system. Two possible LSW mechanisms can be observed by ion tracking: rock dissolution and multi-ion exchange (PDI). The rapid increase of  $Ca^{2+}$  and  $Mg^{2+}$  ions and the fact that the concentration of these ions stably remained at least twice as high as the initial concentration of the injected brine proved the rock dissolution during the core flooding experiment. Soon after an increase in the temperature, an increase in the concentration of cations and  $SO_4^{2-}$  was observed, which shows rock dissolution and helps to increase the oil recovery as one of the mechanisms involved during

the hybrid EOR. It can be noticed that the process of PDI fluctuation was more active in brines with double concentration, i.e., 5D 2Mg\*2SO4 and 5D 2Ca\*2Mg\*2SO4, than 5D SW and 5D 2Ca\*2SO4 brines, which also corresponds with the results of core flooding experiments. The calcite dissolution mechanism, which can be interpreted by an increase in  $C/C_0$  during injected PV, was the most active in 5D 2Ca\*2Mg\*2SO4 brine. The same trend was observed for multi-ion exchange, i.e., adsorption of PDI mechanisms on the rock surface that causes oil release from the surface. An increase in the temperature during the core flooding experiments from 20°C to 50°C and from 50°C to 70°C caused more active reactions between the rock surface, crude oil, and injected brine, proving the statement about direct dependence of the efficiency of LSW mechanisms on temperature.

To summarize, the increase in the concentration of all ions is evidence of rock dissolution. The decrease of  $C/C_0$  indicated about PDIs adsorption into the carbonate surface and, hence, additional oil displacement. The results of all ion chromatography analyses, from pellet aging and core flooding tests, show that the active mechanisms of LSW/EW interactions are stronger at higher temperatures. However, the effect of LSW mechanisms was found to be insufficiently effective in displacing heavy oil with a viscosity of more than 900 cp during core flooding experiments. Hence, the hybrid method is recommended to activate both thermal EOR and LSW flooding mechanisms.

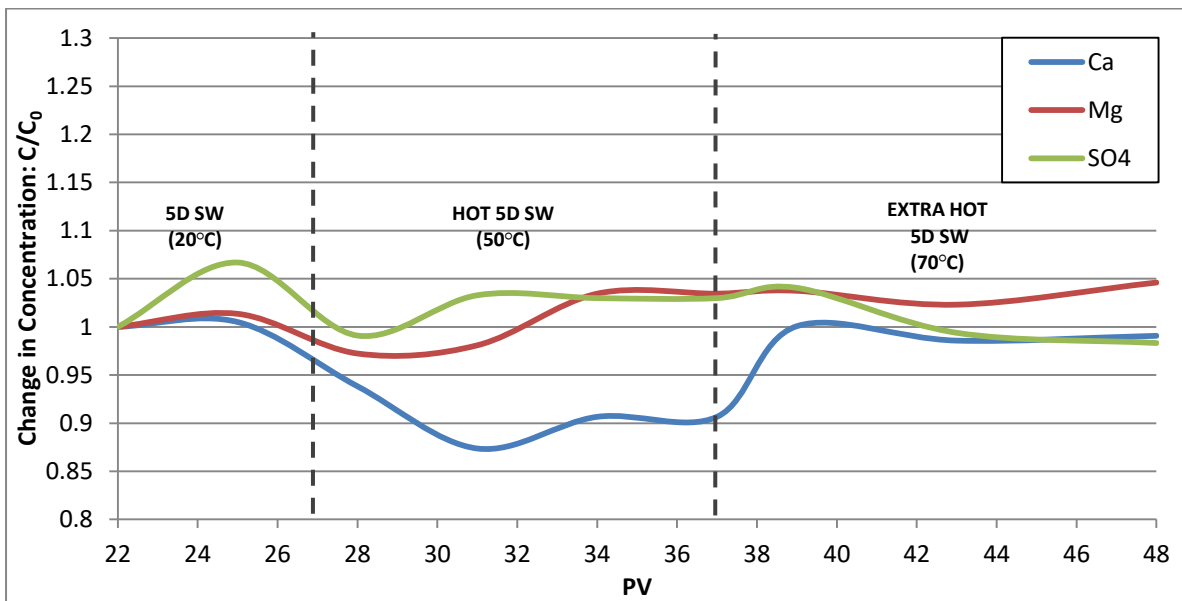


Figure 51. Change of PDIs concentration during 5D SW brine injection

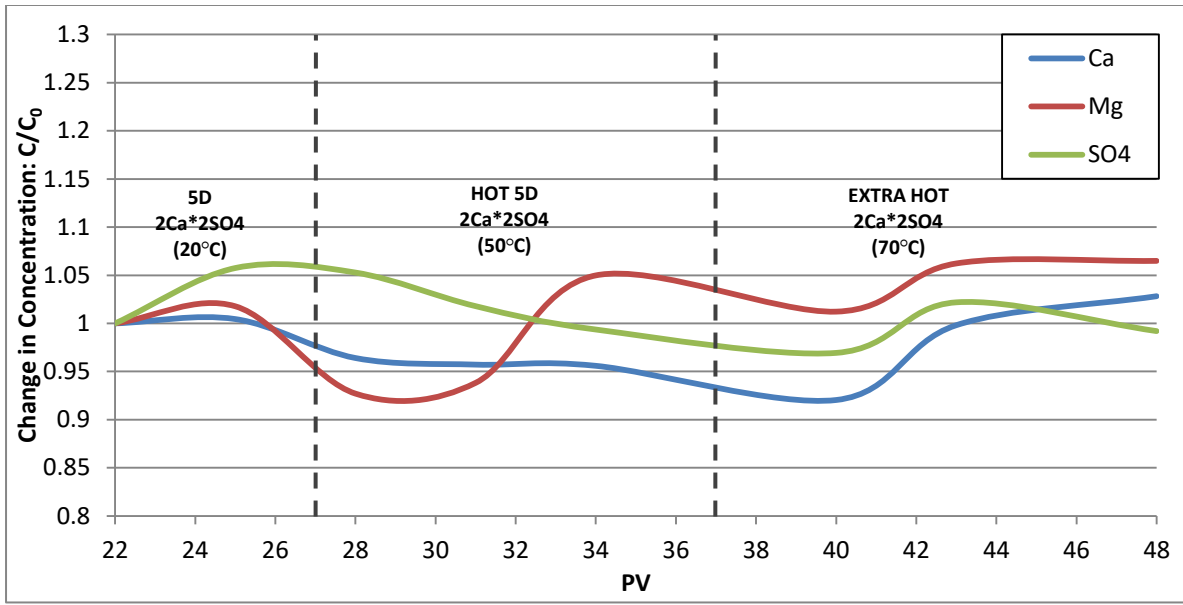


Figure 52. Change of PDI's concentration during 5D 2Ca\*2SO4 brine injection

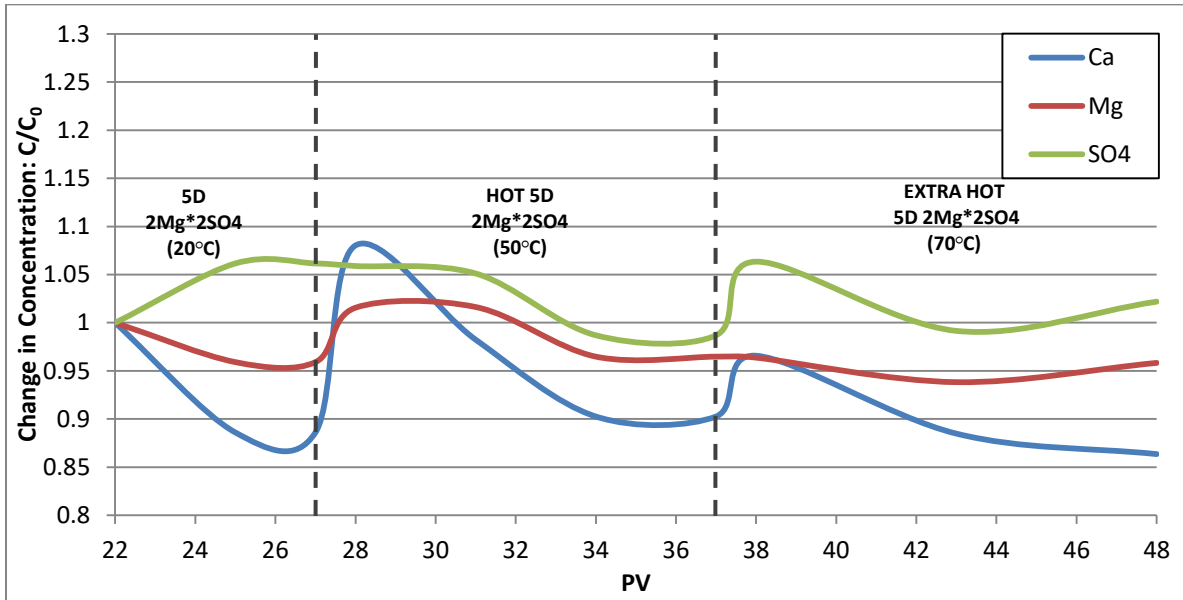


Figure 53. Change of PDI's concentration during 5D 2Mg\*2SO4 brine injection

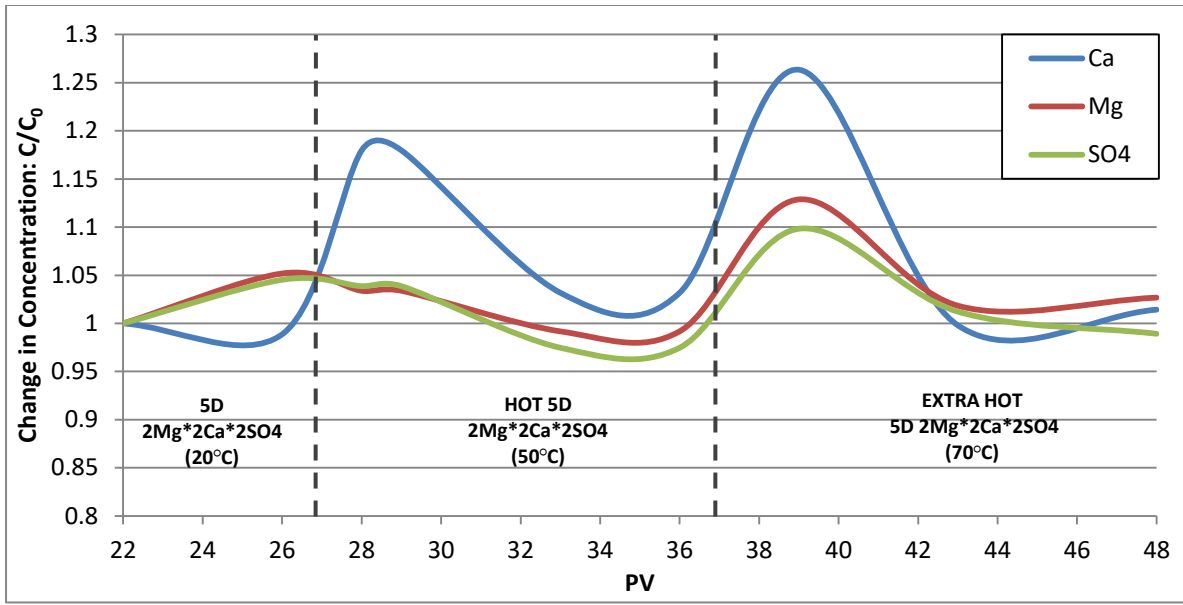


Figure 54. Change of PDI's concentration during 5D 2Mg\*2Ca\*2SO4 brine injection

#### 4. CONCLUSION AND RECOMMENDATIONS

In this study, the performance of standalone LSW and hybrid LSHW injection (direct after SW and following LSW injection) in heavy oil carbonate cores was experimentally investigated under different temperatures from 20 to 70°C to study the effect of LSW mechanisms on the rock surface and synergistic effects of the hybrid EOR approach. Contact angle measurements were conducted on core slices for 168 hours at 20°C and 80°C to estimate the optimal dilution of SW and observe the effect of different PDIs concentrations on the wettability alteration of rock surface. 5D SW, 5D 2Ca\*2SO<sub>4</sub>, 5D 2Mg\*2SO<sub>4</sub>, and 5D 2Ca\*2Mg\*2SO<sub>4</sub> brines were prepared for six core flooding experiments and conducted at 20°C, 50°C, and 70°C to evaluate the LSW and LSHW flooding in different conditions and design techniques. Water samples for ion chromatography analysis were taken from the core slices aging and core flooding experiments to track the change in PDI concentration during the time and injected PV, investigate the difference in the performance of LSW mechanisms at various temperatures, and estimate the dependence of the efficiency of mechanisms on temperature. Based on the laboratory results, the following conclusions can be drawn:

- 5-times diluted SW showed the most significant change in contact angle after 168 hours, indicating the optimal ionic concentration for the wettability alteration. Due to the low concentration of PDIs, LSW was not very effective at higher dilution levels, even at the higher temperature. 5-times diluted SW was chosen as an optimal dilution for injected brine in core flooding experiments.
- Standalone LSW injection without thermal approach was ineffective for heavy oil displacement due to very low and almost zeros oil production. 5D-2Ca\*2Mg\*2SO<sub>4</sub> brine injection at 20°C showed the highest additional oil recovery of 3.37% OOIP (or 10.14% of the remaining oil) among all 4-steps core flooding experiments. However, it was still not significant enough to evaluate the performance of this brine as effective in core-scale flooding.
- Hybrid LSHW injection following LSW showed high efficiency in heavy oil carbonate cores. Combinations of double concentrations of Ca<sup>2+</sup>, Mg<sup>2+</sup>, and SO<sub>4</sub><sup>2-</sup> ions resulted in the highest oil displacement, where 60.00% and 54.89% of residual oil were recovered at 50°C and 70°C. The injection of LSHW directly after SW resulted in the production of 55.74%

and 27.18% of the remaining oil at 50°C and 70°C, respectively. Compared to the results of the conventional hot seawater injection, which showed 35.21% and 11.36% of the displaced remaining oil, PDI tuning was highly recommended during LSHW injection. Since standalone LSW injection was not effective, it was recommended to avoid it and directly start the injection of a more effective and practical hybrid LSHW injection design with PDI tuning.

- PDIs and calcite dissolution were defined as the main mechanisms of LSW by the results of ion chromatography analyses, leading to the wettability alteration from oil-wet to water-wet. An increase in temperature showed more active multi-ion exchange and rock dissolution, leading to the additional release of oil carboxylic groups from the carbonate surface.

The following recommendations are offered for a better understanding of the impact of LSW mechanisms on the oil recovery process in carbonates:

- To design more solutions of PDI tuning in injected LSW brines, such as  $2Ca*3Mg*2SO_4$ ,  $3Ca*2Mg*2SO_4$ , and so on, i.e., change the proportional concentration of PDI and study the effect of this tuning on the wettability change.
- To perform core flooding experiments at higher temperature conditions (80, 90, 100°C, etc.) in order to determine the dependency of active LSW mechanisms (linear, exponential, etc.) on temperature increase.
- To investigate the impact of incompatibility between the injected water and rock mineralogy.
- To study the influence of ionic concentration of pore water on oil displacement during LSW and LSHW injection.
- To investigate the problem of the change of influence of LSW mechanisms during the increase of the research scale from the core- to reservoir-scale by numerical simulations methods.

## 5. REFERENCES

1. Abass. E. & Fahmi. A. (2013). Experimental investigation of low salinity hot water injection to enhance the recovery of heavy oil reservoirs. *In: North Africa Technical Conference and Exhibition*. Cairo. Egypt. <https://doi.org/10.2118/164768-ms>
2. Al Saedi. H. N., Williams. A. & Flori. R. E. (2018). Comparison between cold/hot smart water flooding in sandstone reservoirs. *Journal of Petroleum & Environmental Biotechnology*. 09(02). <https://doi.org/10.4172/2157-7463.1000365>
3. Alameri. W., Teklu. T., Graves. R., Kazemi. H. & AlSumaiti. A. (2015). Low-salinity water-alternate-surfactant in low-permeability carbonate reservoirs. *In: IOR 2015 - 18th European Symposium on Improved Oil Recovery*. Dresden. Germany. <https://doi.org/10.3997/2214-4609.201412158>
4. Aleidan. A. & Mamora. D. D. (2010). SWACO<sub>2</sub> and WACO<sub>2</sub> efficiency improvement in carbonate cores by lowering water salinity. *In: Canadian Unconventional Resources and International Petroleum Conference*. Alberta. Canada. <https://doi.org/10.2118/137548-ms>
5. Almansour. A.O., AlQuraishi. A.A., AlHussin. S.N. *et al.* Efficiency of enhanced oil recovery using polymer-augmented low salinity flooding. *J Petrol Explor Prod Technol* 7. 1149–1158 (2017). <https://doi.org/10.1007/s13202-017-0331-5>
6. Al-Murayri. M. T., Kamal. D. S., Al-Sabah. H. M., AbdulSalam. T., Al-Shamali. A., Quttainah. R., Glushko. D., Britton. C., Delshad. M., Liyanage. J., & Dean. R. M. (2019). Low-salinity polymer flooding in a high-temperature low-permeability carbonate reservoir in West Kuwait. *In: SPE Kuwait Oil & Gas Show and Conference*. Mishref. Kuwait. <https://doi.org/10.2118/198000-ms>
7. Alotaibi. M. B., Nasr-El-Din. H. A. & Fletcher. J. J. (2011). Electrokinetics of limestone and dolomite rock particles. *SPE Reservoir Evaluation & Engineering*. 14(05). 594-603. <https://doi.org/10.2118/148701-pa>
8. Al-Shalabi. E. W. & Sepehrnoori. K. (2016). A comprehensive review of low salinity/engineered water injections and their applications in sandstone and carbonate rocks. *Journal of Petroleum Science and Engineering*. 139. 137–161. <https://doi.org/10.1016/j.petrol.2015.11.027>

9. AlSofi. A. M., Liu. J. S., Han. M. & Aramco. S. (2013). Numerical simulation of surfactant–polymer coreflooding experiments for carbonates. *Journal of Petroleum Science and Engineering*. 111. 184–196. <https://doi.org/10.1016/j.petrol.2013.09.009>
10. Altahir. M., Yu. M. & Hussain. F. (2017). Low Salinity Water Flooding in Carbonates - Dissolution Effect. In: *International Symposium of the Society of Core Analysts*. Vienna. Austria. 1–8.
11. Alvarado. V. & Manrique. E. (2010). *Enhanced Oil Recovery: Field Planning and Development Strategies*. Burlington: Elsevier Science. <https://doi.org/10.1016/C2009-0-30583-8>
12. Alzayer. H. & Sohrabi. M. (2013). Numerical simulation of improved heavy oil recovery by low-salinity water injection and polymer flooding. In: *SPE Saudi Arabia Section Technical Symposium and Exhibition*. Al-Khobar. Saudi Arabia. <https://doi.org/10.2118/165287-ms>
13. Askarova. A., Turakhanov., A. Markovic. S., Popov. E., Maksakov. K., Usachev. G., Karpov. V. & Cheremisin. A. (2020). Thermal enhanced oil recovery in deep heavy oil carbonates: Experimental and numerical study on a hot water injection performance. *Journal of Petroleum Science and Engineering*. 194. 107456. <https://doi.org/10.1016/j.petrol.2020.107456>
14. Assef. Y. Arab. D. & Pourafshary. P. (2014). Application of nanofluid to control fines migration to improve the performance of low salinity water flooding and alkaline flooding. *Journal of Petroleum Science and Engineering*. 124. 331-340. <https://doi.org/10.1016/j.petrol.2014.09.023>
15. Assef. Y., Pourafshary. P. & Hejazi. H. (2016). Controlling interactions of colloidal particles and porous media during low salinity water flooding and alkaline flooding by mgo nanoparticles. In *SPE EOR Conference at Oil and Gas West Asia. Muscat. Oman*. <https://doi.org/10.2118/179768-ms>
16. Austad. T., RezaeiDoust., A. & Puntervold. T. (2010). Chemical mechanism of low salinity water flooding in sandstone reservoirs. In: *SPE Improved Oil Recovery Symposium*. Tulsa. Oklahoma. USA. <https://doi.org/10.2118/129767-ms>
17. Austad. T., Strand. S., Høgnesen. E. & Zhang. P. (2005). Seawater as IOR fluid in fractured chalk. In: *SPE International Symposium on Oilfield Chemistry*. Texas. USA. <https://doi.org/10.2118/93000-ms>

18. Ayirala. A. S., Sofi. Z., Li.& Z. Xu (2011). Surfactant and surfactant-polymer effects on wettability and crude oil liberation in carbonates. *Journal of Petroleum Science and Engineering*. vol. 207. 109117. <https://doi.org/10.1016/j.petrol.2021.109117>
19. Ayirala. S. C., Saleh. S. H., Enezi. S. M. & Al-Yousef. A. A. (2018). Effect of salinity and water ions on electrokinetic interactions in carbonate reservoir cores at elevated temperatures. *SPE Reservoir Evaluation & Engineering*. 21(03). 733-746. <https://doi.org/10.2118/189444-pa>
20. Bealesio. B. A., Blázquez Alonso. N. A., Mendes. N. J., Sande. A. V. & Hascakir. B. (2021). A review of Enhanced Oil Recovery (EOR) methods applied in Kazakhstan. *Petroleum*. 7(1). 1-9. <https://doi.org/10.1016/j.petlm.2020.03.003>
21. Burchette. T. P. (2012). Carbonate rocks and petroleum reservoirs: A geological perspective from the industry. *Geological Society. London. Special Publications*. 370(1). 17–37. <https://doi.org/10.1144/sp370.14>
22. Burger. J., Sourieau. P. & Combarous. M. (1985). *Thermal Methods of Oil Recovery*. Paris. France: Editions Technip.
23. Chandrasekhar. S. & Mohanty. K. K. (2013). Wettability alteration with brine composition in high temperature carbonate reservoirs. In: *SPE Annual Technical Conference and Exhibition*. New Orleans. Louisiana. USA. <https://doi.org/10.2118/166280-ms>
24. Diab. W. N. & Al-Shalabi. E. W. (2019). Recent developments in polymer flooding for carbonate reservoirs under harsh conditions. In: *Offshore Technology Conference Brasil*. Rio De Janeiro. Brazil. <https://doi.org/10.4043/29739-ms>
25. Ding. H. & Rahman. S. R. 2018. Investigation of the impact of potential determining ions from surface complexation modeling. *Energy & Fuels*. 32(9). 9314-9321. <https://doi.org/10.1021/acs.energyfuels.8b02131>
26. Ding. Y., Zheng. S., Meng. X. & Yang. D. (2019). Low salinity hot water injection with addition of nanoparticles for Enhancing Heavy Oil Recovery. *Journal of Energy Resources Technology*. 141(7). <https://doi.org/10.1115/1.4042238>
27. Duan. Z. & Sun. R. (2003). An improved model calculating CO<sub>2</sub> solubility in pure water and aqueous NaCl solutions from 273 to 533 K and from 0 to 2000 bar. *Chemical Geology*. 193(3-4). 257–271. [https://doi.org/10.1016/s0009-2541\(02\)00263-2](https://doi.org/10.1016/s0009-2541(02)00263-2)
28. Enhanced Oil Recovery Scoping Study. ERPI. Palo Alto. CA: 1999. TR-113836.

29. Enick. R. & Klara. S. (1990). CO<sub>2</sub> solubility in water and brine under reservoir conditions. *Chemical Engineering Communications*. 90(1). 23–33. <https://doi.org/10.1080/00986449008940574>
30. Gachuz-Muro. H. &Sohrabi. M. (2014). Smart water injection for heavy oil recovery from naturally fractured reservoirs. *In: SPE Heavy and Extra Heavy Oil Conference: Latin America*. Medellín. Colombia. <https://doi.org/10.2118/171120-ms>
31. Hallenbeck. L. D., Sylte. J. E., Ebbs. D. J. & Thomas. L. K.(1991). Implementation of the Ekofisk field waterflood.*SPE Formation Evaluation*. 6(3). 284-290. <https://doi.org/10.2118/19838-PA>
32. Hein. F.J. (2006). Heavy Oil and Oil (Tar) Sands in North America: An Overview & Summary of Contributions. *Nat Resour Res* 15. 67–84. <https://doi.org/10.1007/s11053-006-9016-3>
33. Hiorth. A., Cathles. L. M. &Madland. M. V.(2010). The impact of pore water chemistry on carbonate surface charge and oil wettability. *Transport in Porous Media*.85(1). 1-21. <https://doi.org/10.1007/s11242-010-9543-6>
34. Ismail. I.,Kazemzadeh.Y., Gaganis. V. &Bassias. Y. (2021). Increasing medium-heavy oil recovery in carbonate reservoirs using smart water injection. *In: 82nd EAGE Annual Conference & Exhibition*. <https://doi.org/10.3997/2214-4609.202011756>
35. Jamaloei. B. Y. & Singh. A. R. (2016). Hot water flooding and cold water flooding in heavy oil reservoirs. *Energy Sources. Part A: Recovery. Utilization. and Environmental Effects*. 38(14). 2009–2017. <https://doi.org/10.1080/15567036.2014.1004004>
36. Jiang. H.,Nuryaningsih. L. &Adidharma. H.(2010). The effect of salinity of injection brine on water alternating gas performance in tertiary miscible carbon dioxide flooding: Experimental study. *In: SPE Western Regional Meeting*. Anaheim. California. USA. <https://doi.org/10.2118/132369-ms>
37. Karimov. D.,Hashmet. M. R. &Pourafshary. P. (2020). A laboratory study to optimize ion composition for the hybrid low salinity water/polymer flooding. *In: Offshore Technology Conference Asia*. Kuala Lumpur. Malaysia. <https://doi.org/4043/30136-ms>
38. Kasha. A.,Sauerer. B., Al-Hashim. H.& Abdallah.W.. 2021. Interplay between ca<sup>2+</sup>. mg<sup>2+</sup>. and so<sub>4</sub><sup>2-</sup> ions and their influence on the Zeta-potential of limestone during controlled-

- salinity waterflooding. *Energy & Fuels*.35(16). 12982-12992.  
<https://doi.org/10.1021/acs.energyfuels.1c00940>
39. Katende. A. &Sagala. F. (2019). A critical review of low salinity water flooding: Mechanism. laboratory and Field Application. *Journal of Molecular Liquids*.278. 627-649.  
<https://doi.org/10.1016/j.molliq.2019.01.037>
40. Koottungal. K. (2010.). Special Report 2010 worldwide EOR survey. *Oil and Gas Journal*. 108. 41–53.
41. Lee. J. H.& Lee. K. S. (2018). Geochemical evaluation of low salinity hot water injection to enhance heavy oil recovery from carbonate reservoirs. *Petroleum Science*.16(2). 366-381.  
<https://doi.org/10.1007/s12182-018-0274-6>
42. Lee. J. H., Jeong. M. S., Lee. K. S. &Mohammadi. A. H. (2017). Modeling of Low-Salinity Waterflood with Temperature-Dependent Geochemical Reactions for Heavy Oil Carbonate Reservoirs . In *Heavy Oil: Characteristics. Production and Emerging Technologies* (pp. 1–21). Nova Science Publishers.
43. Lee. K. S. & Lee. J. (2019). *Hybrid enhanced oil recovery using smart waterflooding*. Gulf Professional Publishing. <https://doi.org/10.1016/C2018-0-01195-0>
44. Lee. Y., Lee. W., Jang. Y. & Sung. W. (2019). Oil recovery by low-salinity polymer flooding in carbonate oil reservoirs. *Journal of Petroleum Science and Engineering*. 181. 106211. <https://doi.org/10.1016/j.petrol.2019.106211>
45. Li. Y.-K. & Nghiem. L. X. (1986). Phase equilibria of oil. gas and water/brine mixtures from a cubic equation of state and Henry's Law. *The Canadian Journal of Chemical Engineering*. 64(3). 486–496. <https://doi.org/10.1002/cjce.5450640319>
46. Liu. W. Z. (1998). *The development models of heavy oil reservoirs by thermal recovery*. Beijing: Petroleum Industry Press.
47. Lo. H. Y. &Mungan. N. (1973). Effect of temperature on water-oil relative permeabilities in oil-wet and water-wet systems. In: *Fall Meeting of the Society of Petroleum Engineers of AIME*. Las Vegas. Nevada. USA.<https://doi.org/10.2118/4505-ms>
48. Mahani. H., Keya. A. L., Berg. S. &Nasralla. R. (2017). Electrokinetics of Carbonate-Brine Interface in Low-Salinity-Waterflooding: Effect of Brine Salinity. Composition. Rock Type and pH on Zeta-Potential and A Surface Complexation Model .*SPE Journal*. 22(01). 53–68.  
<https://doi.org/10.2118/181745-pa>

49. Mahani. H., Keya. A. L., Berg. S., Bartels. W., Nasralla. R. & Rossen. W. R. (2015). Insights into the mechanism of wettability alteration by low-salinity flooding (LSF) in carbonates. *Energy & Fuels*.29(3). 1352-1367. <https://doi.org/10.1021/ef5023847>
50. Mahmoudpour. M. & Pourafshary. P.(2021). Investigation of the effect of engineered water/nanofluid hybrid injection on enhanced oil recovery mechanisms in carbonate reservoirs. *Journal of Petroleum Science and Engineering*.196. 107662. <https://doi.org/10.1016/j.petrol.2020.107662>
51. Manrique. E., Thomas. C., Ravikiran. R., Izadi. M., Lantz. M., Romero. J. & Alvarado. V. (2010). EOR: Current status and opportunities. In: *17th SPE Improved Oil Recovery Symposium*. Tulsa. Oklahoma. USA. <https://doi.org/10.2118/130113-ms>
52. Masoomi. R. & Torabi. F. (2022). A new computational approach to predict hot-water flooding (HWF) performance in unconsolidated heavy oil reservoirs. *Fuel*. 312. 122861. <https://doi.org/10.1016/j.fuel.2021.122861>
53. Mehana. M. & Fahes. M. M. (2018). Investigation of double layer expansion in low-salinity waterflooding: Molecular simulation study. In: *Fall Meeting of the Society of Petroleum Engineers of AIME. Las Vegas. Nevada. USA*. <https://doi.org/10.2118/190106-ms>
54. Meyer. R. F., Attanasi. E. D. & Freeman. P. A. (2007). Heavy oil and natural bitumen resources in geological basins of the world. *U.S. Geological Survey*. <https://doi.org/10.3133/ofr20071084>
55. Montaron. B. A., Bradley. D. C., Cooke. A., Prouvost. L. P., Raffn. A. G., Vidal. A. & Wilt. M. (2007). Shapes of flood fronts in heterogeneous reservoirs and oil recovery strategies. In: *SPE/EAGE Reservoir Characterization and Simulation Conference*. Abu Dhabi. UAE. Oct. 2007. <https://doi.org/10.2118/111147-MS>
56. Moradi. B., Pourafshary. P., Jalali. F. & Mohammadi. M. (2017). Effects of nanoparticles on gas production, viscosity reduction, and foam formation during nanofluid alternating gas injection in low and high permeable carbonate reservoirs. *The Canadian Journal of Chemical Engineering*. 95(3). 479–490. <https://doi.org/10.1002/cjce.22699>
57. Moradpour. N., Pourafshary. P. & Zivar. D. (2021). Experimental analysis of hybrid low salinity water alternating gas injection and the underlying mechanisms in carbonates. *Journal of Petroleum Science and Engineering*.202. 108562. <https://doi.org/10.1016/j.petrol.2021.108562>

58. Myint. P. C. &Firoozabadi. A. (2015). Thin liquid films in improved oil recovery from low-salinity brine. *Current Opinion in Colloid & Interface Science*.20(2). 105–114. <https://doi.org/10.1016/j.cocis.2015.03.002>
59. Nasralla. R. A.,Mahani. H., Van der Linde. H. A.,Marcelis. F. H., Masalmeh. S. K., Sergienko. E., Basu. S. (2018). Low salinity waterflooding for a carbonate reservoir: Experimental Evaluation and Numerical Interpretation. *Journal of Petroleum Science and Engineering*.164. 640-654. <https://doi.org/10.1016/j.petrol.2018.01.028>
60. Penney. R. K., Moosa. R., Shahin. G. T., Hadrami. F., Kok. A., Engen. G., van Ravesteijn. O., Rawnsley. K., & Kharusi. B. (2005). Steam injection in fractured carbonate reservoirs: Starting a new trend in EOR. *In: International Petroleum Technology Conference*. Doha. Qatar.<https://doi.org/10.2523/iptc-10727-ms>
61. Pourafshary. P. &Moradpour. N. (2019). Hybrid EOR methods utilizing low-salinity water. *Enhanced Oil Recovery Processes - New Technologies*. <https://doi.org/10.5772/intechopen.88056>
62. RezaeiDoust. A.,Punternvold. T., Strand. S., &Austad. T. (2009). Smart water as wettability modifier in carbonate and sandstone: A discussion of similarities/differences in the chemical mechanisms. *Energy & Fuels*.23(9). 4479-4485. <https://doi.org/10.1021/ef900185q>
63. Sadatshojaei. E., Jamialahmadi. M., Esmaeilzadeh. F. &Ghazanfari. M. H. (2016). Effects of low-salinity water coupled with silica nanoparticles on wettability alteration of dolomite at Reservoir Temperature. *Petroleum Science and Technology*. 34(15). 1345–1351. <https://doi.org/10.1080/10916466.2016.1204316>
64. Sagbana. P. I.,Sarkodie. K. & Nkrumah. W. A. (2022). A critical review of carbonate reservoir wettability modification during low salinity waterflooding. *Petroleum*.<https://doi.org/10.1016/j.petlm.2022.01.006>
65. Sánchez-Rodríguez. J., Gachuz-Muro. H. &Sohrabi. M. (2015). Application of low salinity water injection in heavy oil carbonate reservoirs. *In: EUROPEC 2015*. Madrid. Spain. <https://doi.org/10.2118/174391-ms>
66. Saw. R. K. & Mandal. A.. 2020. A mechanistic investigation of low salinity water flooding coupled with ion tuning for Enhanced Oil Recovery. *RSC Advances*.10(69). 42570-42583. <https://doi.org/10.1039/d0ra08301a>

67. Seethepalli. A., Adibhatla. B. & Mohanty. K. K. (2004). Physicochemical interactions during surfactant flooding of fractured carbonate reservoirs. *SPE Journal*. 9(04). 411–418. <https://doi.org/10.2118/89423-pa>
68. Sekerbayeva. A., Pourafshary. P. & Hashmet. M. R. (2020). Application of anionic surfactant-engineered water hybrid EOR in carbonate formations: An experimental analysis. *Petroleum*. <https://doi.org/10.1016/j.petlm.2020.10.001>
69. Shafiei. A., Dusseault. M. B., Memarian. H. & Sadeh. B. S. (2007). Production Technology Selection for Iranian naturally fractured heavy oil reservoirs. In: *Canadian International Petroleum Conference*. Calgary, Canada. <https://doi.org/10.2118/2007-145>
70. Shakeel. M., Pourafshary. P. & Hashmet. M. R. (2020). Hybrid engineered water–polymer flooding in carbonates: A review of mechanisms and case studies. *Applied Sciences*. 10(17). 6087. <https://doi.org/10.3390/app10176087>
71. Shakeel. M., Samanova. A., Pourafshary. P. & Hashmet. M. R. (2021). Experimental analysis of oil displacement by hybrid engineered water / chemical EOR approach in carbonates. *Journal of Petroleum Science and Engineering*. 207. 109297. <https://doi.org/10.1016/j.petrol.2021.109297>
72. Skrettingland. K., Holt. T., Tweheyo. M. T. & Skjevrak. I. (2011). Snorre low-salinity-water injection—Coreflooding experiments and single-well field pilot. *SPE Reservoir Evaluation & Engineering*. 14(02). 182-192. <https://doi.org/10.2118/129877-pa>
73. Standnes. D. C. & Austad. T. (2000). Wettability Alteration in Chalk 2. Mechanism for Wettability Alteration from Oil-Wet to Water-Wet Using Surfactants. *Journal of Petroleum Science and Engineering*. 28(3). 123–143. [https://doi.org/10.1016/s0920-4105\(00\)00084-x](https://doi.org/10.1016/s0920-4105(00)00084-x)
74. Strand. S., Henningsen. S. C., Puntervold. T. & Austad. T. (2017). Favorable temperature gradient for maximum low-salinity enhanced oil recovery effects in carbonates. *Energy & Fuels*. 31(5). 4687-4693. <https://doi.org/10.1021/acs.energyfuels.6b03019>
75. Strand. S., Høgenesen. E. J. & Austad. T. (2006). Wettability alteration of carbonates: effects of potential determining ions ( $\text{Ca}^{2+}$  and  $\text{SO}_4^{2-}$ ) and temperature. *Colloids and Surfaces A: Physicochemical and Engineering Aspects*. 275(1). 110. <https://doi.org/10.1016/j.colsurfa.2005.10.061>

76. Strand. S., Standnes. D. C. & Austad. T. (2003). Spontaneous imbibition of aqueous surfactant solutions into neutral to oil-wet carbonate cores: effects of brine salinity and composition. *Energy & Fuels*. 17(5). 1133–1144. <https://doi.org/10.1021/ef030051s>
77. T. Knott. Less Salt. More Oil. *BP Magazine of Technology and Innovation*. 2009. 1–12.
78. Tahir. M., Hincapie. R. E., Foedisch. H., Abdullah. H. & Ganzer. L. (2018). Impact of sulphates presence during application of smart water flooding combined with polymer flooding. In: *SPE Europec Featured at 80th EAGE Conference and Exhibition*. Copenhagen. Denmark. <https://doi.org/10.2118/190796-ms>
79. Teklu, T., Alameri, W., Kazemi, H., & Graves, R. M. (2015). Contact angle measurements on conventional and unconventional reservoir cores. In: *SPE/AAPG/SEG Unconventional Resources Technology Conference*, San Antonio, Texas, USA. <https://doi.org/10.15530/urtec-2015-2153996>
80. Torrijos P. I. D., Puntervold. T., Strand. S., Austad. T., Bleivik. T. H. & Abdullah. H. I. (2018). An experimental study of the low salinity smart water - polymer hybrid EOR effect in sandstone material. *Journal of Petroleum Science and Engineering*. 164. 219-229. <https://doi.org/10.1016/j.petrol.2018.01.031>
81. Tweheyo. M. T., Zhang. P., & Austad. T., 2006. The effects of temperature and potential determining ions present in seawater on oil recovery from fractured carbonates. In: *PE/DOE Symposium on Improved Oil Recovery*. Tulsa. Oklahoma. USA. <https://doi.org/10.2118/99438-ms>
82. Verma. M. K. (2015). *Fundamentals of carbon dioxide-enhanced oil recovery (CO<sub>2</sub>-EOR): a supporting document of the assessment methodology for hydrocarbon recovery using CO<sub>2</sub>-EOR associated with carbon sequestration* (Vol. 19. pp. 1–24). Reston. Virginia: U.S. Geological Survey. <https://dx.doi.org/10.3133/ofr20151071>
83. Vishnyakov. V., Suleimanov. B., Salmanov. A., & Zeynalov. E. (2020). Hydrocarbon and oil reserves classification. In *Primer on Enhanced Oil Recovery* (pp. 5-26). Cambridge. MA: Gulf Professional Publishing. <https://doi.org/10.1016/B978-0-12-817632-0.00002-5>
84. Vledder. P., Fonseca. J. C., Wells. T., Gonzalez. I., & Ligthelm. D. (2010). Low salinity water flooding: Proof of wettability alteration on a field wide scale. In: *SPE Improved Oil Recovery Symposium*. Tulsa. Oklahoma. USA. <https://doi.org/10.2118/129564-ms>

85. Winsauer. W.O. and W.M. McCardell. "Ionic Double-Layer Conductivity in Reservoir Rock." *J Pet Technol* 5 (1953): 129–134. <https://doi.org/10.2118/953129-G>
86. Xu. Z.-X., Li. S.-Y., Li. B.-F., Chen. D.-Q., Liu. Z.-Y. & Li. Z.-M. (2020). A review of development methods and EOR technologies for carbonate reservoirs. *Petroleum Science*. 17(4). 990–1013. <https://doi.org/10.1007/s12182-020-00467-5>
87. Yongmao. H., Mingjing. L., Chengshun. D., Jianpeng. J., Yuliang. S. & Guanglong. S. (2016). Experimental investigation on oil enhancement mechanism of hot water injection in tight reservoirs. *Open Physics*. 14(1). 703–713. <https://doi.org/10.1515/phys-2016-0079>
88. Yousef. A. A., Al-Saleh. S. & Al-Jawfi. M. (2012). Improved/enhanced oil recovery from carbonate reservoirs by tuning injection water salinity and Ionic content. In: *SPE Improved Oil Recovery Symposium*. Tulsa. Oklahoma. USA. <https://doi.org/10.2118/154076-MS>
89. Yousef. A. A., Al-Saleh. S., Al-Kaabi. A. & Al-Jawfi. M. (2011). Laboratory investigation of the impact of injection-water salinity and ionic content on oil recovery from Carbonate Reservoirs. *SPE Reservoir Evaluation & Engineering*. 14(05). 578–593. <https://doi.org/10.2118/137634-pa>
90. Zaeri. M. R., Hashemi. R., Shahverdi. H. & Sadeghi. M. (2018). Enhanced oil recovery from carbonate reservoirs by spontaneous imbibition of low salinity water. *Petroleum Science*. 15(3). 564–576. <https://doi.org/10.1007/s12182-018-0234-1>
91. Zhang. P. & Austad. T. (2006). Wettability and oil recovery from carbonates: Effects of temperature and potential determining ions. *Colloids and Surfaces A: Physicochemical and Engineering Aspects*. 279(1-3). 179-187. <https://doi.org/10.1016/j.colsurfa.2006.01.009>
92. Zhang. P., Tweheyo. M. T. & Austad. T. (2006). Wettability alteration and improved oil recovery in Chalk: the effect of calcium in the presence of sulfate. *Energy and Fuels*. 20(5). 2056-2062. <https://doi.org/10.1021/ef0600816>
93. Zhang. P., Tweheyo. M. T. & Austad. T. (2007). Wettability alteration and improved oil recovery by spontaneous imbibition of seawater into chalk: Impact of the potential determining ions  $Ca^{2+}$ ,  $Mg^{2+}$ , and  $SO_4^{2-}$ . *Colloids and Surfaces A: Physicochemical and Engineering Aspects*. 301(1-3). 199-208. <https://doi.org/10.1016/j.colsurfa.2006.12.058>